Regulation of the *dsr* operon and function of the proteins DsrR and DsrS in the purple sulfur bacterium *Allochromatium vinosum*

Dissertation

zur

Erlangung des Doktorgrades (Dr. rer. nat.)

der

Mathematisch-Naturwissenschaftlichen Fakultät

der

Rheinischen Friedrich-Wilhelms-Universität Bonn

vorgelegt von

Frauke Grimm

aus

Bonn

Bonn 2011

Angefertigt mit Genehmigung der Mathematisch-Naturwissenschaftlichen Fakultät der Rheinischen Friedrich-Wilhelms-Universität Bonn

1. Gutachter: apl. Prof. Dr. Christiane Dahl
2. Gutachter: Prof. Dr. Uwe Deppenmeier

Tag der Promotion: 25. April 2012
Erscheinungsjahr: 2012

Meiner Familie

To my family

List of contents

I. Introduction 1

II. Materials and Methods 12

1. Chemicals and materials 12
   - 1.1. Chemicals 12
   - 1.2. Kits 12
   - 1.3. Enzymes 13
   - 1.4. Standards for DNA, RNA and protein gel electrophoresis 13
   - 1.5. Antibodies 13
   - 1.6. Other materials 13
2. Software and online tools 14
3. Bacterial strains, plasmids and primers 15
   - 3.1. Bacterial strains 15
   - 3.2. Plasmids 16
   - 3.3. Primers 17
4. Cultivation techniques 19
   - 4.1. Cultivation of *A. vinosum* strains 19
     - 4.1.1. RCV medium 19
     - 4.1.2. Modified Pfennig's medium 20
   - 4.2. Conservation of *A. vinosum* strains 21
   - 4.3. Cultivation of *E. coli* strains 21
     - 4.3.1. LB medium 21
     - 4.3.2. 2 x YT medium 21
   - 4.4. Preparation of competent *E. coli* cells 22
   - 4.5. Turnover of reduced sulfur compounds by *A. vinosum* wild-type and mutant strains 22
5. Methods in molecular biology: DNA 23
   - 5.1. DNA preparation 23
     - 5.1.1. Isolation of genomic DNA from *A. vinosum* 23
     - 5.1.2. Isolation of genomic DNA from *E. coli* 23
     - 5.1.3. Isolation of plasmid DNA 24
   - 5.2. Photometric determination of DNA concentration and purity 24
   - 5.3. *In vitro* amplification of DNA by PCR 24
     - 5.3.1. Standard PCR protocol 25
     - 5.3.2. Colony PCR 25
     - 5.3.3. Construction of digoxigenin-labelled DNA probes by PCR 26

5.3.4. Gene splicing by overlap extension 26
5.4. Electrophoretic separation of DNA 26
5.4.1. Agarose gel electrophoresis 26
5.4.2. Purification of DNA fragments from agarose gels 27
5.5. Enzymatic modification of DNA 27
5.5.1. DNA restriction digestion 27
5.5.2. Dephosphorylation by alkaline phosphatase 27
5.5.3. Purification of DNA after PCR or restriction digestion 28
5.5.4. Ligation 28
5.6. Cloning 28
5.6.1. Transformation of competent *E. coli* cells 28
5.7. Conjugative transfer of plasmid DNA from *E. coli* to *A. vinosum* 28
5.8. DNA-DNA hybridization 29
5.8.1. Southern transfer 29
5.8.2. Hybridization with digoxigenin-labelled DNA probes 29
5.8.3. Chemiluminescence detection 30
6. Methods in molecular biology: RNA 31
6.1. Isolation of RNA from *A. vinosum* 31
6.2. Photometric determination of RNA concentration and purity 32
6.3. Denaturating formaldehyde agarose gel electrophoresis 32
6.4. Quantitative real-time RT-PCR 32
6.4.1. Generation of RNA standards 33
6.4.2. Standard real-time RT-PCR protocol 33
6.4.3. Analysis of the melting temperature 34
7. Protein techniques 35
7.1. Production of recombinant protein in *E. coli* 35
7.2. Cell harvesting and disruption 35
7.3. Determination of protein concentration 36
7.3.1. BCA Protein Assay Reagent Kit 36
7.3.2. Modified Bradford method 36
7.4. Electrophoretic separation of proteins 36
7.4.1. SDS-PAGE 36
7.4.2. Coomassie staining 37
7.4.3. Silver staining 37
7.5. Western blot 38
7.6. Immunological detection methods 38
7.6.1. Colorimetric detection method 39

7.6.2. Chemiluminescent detection method 40
7.7. Desalting of protein solutions....40
7.7.1. Desalting of protein solutions by dialysis....40
7.7.2. Desalting of protein solutions by HiTrap Desalting Column....40
7.8. Concentration of protein solutions....41
7.9. Chromatography methods....41
7.9.1. Nickel-chelate affinity chromatography....41
7.9.2. Gel filtration chromatography....42
7.10. UV-visible absorption spectra....42
7.11. Removal of the His-tag by thrombin digestion....43
7.12. Iron- and iron-sulfur cluster-binding assay of DsrR....43
7.13. Coprecipitation....43
7.14. Electrophoretic mobility shift assay....44
7.15. β-Galactosidase assays....44
8. Analytical determination of sulfur compounds.... 45
8.1. Determination of thiols using HPLC....45
8.2. Determination of sulfate using HPLC....46
8.3. Determination of elemental sulfur....47
III. Results 48
1. Insights into the regulation of the *dsr* operon.... 48
1.1. Expression studies with reporter gene fusions....48
1.1.1. Construction of reporter gene fusion plasmids....49
1.1.2. Expression of *dsrA* under sulfur-oxidizing conditions....50
1.1.3. The time-course of *dsrA* expression under sulfur-oxidizing conditions....51
1.1.4. Inhibition of *dsrA* expression by malate and sulfite....52
1.2. Expression studies using real-time RT-PCR....53
1.2.1. Construction of gene-specific RNA standards....54
1.2.2. Expression of *dsr* genes in the wild-type and the mutants 21D and 34D....55
1.3. Electrophoretic mobility shift assays with the *dsrA* promoter region and DsrC....59
2. Characterization of the DsrR protein.... 62
2.1. Sequence analyses....62
2.2. Biochemical characterization of DsrR....65
2.2.1. Production and purification of recombinant DsrR protein....65

2.2.2. Testing of DsrR-specific antiserum and detection of DsrR in *A. vinosum* 66
2.2.3. State of oligomerization of DsrR....67
2.2.4. Iron and iron-sulfur cluster binding of DsrR 68
2.2.5. Solution structure of DsrR 70
2.2.6. Interaction of DsrR with other Dsr proteins....73
2.3. Physiological characterization of DsrR....75
2.3.1. Complementation of a *dsrR* deletion mutant....75
2.3.2. Phenotypical characterization of the complementation mutant ..76
2.3.3. Formation of Dsr proteins in the deletion and complementation mutant....78
2.4. Influence of the *dsrR* deletion on the expression of other *dsr* genes....79
2.4.1. Expression studies by real-time RT-PCR 80
2.4.2. Expression studies by reporter gene fusions....81
3. Characterization of the DsrS protein 84
3.1. Sequence analyses 84
3.2. Biochemical characterization of DsrS 89
3.2.1. Production and purification of recombinant DsrS protein....89
3.2.2. Testing of DsrS-specific antiserum and detection of DsrS in *A. vinosum* 90
3.2.3. State of oligomerization of DsrS....91
3.3. Physiological characterization of DsrS....92
3.3.1. Complementation of a *dsrS* deletion mutant....92
3.3.2. Phenotypical characterization of the complementation mutant ..93
3.3.3. Formation of Dsr proteins in the deletion and complementation mutant....95
3.4. Influence of the *dsrS* deletion on the expression of other *dsr* genes....96
3.4.1. Expression studies by real-time RT-PCR 97
3.4.2. Expression studies by reporter gene fusions....98
IV. Discussion....101
V. Summary 112
VI. References 113
VII. Publications 128
VIII. Acknowledgments 130

Abbreviations

Ap	ampicillin
APS	adenosine-5'-phosphosulfate
aa	amino acid(s)
bp	base pair(s)
BSA	bovine serum albumine
CDP-*Star*	disodium 2-chloro-5-(4-methoxyspiro {1,2-dioxetane-3,2'-(5'-chloro)tricyclo[3.3.1.13,7]decan}-4-yl) phenyl phosphate
CV	column volume
Da	Dalton
DEPC	diethyl dicarbonate
dig	digoxigenin
EDTA	ethylenediaminetetraacetate
g	earth acceleration / gravitational constant
HEPES	N-[2-hydroxyethyl]-piperazine-N´-[2-ethanesulfonic acid]
HPLC	high-performance liquid chromatography
IPTG	isopropyl-β-S-thiogalactoside
kb	10^3 bases
Km	kanamycin
MOPS	3-(N-morpholino)propanesulfonic acid
MWCO	molecular weight cut off
NMR	nuclear magnetic resonance
Ni-NTA	nickel-nitrilotriacetic acid
OD	optical density
ONPG	*o*-nitrophenyl-β-galactoside
PAGE	polyacrylamide gel electrophoresis
PAPS	3'-phosphoadenosine-5'-phosphosulfate
PCR	polymerase chain reaction
rbs	ribosome binding site
Rif	rifampicin
r.m.s.d.	root mean square deviation
rpm	rounds per minute
RT	room temperature
RT-PCR	reverse transcriptase-PCR
SDS	sodium dodecyl sulfate
Sm	streptomycin
TCEP	tris (2-carboxyethyl) phosphine
TEMED	tetramethylendiamine
T_a	annealing temperature
T_m	melting temperature
Tris	trishydroxymethylaminomethane
X-gal	5-bromo-4-chloro-3-indolyl-β-D-galactopyranoside

I. Introduction

The biological sulfur cycle

Sulfur is a highly versatile element due to its ability to occur in nine different oxidation states (ranging from -2 (sulfide) to +6 (sulfate)). Additionally, sulfur of the oxidation state zero tends to catenate, making sulfur the element with the largest number of known allotropes (Steudel, 2000). Geochemically, sulfur is quite abundant; it mainly occurs as sulfate or sulfide in water and soil and sulfur dioxide in the atmosphere (Brown, 1982; Middelburg, 2000). To all living organisms sulfur is essential as sulfur atoms are components of important biologically active molecules like amino acids, (poly)peptides, enzyme cofactors, antibiotics, sulfolipids, vitamins or carbohydrates (Brüser *et al.*, 2000; Dahl *et al.*, 2002).

Inorganic sulfur compounds can be assimilated and incorporated in the above mentioned organic sulfur compounds, or serve as electron donors or acceptors for energy-yielding processes. The sulfur atom is thus cycled between the oxidation states of -2 and +6 (Lens and Kuenen, 2001). The assimilatory reduction of sulfate is very common in prokaryotes, plants, and fungi, whereas the dissimilatory pathways are restricted to prokaryotes (Brüser *et al.*, 2000; Dahl *et al.*, 2008a).

The dissimilatory reduction of sulfate is carried out by a metabolically versatile, obligately anaerobic group of prokaryotes, including members of the δ-subdivision of the Proteobacteria (*e. g*. *Desulfovibrio*, *Desulfolobus*, *Desulfobacter*), the Gram-positive genus *Desulfotomaculum*, the Gram-negative genus *Thermodesulfobacterium*, and the archaean genus *Archaeoglobus* (Lens and Kuenen, 2001; Pereira *et al.*, 2011). Sulfate-reducing organisms are widespread in the anaerobic zones of a multitude of environments like soil, sediments, marine and fresh waters as well as the mouth and gut of many animals (Matias *et al.*, 2005). Sulfate is utilized as electron acceptor for anaerobic respiration, forming sulfide as final product. Organic compounds (*e.g.* lactate, ethanol, propionate) or molecular hydrogen serve as electron donors. Due to its extremely low redox potential, sulfate has to be activated prior to its reduction. The activation is catalyzed by the enyzme ATP sulfurylase and two ATP equivalents per sulfate molecule are expended, yielding adenosine-5'-phosphosulfate (APS). APS is reduced by the iron-sulfur flavoprotein APS reductase to sulfite, which is subsequently reduced by the dissimilatory sulfite reductase to the final product sulfide (Brüser *et al.*, 2000; Lens and Kuenen, 2001; Matias *et al.*, 2005). Most sulfite reductases are reported to contain iron-sulfur clusters and siroheme-[Fe_4S_4] coupled cofactors. In *Desulfovibrio vulgaris* and *Desulfovibrio gigas*, the non-catalytic subunit of sulfite reductase contains the iron-free form of siroheme, sirohydrochlorin (Oliveira *et al.*, 2008; Hsieh *et al.*, 2010). Siroamide, the amidated form of siroheme, has been described to be the cofactor in some dissimilatory sulfite reductases from *Desulfovibrio* species (Matthews *et al.*, 1995). Several

sulfate reducers, as well as members of the genus *Desulfuromonas* and many hyperthermophilic Archaea (*Pyrococcus*, *Desulfurococcus*, *Thermococcus*), are also able to utilize elemental sulfur as electron acceptor, reducing it to sulfide. Furthermore, some sulfur respirers can in addition use sulfite, thiosulfate, organic sulfoxides, inorganic polysulfides, and/or organic disulfanes as terminal electron acceptor (Dahl *et al.*, 2008a).

The ability to grow lithotrophically with reduced sulfur compounds is phylogenetically widespread (Ghosh and Dam, 2009). It occurs in organisms that reside in environments abundant with sulfide, like stratified water bodies, organic nutrient-rich anoxic sediments or hydrothermal vents. Most groups of phototrophic prokaryotes are able to utilize reduced sulfur compounds as electron donors for the photosynthetic CO_2 fixation (Brune, 1989; Brune, 1995b). Classic examples are green sulfur bacteria (*Chlorobiaceae*) and purple sulfur bacteria (*Chromatiaceae* and *Ectothiorhodospiraceae*). But even some members of the purple non-sulfur bacteria, the filamentous anoxygenic phototrophs (*Chloroflexaceae*) and a couple of the strictly anaerobic Gram-positive Heliobacteria (Bryantseva *et al.*, 2000) are able to utilize reduced sulfur compounds as electron donors. Also, certain Cyanobacteria species can perform anoxygenic photosynthesis at the expense of sulfide as electron donor (Brune, 1989; Shahak and Hauska, 2008). The classic non-taxonomical group of colorless sulfur bacteria describes the physiological group of non-photosynthetic prokaryotes that gain energy by oxidizing reduced sulfur compounds using either oxygen or nitrate as electron acceptor. The group encompasses bacteria (*Beggiatoa*, *Thiobacillus*, *Thiothrix*, *Thiomicrospira*, *Thioploca etc.*) as well as archaea (*e.g. Sulfolobus*, *Acidianus*) (Brüser *et al.*, 2000; Lens and Kuenen, 2001). Reduced sulfur compounds are also utilized as energy source by endosymbiontic chemoautotrophic sulfur bacteria associated with marine invertebrates (Cavanaugh *et al.*, 2006). The symbiotic bacteria utilize the energy gained by sulfur oxidation for CO_2 fixation and supply the invertebrate with reduced carbon. In return, the host provides the bacteria with sulfide and oxygen. Sulfide oxidizing properties were also proposed as an evolutionary holdover for eukaryotic mitochondria (Hildebrandt and Grieshaber, 2008; Theissen and Martin, 2008).

Reduced sulfur compounds, like sulfide, polysulfides, sulfur, sulfite, thiosulfate, and various polythionates are usually oxidized to sulfate. However, as there are various sulfur oxidation pathways, depending on the organism, different sulfur compounds are used as substrate, various intermediates may be formed and miscellaneous end products are produced (Brune, 1995b; Brüser *et al.*, 2000; Dahl *et al.*, 2008a; Ghosh and Dam, 2009). In some organisms, globules of polymeric, water-insoluble sulfur accumulate as an intermediary product during the oxidation. These sulfur globules are either deposited extracellularly, as is the case for the *Chlorobiaceae*, *Ectothiorhodospiraceae* and some thiobacilli, or intracellularly, inside the periplasm, as it occurs in *Chromatiaceae*, *Beggiatoa* species and chemotrophic sulfur-

oxidizing bacterial symbionts of marine invertebrates like *Riftia pachyptila* and *Calyptogena okutanii* (Dahl and Prange, 2006).

Allochromatium vinosum

The anoxygenic purple sulfur bacterium *Allochromatium vinosum* is a representative of the *Gammaproteobacteria* familiy *Chromatiaceae* (Imhoff *et al.*, 1998). The rod-shaped bacterium contains a vesicular photosynthetic membrane system. The natural habitats of *A. vinosum* are ponds and lakes with stagnant, sulfide-containing freshwater (Pfennig and Trüper, 1989; Imhoff *et al.*, 1998). Metabolically, *A. vinosum* is quite versatile. The bacterium grows phototrophically under anoxic conditions, but some strains of the species may also grow chemoautotrophically or mixotrophically under micro- to semioxic conditions (Kämpf and Pfennig, 1980). Reduced sulfur compounds like sulfide, thiosulfate, sulfur, and sulfite, as well as molecular hydrogen, formiate, acetate, propionate, pyruvate, fumarate, malate, and succinate can all be utilized as photosynthetic electron donors (Pfennig and Trüper, 1989). Sulfur of the oxidation state zero is formed as an obligatory intermediate during the oxidation of reduced sulfur compounds and stored in the form of highly refractile globules inside the cells. Sulfate is the ultimate oxidation product (Imhoff *et al.*, 1998). Photosynthetic CO_2 fixation is achieved via the reductive pentose phosphate pathway (Brune, 1989).

A. vinosum is one of the best researched purple sulfur bacteria. Its high metabolic flexibility and genetic accessability (Pattaragulwanit and Dahl, 1995) allow the creation of viable mutants with defects in sulfur metabolism. Therefore, *A. vinosum* represents the ideal organism for the investigation of oxidative sulfur metabolism in phototrophic sulfur bacteria.

Oxidative sulfur metabolism in *A. vinosum*

In phototrophic sulfur bacteria, the oxidation of reduced sulfur compounds to sulfate consists of three major steps (Trüper and Fischer, 1982; Trüper, 1984; Dahl and Trüper, 1994). At first, the above mentioned sulfur globules are formed as an obligate intermediate during the oxidation of sulfide or thiosulfate. This is followed by the oxidation of the intermediary stored sulfur to sulfite, and lastly by the formation of sulfate as end product that is excreted into the medium.

In *A. vinosum*, thiosulfate appears to be metabolized via two different pathways (Hensen *et al.*, 2006). Under acidic conditions, *A. vinosum* oxidizes two thiosulfate anions to tetrathionate catalyzed by thiosulfate dehydrogenase. Tetrathionate is not further metabolized (Hensen *et al.*, 2006; Denkmann, 2011). Thiosulfate is completely oxidized to sulfate via the second pathway. Here, the more reduced sulfane sulfur atom and the more oxidized sulfone sulfur atom of the thiosulfate molecule are processed differently. The sulfone sulfur atom is rapidly converted to sulfate and excreted, whereas the sulfane sulfur atom accumulates in

intermediary sulfur globules as zero-valent sulfur before it is further oxidized (Smith and Lascelles, 1966; Schedel and Trüper, 1980). The thiosulfate oxidation of the second pathway is strictly dependent on the presence of three periplasmic Sox proteins SoxXAK, SoxB, and SoxYZ (Hensen *et al.*, 2006; Lehmann, 2010). Homologous proteins have been described earlier for the chemotrophic sulfur oxidizer *Paracoccus pantotrophus* (Mittenhuber *et al.*, 1991; Friedrich *et al.*, 2001). In this organism, the Sox proteins SoxXA, SoxYZ, and SoxB together with SoxCD, which is missing in *A. vinosum*, form a periplasmic multienzyme complex that is responsible for the complete oxidation of thiosulfate to sulfate without forming sulfur deposits as intermediary product. SoxYZ has been identified as the substrate-binding molecule of the complex. SoxXA, a *c*-type cytochrome, is reduced while oxidatively coupling the sulfur compound to SoxYZ. SoxB has been proposed to act as thiol esterase or sulfate thiol hydrolase and is responsible for hydrolytic cleavage of a sulfate group from the bound sulfur substrate (Friedrich *et al.*, 2005). SoxCD oxidizes the remaining sulfane sulfur, acting as a sulfur dehydrogenase. Further action of SoxB releases a second sulfate molecule and thereby restores SoxYZ (Friedrich *et al.*, 2001).

In *A. vinosum* and the green sulfur bacterium *Chlorobaculum tepidum* SoxXA occurs in a tight complex together with the SoxXA binding protein SoxK, the product of the gene immediately downstream of *soxA* (Ogawa *et al.*, 2008; Lehmann, 2010). Also, as *A. vinosum* lacks SoxCD, the sulfane sulfur cannot be further oxidized to sulfate directly. It has been proposed that the sulfane sulfur is transferred from SoxYZ to sulfur globules in an as of yet unkown manner (Hensen *et al.*, 2006), though a possible candidate for a sulfur transferase is the rhodanese-like protein SoxL that is encoded immediately downstream of the *soxXAK* locus (Welte *et al.*, 2009).

Contrary to *P. pantotrophus*, the Sox proteins of *A. vinosum* are not involved in sulfide oxidation (Hensen, 2006). The mechanism of the oxidation of sulfide in *A. vinosum* is as of yet uncertain. The involvement of two enzymes has been considered. *In vitro*, the periplasmic FAD-containing flavocytochrome *c* catalyzes the electron transfer from sulfide to a variety of small *c*-type cytochromes. But in *A. vinosum*, flavocytochrome *c* is not essential for sulfide oxidation as a flavocytochrome-deficient mutant exhibited the same rates of sulfide oxidation as the wild-type (Reinartz *et al.*, 1998). The other candidate is the membrane-bound sulfide:quinone oxidoreductase (SQR) that could transfer the electrons from sulfide into the quinone pool of the membrane. The primary products of SQR *in vitro* are soluble polysulfides (Griesbeck *et al.*, 2002), which have been found in *A. vinosum* as an intermediary product of sulfide oxidation (Prange *et al.*, 2004). Although the enzyme has so far not been isolated, *A. vinosum* membranes exhibit SQR activity and the recent genome sequence of *A. vinosum* revealed two potential SQR encoding genes (Dahl, 2008; Weissgerber *et al.*, 2011).

The obligate, intermediary sulfur globules during the oxidation of thiosulfate or sulfide are formed by an unknown enzymatic mechanism. The periplasmic globules contain long chains of sulfur with organic residues at one or both ends (Prange *et al.*, 1999; Prange *et al.*, 2002) and are surrounded by an unimolecular envelope, consisting of three hydrophobic sulfur globule proteins that most likely possess only structural function (Schmidt *et al.*, 1971; Brune, 1995a; Pattaragulwanit *et al.*, 1998). The oxidative degradation of these sulfur deposits is one of the least understood areas of sulfur metabolism, as the process does not only involve the oxidation of the sulfur but must also include binding, activation, and transport of sulfur atoms into the cytoplasm. The enzyme identified as being essential for the oxidation of periplasmically stored sulfur is the cytoplasmic siroamide-containing reverse sulfite reductase. It has been proposed that the enzyme, in a reverse-action of the function of the homologous protein in sulfate-reducing prokaryotes, oxidizes sulfide to sulfite (Schedel *et al.*, 1979; Hipp *et al.*, 1997). The intermediary stored sulfur must therefore be reductively activated and transported through the membrane in an as of yet unknown manner, though the involvement of a perthiolic carrier molecule has been suggested (Dahl, 2008).

The last step of reduced sulfur compound oxidation in *A. vinosum* is the oxidation of sulfite to the end product sulfate. The mechanism of sulfite oxidation in phototrophic sulfur-oxidizing bacteria is still under debate, though two different pathways have been suggested. Sulfite can be oxidized to sulfate indirectly via the enzymes APS reductase and ATP sulfurylase. In a first step, APS is formed from sulfite and AMP by APS reductase. Subsequently, the AMP moiety of APS is transferred to pyrophosphate by ATP sulfurylase and sulfate is released (Dahl, 2008). Insertional gene inactivation experiments showed this pathway to be non-essential in *A. vinosum* (Dahl, 1996). Until recently, the main candidate for the alternative and most likely main pathway was the periplasmic molybdenum-containing sulfite dehydrogenase that catalyzes the direct oxidation of sulfite to sulfate (Dahl, 1996; Kappler, 1999; Sanchez *et al.*, 2001; Kappler and Dahl, 2001). Even though it has been shown that tungstate, a specific antagonist of molybdate, inhibits sulfite oxidation in *A. vinosum* (Dahl, 1996), the corresponding enzyme could not be isolated. The recently resolved genome sequence did not reveal potential sulfite dehydrogenase genes (Weissgerber *et al.*, 2011). It is unclear by which mechanism *A. vinosum* mainly catalyzes the oxidation of sulfite to the final product sulfate.

The *dsr* operon

The key enzyme for the oxidation of intermediary stored sulfur, the reverse-acting dissimilatory sulfite reductase, consists of two subunits in an $\alpha_2\beta_2$-configuration. The genes encoding the subunits were discovered in 1997 in *A. vinosum* (Hipp *et al.*, 1997). Since then, it has been found that the *d*issimilatory *s*ulfite *r*eductase (*dsr*) subunit genes, *dsrAB*, are

organized together with thirteen other genes in an operon (*dsrABEFHCMKLJOPNRS*) (Pott and Dahl, 1998; Pott-Sperling, 2000; Dahl *et al.*, 2005) (Figure I.1). The *dsr* gene cluster is the only gene region known to encode proteins responsible for the oxidation of intermediary stored zero-valent sulfur (Grimm *et al.*, 2008; Dahl, 2008; Frigaard and Dahl, 2009; Sander and Dahl, 2009).

The cytoplasmically located sulfite reductase DsrAB has been proposed to catalyze the six electron oxidation from sulfide to sulfite in a reaction reverse to that of the homologous enzymes of sulfate-reducing prokaryotes (Schedel *et al.*, 1979). The prosthetic group of DsrAB is siroamide-[Fe_4S_4], with siroamide being an amidated form of the classic siroheme. The *dsrN* encoded protein resembles cobyrinic acid *a,c*-diamide synthases and catalyzes the glutamine-dependent amidation of siroheme (Dahl *et al.*, 2005; Lübbe *et al.*, 2006). A *dsrN* deletion mutant showed a reduced sulfur oxidation rate, indicating that *A. vinosum* is capable of utilizing siroheme instead of siroamide as prosthetic group, thereby retaining some function of the enzyme (Lübbe *et al.*, 2006).

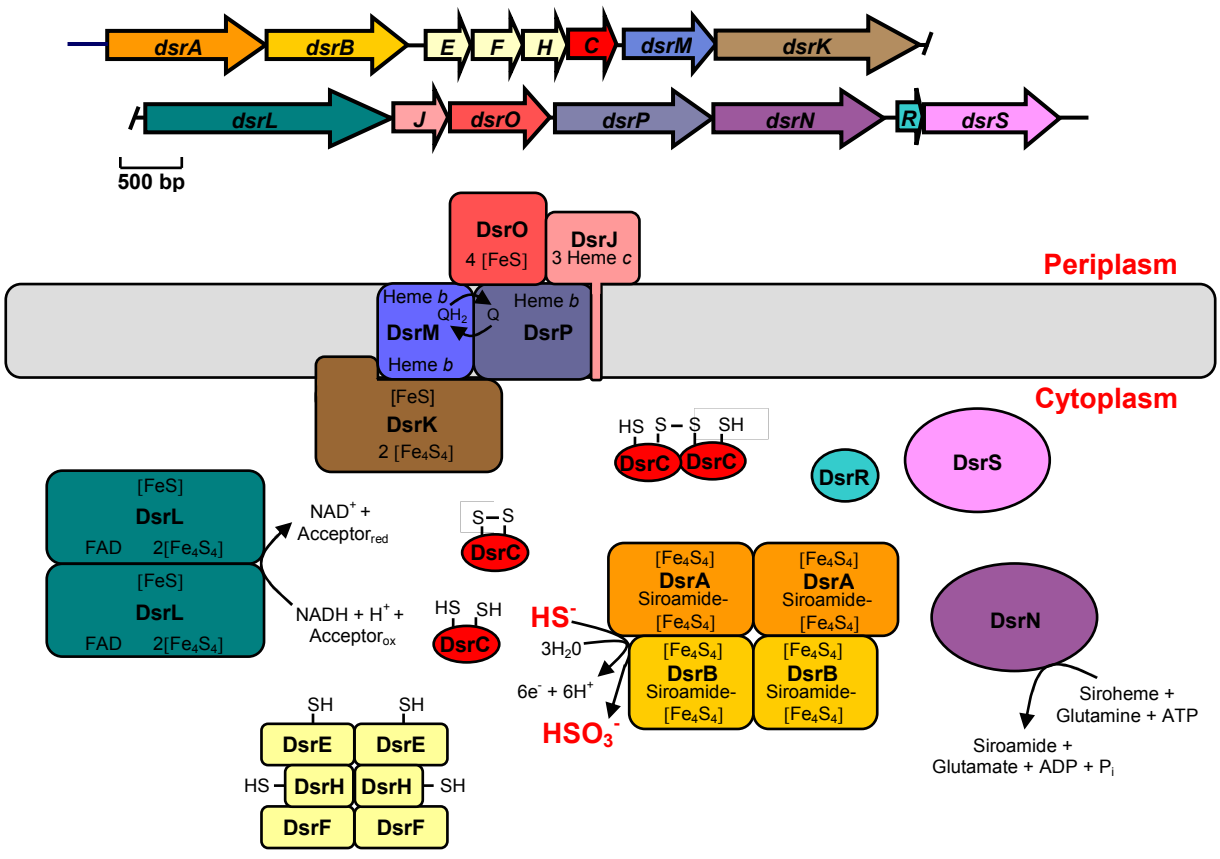

Figure I.1. Schematic representation of the *dsr* operon and its encoded proteins.

Downstream of *dsrAB*, the genes *dsrEFH* are located. The products of these three genes show significant similarity to each other and form a single tight complex with an $\alpha_2\beta_2\gamma_2$ structure. Conserved cysteine residues have been identified in DsrE and DsrH (Dahl *et al.*,

2005; Dahl *et al.*, 2008b). Adjacent to *dsrEFH*, the gene encoding DsrC is situated. DsrC is a small soluble cytoplasmic protein with a highly conserved, mobile C-terminal arm that contains two invariant cysteine residues. The protein occurs in a monomeric and dimeric configuration (Cort *et al.*, 2008). The crystal structure of sulfite reductases with bound DsrC of sulfate-reducing bacteria *Desulfovibrio vulgaris*, *Desulfovibrio gigas*, and *Desulfomicrobium norvegicum* showed the C-terminal arm of DsrC to be able to reach into the active site of the reductase (Oliveira *et al.*, 2008; Hsieh *et al.*, 2010; Oliveira *et al.*, 2011). Proteins closely related to DsrEFH and DsrC have been shown to act as parts of a sulfur relay system involved in thiouridine biosynthesis at tRNA wobble positions in *E. coli* (Ikeuchi *et al.*, 2006; Numata *et al.*, 2006). Taken together, these facts opened up the possibility that DsrEFH and DsrC could act as substrate donors to the reverse sulfite reductase DsrAB. DsrEFH could act as a cytoplasmic acceptor for the persulfide sulfur transported through the membrane. DsrC could accept a sulfur atom from DsrEFH and then present the sulfur bound to its flexible C-terminal arm immediately to the active site of DsrAB. The bound sulfur would be oxidized and DsrC would leave the sulfite reductase carrying a sulfonate group. Finally, sulfite could be reductively released by formation of a disulfide between the two conserved C-terminal cysteines of DsrC (Cort *et al.*, 2008).

The genes *dsrMKJOP* encode an electron-transporting transmembrane complex that is highly similar to the DsrMKJOP complex of sulfate-reducing prokaryotes which is responsible for the transfer of electrons to the sulfite reductase (Pires *et al.*, 2006). Individual in frame deletions of the *dsrMKJOP* genes lead to the complete inability of the mutants to oxidize stored sulfur (Sander *et al.*, 2006). DsrM is an integral membrane protein and contains two *b*-type cytochromes as prosthetic groups. The other integral membrane protein of the complex, DsrP, has also been identified as a *b*-type cytochrome. Both proteins might interact with the quinone pool of the membrane; while DsrM may work as a quinol oxidase donating electrons to DsrK, DsrP could act as a quinone reductase (Grein *et al.*, 2010a). The periplasmic protein DsrJ is a triheme *c*-type cytochrome. The signal peptide of the protein is not cleaved off but serves as membrane anchor. An involvement in the catalytic sulfur chemistry has been suggested for DsrJ (Grein *et al.*, 2010b). The *dsrO* encoded protein is a periplasmically located iron-sulfur cluster-containing protein (Dahl *et al.*, 2005). The cytoplasmic iron–sulfur protein DsrK is monotopically anchored in the membrane via an amphipathic α-helix. The protein exhibits relevant similarity to the catalytic subunit of (hetero)disulfide reductases and might represent the catalytic subunit of the complex (Dahl *et al.*, 2005). Interestingly, there is some evidence that DsrK interacts with DsrC (Grein *et al.*, 2010a).

It has been proposed that the electron flow through the DsrMKJOP complex of *A. vinosum* is analogous to that of sulfate-reducing prokaryotes (Grein *et al.*, 2010a). DsrJ could be involved in the oxidation of an unknown sulfur substrate in the periplasm. The released

electrons would then be transported via the iron-sulfur clusters of DsrO possibly to the heme *b* group(s) of DsrP. Since DsrP and DsrM are both quinone-interacting proteins, they could be connected via the quinone pool. DsrM would then donate electrons to DsrK, which could reduce the intramolecular disulfide formed by the conserved cysteines in DsrC to generate free thiols. This would enable DsrC to restart a cycle of sulfur transfer from DsrEFH to DsrAB.

The *dsrL* encoded protein is a cytoplasmic, homodimeric iron-sulfur flavoprotein with NADH:acceptor oxidoreductase activity. The protein carries a thioredoxin motif immediately preceding the carboxy-terminal iron-sulfur cluster binding sites that could indicate a potential disulfide reductase activity (Lübbe, 2005; Kammler, 2009). DsrL is co-purified together with DsrAB and an in frame deletion of *dsrL* completely stopped the oxidation of stored sulfur (Lübbe *et al.*, 2006). The exact role of DsrL in sulfur oxidation has so far not been elucidated, but several potential functions have been proposed. DsrL could use NADH as electron donor for the reduction of a di- or persulfidic compound. It could either be involved in the reductive release of sulfide from a perthiolic carrier molecule (Dahl *et al.*, 2005; Dahl, 2008) or it could be involved in the reduction of the intramolecular disulfide bond in DsrC (Cort *et al.*, 2008). However, a disulfide reductase activity could so far not be shown for DsrL (Kammler, 2009). Another possible function for DsrL is the transfer of electrons that have been gained by the oxidation of sulfide to sulfite, to NAD^+ thus forming NADH + H^+. The electrons could thereby become available to energy metabolism (Dahl *et al.*, 2005; Kammler, 2009).

Concerning the last two genes of the operon, *dsrR* and *dsrS*, almost nothing is known. The penultimate gene of the operon, *dsrR*, encodes a soluble cytoplasmic 11.4 kDa protein of unknown function. A gene homologous to *dsrR* was found in the *dsr* operon of the chemotrophic sulfur oxidizer *Thiobacillus denitrificans* (Pott-Sperling, 2000; Dahl *et al.*, 2005; Beller *et al.*, 2006a). An *A. vinosum dsrR* deletion mutant exhibited a severely affected oxidation of stored sulfur, implicating DsrR to be involved in the process (Grimm, 2004). DsrR exhibits a weak similarity to the A-type scaffold IscA, but lacks the highly conserved cysteine residues of this protein (Dahl *et al.*, 2005). A-type scaffolds are involved in the maturation of protein-bound iron-sulfur clusters (Johnson *et al.*, 2005; Ayala-Castro *et al.*, 2008). Iron-sulfur clusters are ubiquitous and evolutionary ancient prosthetic groups. The formation of intracellular iron-sulfur clusters does not occur spontaneously but requires a complex biosynthetic machinery. Three types of iron-sulfur cluster biosynthetic systems have been described. All of them have the requirement for a cysteine desulfurase and the participation of an iron-sulfur cluster scaffolding protein in common. Scaffold proteins provide an intermediate site for the assembly of iron-sulfur clusters or iron-sulfur cluster precursors. A well researched representative is the A-type scaffold IscA. IscA functions either as iron chaperone delivering iron ions to nascent iron-sulfur clusters built on the IscU scaffold (Ding

et al., 2005; Yang *et al.*, 2006), or as an alternative scaffold for [2Fe-2S] or [4Fe-4S] clusters (Ollagnier-de-Choudens *et al.*, 2001; Krebs *et al.*, 2001; Johnson *et al.*, 2005). The protein occurs as a mixture of oligomeric forms with dimer and tetramer predominating (Ollagnier-de-Choudens *et al.*, 2001). The monomers associate to form a dimer of dimers with a central channel within which the conserved cysteine residues, that are characteristic for A-type scaffolds, are presumed to form a "cysteine pocket" and where mononuclear iron or iron-sulfur cluster can be coordinated in a subunit bridging manner (Krebs *et al.*, 2001; Cupp-Vickery *et al.*, 2004; Bilder *et al.*, 2004).

DsrS, the protein encoded by the last gene of the *A. vinosum dsr* operon, is predicted to be a soluble cytoplasmic protein of the calculated molecular mass of 41.1 kDa (Dahl *et al.*, 2005). Neither conserved domains nor motifs could be detected and no significant similarities to proteins of known function could be identified. A homologous gene was found in *T. denitrificans*, though not as part of the *dsr* operon (Dahl *et al.*, 2005; Beller *et al.*, 2006a; Sander *et al.*, 2006). An *A. vinosum* Δ*dsrS* in frame deletion mutant appeared to be slightly affected in the oxidation of stored sulfur, suggesting DsrS to be involved in the process (Grimm, 2004).

Dissimilatory sulfite reductase and other Dsr proteins occur in sulfur-oxidizing bacteria as well as in sulfate-reducing prokaryotes (Hipp *et al.*, 1997; Dahl *et al.*, 2005; Sander *et al.*, 2006; Grimm *et al.*, 2008). Comparison of the *dsr* sequences showed that certain genes, *dsrABCNMKJOP*, represent a core unit, whereas other *dsr* genes are specific for either sulfur-oxidizing or sulfate-reducing prokaryotes. The genes *dsrEFH* and *dsrL*, for example, appear to be restricted to sulfur oxidizers. When the *dsr* sequences of just sulfur-oxidizing bacteria are compared, the genes *dsrABEFHCMKLJOPN* are revealed to be present in all sulfur-oxidizing bacteria that form sulfur globules as intermediate. Interestingly, the genes *dsrR* and *dsrS*, the last two genes of the *dsr* operon in *A. vinosum*, are not part of this common core *dsr* operon in sulfur-oxidizing bacteria, as they are absent in the green sulfur bacterium *Chlorobaculum tepidum* (Sander *et al.*, 2006).

Regulation of the *dsr* gene expression

Upstream of the coding region of *dsrA*, a putative promoter region has been identified. A potential transcriptional terminator, an inverted repeat with a potential for hairpin loop formation, was located downstream of *dsrS*, although the poly(T)-sequence usually located directly downstream of such hairpin loops in typical eubacterial rho-independent transcription terminators is lacking (Pott-Sperling, 2000; Dahl *et al.*, 2005). Downstream of *dsrS*, located on the complementary strand, an incomplete open reading frame homologous to *ruvB* is situated. RuvB is part of the RuvABC resolvasom which is involved in the dissolution of holliday junctions (Dahl *et al.*, 2005). Northern blot analysis confirmed the gene region as

transcriptional unit, showed a higher mRNA amount of the *dsr* genes under sulfur-oxidizing conditions and suggested a secondary promoter for the constitutively expressed *dsrC,* located in *dsrF* (Pott and Dahl, 1998; Dahl *et al.*, 2005).

Even though the genomes of several sulfur-oxidizing bacteria have recently been resolved, hardly any new information was gained concerning the expression of the *dsr* genes. In the chemotrophic sulfur-oxidizer *Thiobacillus denitrificans*, transcriptomic analysis showed the *dsr* genes to be highly and probably constitutively expressed (Beller *et al.*, 2006a; Beller *et al.*, 2006b). The metatranscriptomic analysis of the intracellular thioautotrophic symbionts of the coastal bivalve *Solemya velum* revealed the abundant transcription of genes from diverse pathways of sulfur energy metabolism, including *dsr* genes (Stewart *et al.*, 2011). Genes of the reverse Dsr pathway were among the most highly expressed in the symbiont meta-transcriptome and *dsrC* constituted the single most abundant sulfur gene. In the intracellular symbiont of the deep-sea bivalve *Calyptogena okutanii* the constitutive expression of *dsrAB* under variable environmental conditions (aerobic, semioxic, and aerobic under high pressure) has been shown (Harada *et al.*, 2009). Nothing is known about the expression of *dsr* genes in other sulfur-oxidizing bacteria.

Also, little is known about the expression of the *dsr* genes in sulfate-reducing prokaryotes. In *Desulfobacterium autotrophicum* and *Desulfovibrio vulgaris* the *dsr* genes are expressed constitutively but the mRNA content varied depending on the growth condition and growth phase of the culture (Neretin *et al.*, 2003; Keller and Wall, 2011). In *D. vulgaris* Hildenborough the expression of the *dsr* genes *dsrMKJOP* is downregulated under oxidative or nitrite stress or when the cells are grown on the alternative electron donor H_2 or the alternative acceptor thiosulfate, whereas the expression of the elsewhere located *dsr* genes *dsrABD* was not significantly affected (Haveman *et al.*, 2004; He *et al.*, 2006; Pereira *et al.*, 2008a; Pereira *et al.*, 2008b; Keller and Wall, 2011). It has been speculated that the down-regulation in the presence of nitrite or thiosulfate is due to the toxicity of sulfite at higher concentrations. Nitrite inhibits the sulfite reductase and thus may cause accumulation of sulfite, whereas sulfite is a product of the thiosulfate reduction (Haveman *et al.*, 2004; Pereira *et al.*, 2008a).

Proteins with a potential regulatory function in the expression of the *dsr* genes have not been identified. An interesting candidate might be DsrC, as the NMR-structure of DsrC from the sulfur-reducing archaeon *Pyrobaculum aerophilum*, as well as from *A. vinosum* revealed a putative DNA-binding motif (Cort *et al.*, 2001; Cort *et al.*, 2008).

Objective

Since the first description of the *dsr* operon of *A. vinosum*, research focused on the elucidation of the substrate delivery and electron flow during sulfur oxidation. Regulatory

aspects were scarcely considered. As part of this thesis, a closer examination was performed of the regulation of the *dsr* operon in the phototrophic sulfur-oxidizing bacterium *A. vinosum*. To this end, the expression of several *dsr* genes was investigated under organoheterotrophic and lithoautotrophic conditions and the potential DNA-binding ability of DsrC was tested.
Furthermore, whereas for most of the Dsr proteins at least a potential function has been identified, concerning the function of the proteins encoded by the last two genes of the operon, *dsrR* and *dsrS*, hardly anything is known. Therefore, the identification of potential functions of these two proteins was a further aim of this work. The *dsrR* and *dsrS* deletion mutant strains produced during my diploma thesis were extensively phenotypically characterized and the effects of the deletions on the expression of other *dsr* genes were examined. In case of DsrR, the similarity to the A-type scaffold IscA was investigated in depth in order to elucidate if DsrR could have a similar function. Also, the interaction of DsrR with other Dsr proteins was looked into.

II. Materials and Methods

1. Chemicals and materials

1.1. Chemicals

30 % acrylamide/bisacrylamide	Roth (Karlsruhe, Germany)
4-Chloro-1-naphthol	Sigma-Aldrich (Steinheim, Germany)
Anti-digoxigenin-AP	Roche (Mannheim, Germany)
Blocking reagent	Roche (Mannheim, Germany)
Bradford reagent	Sigma-Aldrich (Steinheim, Germany)
CDP-*Star*	Roche (Mannheim, Germany)
DEPC	Roth (Karlsruhe, Germany)
Developer	Kodak (Rochester, USA)
dig-dUTP	Roche (Mannheim, Germany)
Dithiothreitol (DTT)	Roth (Karlsruhe, Germany)
Fixer	Kodak (Rochester, USA)
p-Hydroxybenzoic acid	Sigma-Aldrich (Steinheim, Germany)
IPTG	Roth (Karlsruhe, Germany)
Methanesulfonic acid	Merck (Darmstadt, Germany)
Monobromobimane	Fluka (Taufkirchen, Germany)
ONPG	Fluka (Taufkirchen, Germany)
TCEP	Merck (Darmstadt, Germany)
4 x Rotiload 1	Roth (Karlsruhe, Germany)

All further chemicals were obtained from the companies Roth (Karlsruhe, Germany), Fluka (Taufkirchen, Germany), Sigma-Aldrich (Steinheim, Germany) and Merck (Darmstadt, Germany).

1.2. Kits

BCA Protein Assay Reagent Kit	Pierce (Rockford, USA)
First-DNA all-tissue Kit	GEN-IAL (Troisdorf, Germany)
GC-RICH PCR System	Roche (Mannheim, Germany)
PureLink Gel Extraction Kit	Invitrogen (Karlsruhe, Germany)
PureLink PCR Purification Kit	Invitrogen (Karlsruhe, Germany)
PureLink Quick Plasmid Miniprep Kit	Invitrogen (Karlsruhe, Germany)
QIAprep Spin Miniprep Kit	Qiagen (Hilden, Germany)
QIAquick Gel Extraction Kit	Qiagen (Hilden, Germany)
QuantiTect SYBR Green RT-PCR Kit	Qiagen (Hilden, Germany)
Riboprobe in vitro Transcription Systems	Promega (Madison, USA)
RNeasy Mini Kit	Qiagen (Hilden, Germany)
SuperSignal West Pico Chemiluminescent Substrate	Pierce (Rockford, USA)
Thrombin Cleavage Capture Kit	Novagen (Madison, USA)

1.3. Enzymes

Alkaline phosphatase (CIAP)	Fermentas (St. Leon-Rot, Germany)
Complete protease inhibitor cocktail, EDTA-free	Roche (Mannheim, Germany)
Desoxyribonuclease II	Roth (Karlsruhe, Germany)
Lysozyme	Fluka (Taufkirchen, Germany)
Pfu DNA polymerase	Fermentas (St. Leon-Rot, Germany)
Restriction enzymes	Invitrogen (Karlsruhe, Germany)
Restriction enzymes	Fermentas (St. Leon-Rot, Germany)
Ribonuclease A	Sigma-Aldrich (Steinheim, Germany)
RNase-free DNase	Qiagen (Hilden, Germany)
RNasin ribonuclease inhibitor	Promega (Madison, USA)
T4 DNA ligase	Fermentas (St. Leon-Rot, Germany)
Taq DNA polymerase	Fermentas (St. Leon-Rot, Germany)

1.4. Standards for DNA, RNA and protein gel electrophoresis

1 kb DNA ladder	Invitrogen (Karlsruhe, Germany)
100 bp DNA ladder	Invitrogen (Karlsruhe, Germany)
RiboRuler RNA Ladder High Range	Fermentas (St. Leon-Rot, Germany)
PageRuler Prestained Protein Ladder	Fermentas (St. Leon-Rot, Germany)

1.5. Antibodies

Dsr protein-specific antisera	Eurogentec (Seraing, Belgium)
DsrC-specific antiserum	Pott-Sperling (2000)
Goat Anti-Mouse IgG HRP conjugate	Novagen (Madison, USA)
Goat Anti-Rabbit IgG HRP conjugate	Sigma-Aldrich (Steinheim, Germany)
His-Tag Monoclonal Antibody	Novagen (Madison, USA)

1.6. Other materials

Anaerocult A + Anaerotest	Merck (Darmstadt, Germany)
Cellulose nitrate filter (conjugation)	Sartorius (Göttingen, Germany)
Centriplus Centrifugal Filter Device	Millipore (Schwalbach, Germany)
ABgene PCR Plates	Thermo Scientific (Karlsruhe, Germany)
Adhesive PCR Film	Thermo Scientific (Karlsruhe, Germany)
Dialysis tube (MWCO 6000, 8000 and 12000)	Serva (Heidelberg, Germany)
Gases (nitrogen, forming gas, carbon dioxide)	Air Products (Hattingen, Germany)
HiTrap Desalting Column	GE Healthcare (Munich, Germany)
GH Polypro hydrophilic polypropylene membrane filters (0.2 µm pore-size)	PALL Life Science (Dreieich, Germany)
Membrane filters (cellulose nitrate) (0.45 µm pore-size)	Whatman (Dassel, Germany)
Li-Chrospher 100 RP-18e (250-4.5 µm)	Merck (Darmstadt, Germany)
Ni-NTA Agarose	Qiagen (Hilden, Germany)
Polypropylene columns	Qiagen (Hilden, Germany)
Protran BA 85 cellulose nitrate membrane (Western blot)	Schleicher & Schuell (Dassel, Germany)
PRP-X100 (4.1 x 150 mm)	Hamilton (Bonaduz, Switzerland)
Roth nylon membrane (Southern hybridization)	Roth (Karlsruhe, Germany)
RNase AWAY	Roth (Karlsruhe, Germany)
Sterile syringe filter	Roth (Karlsruhe, Germany)
HiLoad 16/60 Superdex-75	GE Healthcare (Munich, Germany)
HiLoad 16/60 Superdex-200	GE Healthcare (Munich, Germany)
Whatman 3MM paper	Millipore (Schwalbach, Germany)
X-ray film X-OMAT AR	Kodak (Rochester, USA)

2. Software and online tools

Table II.1. Software and online tools

Software	Function	Source or reference
Adobe Photoshop CS Version 8.0.1	Image processing	Adobe Systems Incorporated
Agilent Technologies Software	Control software for 8453 Diode Array spectrometer	Agilent Technologies (Böblingen, Germany)
BLAST	Comparison of nucleotide or protein sequences with data bank entries	www.ncbi.nlm.nih.gov/BLAST
Clonemanager 5.03	Sequence processing	Scientific & Educational Software
ClustalW	Program for sequence alignments	www.ebi.ac.uk/clustalw/
DINAMelt Server	Tool for predicting the secondary structure of RNA and DNA	http://mfold.rna.abany.edu/?q=DINAMelt/Quickfold
INTAS GDS	Control and documentation software for the INTAS imaging instrument	INTAS (Göttingen, Germany)
Entrez	Sequence database	www.ncbi.nlm.nih.gov/ENTREZ
ExPasy	DNA and protein analysis	www.expasy.ch
IMG Homepage	Comparative analysis and annotation of all publicly available genomes	img.jgi.doe.gov
Microsoft Office 2002	Word, spreadsheet, and presentation processing	Microsoft Corporation
PC1000	HPLC control software	Thermo Electron (Dreieich, Germany)
Reference Manager Version 10	Database program to manage references	ISI ResearchSoft.
UV Winlab 2.80.03	Control software for UV/VIS spectrometer Lambda 11	Perkin-Elmer (Düsseldorf, Germany)
iCycler iQ software	Control software for iCycler iQ Real Time PCR Detection System	Bio-Rad (Munich, Germany)
REPuter	Computation of all duplications and reverse, complemented and reverse complemented repeats in a DNA sequence	bibiserv.techfak.uni-bielefeld.de/reputer
BPROM	A bacterial σ^{70} promoter recognition program	www.softberry.com/berry.phtml
Neural Network Promoter Prediction (NNPP)	Tool for the prediction of prokaryotic or eukaryotic promoter sites	www.fruitfly.org/seq_tools/promoter.html

3. Bacterial strains, plasmids and primers

3.1. Bacterial strains

Table II.2. Bacterial strains

Strains	Genotype or phenotype	Source or reference
Escherichia coli		
DH5α	F^-Φ80d *lacZ*ΔM15 Δ(*lacZYA-argF*) *U169 recA1 endA1 hsdR17* (r_K^- m_K^+) *supE44*λ^- *thi-1 gyrA relA1*	Hanahan (1983)
S17-1	294 (*recA pro res mod*$^+$) Tp^r Sm^r (pRP4-2-Tc::Mu-Km::Tn7)	Simon *et al.* (1983)
BL21(DE3)	F^-*ompT hsdS*$_B$ (r_B^- m_B^-) *gal dcm met* (DE3)	Novagen
K-12	Wild-type	DSM 498
Allochromatium vinosum		
Rif50	Rif^r, spontaneous rifampicin-resistant mutant of *A. vinosum* DSM 180^T	Lübbe *et al.* (2006)
21D	Sm^r, Km^r, *dsrB*::KmΩ	Pott and Dahl (1998)
34D	Sm^r, Km^r, *dsrH*::KmΩ	Pott and Dahl (1998)
ΔdsrR	Rif^r, *ΔdsrR* (264 bp deletion of *dsrR*)	Grimm (2004)
ΔdsrS	Rif^r, *ΔdsrS* (645 bp deletion of *dsrS*)	Grimm (2004)
ΔdsrR+*dsrR*	Rif^r, Km^r, complementation of *ΔdsrR* with plasmid pBBR*dsr*PT-*dsrR*	This work
ΔdsrS+*dsrS*	Rif^r, Km^r, complementation of *ΔdsrS* with plasmid pBBR*dsr*PT-*dsrS*	This work
Rif50+pTS	Rif^r, Km^r, plasmid pTS integrated into Rif50 genome	This work
ΔdsrR+pTS	Rif^r, Km^r, plasmid pTS integrated into *ΔdsrR* genome	This work
ΔdsrS+pTS	Rif^r, Km^r, plasmid pTS integrated into *ΔdsrS* genome	This work
Rif50+pTL	Rif^r, Km^r, plasmid pTL integrated into Rif50 genome	This work
ΔdsrR+pTL	Rif^r, Km^r, plasmid pTL integrated into *ΔdsrR* genome	This work
ΔdsrS+pTL	Rif^r, Km^r, plasmid pTL integrated into *ΔdsrS* genome	This work

3.2. Plasmids

All plasmids containing inserts were confirmed by DNA sequencing by Sequiserve (Vaterstetten, Germany) or GATC (Konstanz, Germany).

Table II.3. Plasmids

Plasmids	Genotype	Source or reference
pET-15b	Ap^r, His-Tag (N-terminal)	Novagen (Madison, USA)
pET-22b	Ap^r, His-Tag (C-terminal)	Novagen (Madison, USA)
pETCEX	Ap^r, *Nde*I–*Bam*HI fragment of *dsrC* in pET-15b	Cort *et al.* (2008)
pETEFH	Ap^r, *Nde*I–*Xho*I fragment of *dsrEFH* in pET-15b	Dahl *et al.* (2007)
pNREX	Ap^r, *Nde*I–*Xho*I fragment of *dsrNR* in pET-15b	This work
pREX	Ap^r, *Nde*I–*Xho*I fragment of *dsrR* in pET-15b	This work
pDsrS-N	Ap^r, *Nde*I–*Xho*I fragment of *dsrS* in pET-15b	This work
pDsrS-C	Ap^r, *Nde*I–*Xho*I fragment of *dsrS* in pET-22b	This work
pTISCA	Km^r, *Nde*I-*Blp*I fragment of *iscA* in pET-28b	Ding and Clark (2004)
pBBR1MCS-2	Km^r, *lacZ*', Mob^+	Kovach *et al.* (1995)
pBBR*dsr*PT1	Km^r, *Xba*I–*Hin*dIII fragment of PCR-amplified and fused *dsrA* promoter and *dsr* terminator in pBBR1MCS-2	This work
pBBR*dsr*PT-*dsrR*	Km^r, *Nhe*I-*Xma*JI fragment of PCR-amplified *dsrR* in pBBR*dsr*PT1	This work
pBBR*dsr*PT-*dsrS*	Km^r, *Nhe*I-*Xma*JI fragment of PCR-amplified *dsrS* in pBBR*dsr*PT1	This work
pK18*mobsacB*	Km^r, *lacZ*', *sacB*, Mob^+	Schäfer *et al.* (1994)
pKdsrProm	Km^r, *EcoRI-PstI* fragment of PCR-amplified *dsrA* promoter without *rbs* of *dsrA* in pK18*mobsacB*	This work
pTS	Km^r, *Pst*I-*Hin*dIII fragment of PCR-amplified *lacZ* including *rbs* in pKdsrProm	This work
pPHU235	Tc^r, broad-host-range *lacZ* fusion vector	Hübner *et al.* (1991)
pK235	Km^r, *Sal*I-*Eco*RI fragment of promoterless *lacZ* of pPHU235 ligated in *Hin*dIII-*Eco*RI pK18*mobsacB*	Franz (2010)
pTL	Km^r, *Pst*I-*Hin*dIII fragment of PCR-amplified *dsrA* promoter including the first 12 bp of *dsrA* in pK235	This work

3.3. Primers

All primers were obtained from MWG-Biotech AG (Ebersberg, Germany).

Table II.4. Primers. Restriction sites are marked bold, the T7 promoter is underlined.

Primers	Sequence (5'→ 3')	Source
***dsrR* for cloning in pET-15b**		
DsrRNdef1	AATGGAGT**CATATG**ATGTTCAAGCTGACA	This work
DsrRXhor1	CATGATCCG**CTCGAG**CGATCAGCCGC	This work
***dsrNR* for cloning in pET-15b**		
NEXf	GCCGCCCT**CATATG**GCGTCGCTCTA	Lübbe (2005)
***dsrS* for cloning in pET-15b**		
DsrSNdef1	TGTCCGG**CATATG**GACCTCAGTCACGAG	This work
DsrSXhor3	ATCGACGC**CTCGAG**CTAATCCCGGTCC	This work
***dsrS* for cloning in pET-22b**		
DsrSXhor2	ACGCCAG**CTCGAG**ATCCCGGTCCGCGAT	This work
Complementation		
PromDsrHindf1	TCACTGCC**AAGCTT**GAAGACGGAATCGGCG	This work
PromDsrNher1	ATCGACGCCCTAGGCTATGC**GCTAGC**TCTCCTATC	This work
TermDsrXmaJf2	GATAGGAGAGCTAGCGCATAG**CCTAGG**GCGTCGAT	This work
TermDsrXbar1	AGATCTG**TCTAGA**ATCGTGCAACGCTCAGC	This work
DsrRNhef1	TCAATAGG**GCTAGC**ATGATGTTCAAGCTGAC	This work
DsrRXmaJr1	ATGATCCG**CCTAGG**CGATCAGCCGCCG	This work
DsrSNhef1	GCGTGTC**GCTAGC**ATGGACCTCAGTCA	This work
Transcriptional and translational gene fusion		
GfdsrPromf2	CTGC**GAATTC**TGAAGACGGAATC	This work
GfTKdsrProm2	CTCCT**CTGCAG**ATAACCAGGAACG	This work
lacZrbsf1	ACAAT**CTGCAG**CAGGAAACAGCTATG	This work
lacZrbsr1	GCGA**AAGCTT**GCAGACATGGCC	This work
GfdsrPromf1	CTGC**CTGCAG**TGAAGACGG	This work
TLGfdsrPromr1	GTCTC**AAGCTT**GTCGATAGCC	This work

Table II.4. Primers (continued). Restriction sites are marked bold, the T7 promoter is underlined.

Primers	Sequence (5'→ 3')	Source
RT-PCR		
RNAdsrAf1	CGTTCAAGAAGCTGGAGACC	This work
RNAdsrAr1	ATCCATGCGGATGTAGGAAC	This work
RNAdsrEf1	CCGGGTCTTCTTCTATCACG	This work
RNAdsrEr1	GAATTTGGGATGGATGTTGG	This work
RNAdsrCf1	GGAGGGCTATCTCTCCAACC	This work
RNAdsrCr1	CTTCTCCTTGCCGAGCTTCT	This work
RNAdsrLf1	GAACACGTCTGGGACAACCT	This work
RNAdsrLr1	ATACTCCTGCCAGTCCATGC	This work
RNAdsrRf1	CCGATGGAAGCATCGATTAC	This work
RNAdsrRr1	CCTGGGATTGAGGAAGATGA	This work
RNAdsrSf2	GGTATCCGGTCTATCTCAGC	This work
RNAdsrSr2	TTGCCGGCGTCCTCCATC	This work
StandarddsrAf1	TAATACGACTCACTATAGGGCCGCCAGTACTACATCGACA	This work
StandarddsrAr1	CAGTGTGAAGACGTCGAGGA	This work
StandarddsrEf1	TAATACGACTCACTATAGGGCATGATCGAACGACAATCCA	This work
StandarddsrEr1	GAGCTGGTAGACACCGTCGT	This work
StandarddsrCf1	TAATACGACTCACTATAGGGGAATCCTGCCTGAAGTTTGC	This work
StandarddsrCr1	CGGCGAAATAGAACAGGAAG	This work
StandarddsrLf1	TAATACGACTCACTATAGGGCGATCCGAACGAAGAAGAAG	This work
StandarddsrLr1	GTCTTGAGCCTGACCTCGAC	This work
StandarddsrRf1	TAATACGACTCACTATAGGGAGTTTCATCATTCGGCCATC	This work
StandarddsrRr1	GGTATTGGGATTGAGCTGGA	This work
StandarddsrSf1	TAATACGACTCACTATAGGGTCCAGCTCAATCCCAATACC	This work
StandarddsrSr1	GGATCAGAGGACGGGAAGTC	This work
Miscellaneous primers		
Kmfor1	GGCTATGACTGGGCA	This work
Kmrev2	AGCGGCGATACCGTA	This work

4. Cultivation techniques

4.1. Cultivation of *A. vinosum* strains

A. vinosum cultures were grown under anaerobic conditions in the light (1000-2000 lux) at 30°C. Plates were cultivated within an anaerobic jar (Anaerocult A, Merck, Darmstadt, Germany). Antibiotics were added as needed in the following concentrations: rifampicin 50 µg mL^{-1}, kanamycin 10 µg mL^{-1}.

4.1.1. RCV medium

Photoorganoheterotrophic growth of *A. vinosum* strains was achieved utilizing RCV medium of Weaver *et al.* (1975) modified by trace element solution SL 12 (Overmann *et al.*, 1992). 5 % (v/v) of solution A (20 x RÄH) was mixed with 0.05 % (w/v) yeast extract and 0.19 % (w/v) NaOH. The pH value was adjusted to pH 7.0 and the solution was bottled in screw-capped glass bottles and autoclaved. After cooling, 5 % (v/v) sterile solution B (20 x PPB) was added. For conjugational uses, the RCV medium was solidified by the addition of 1.5 % (w/v) agar.

RCV medium:

Solution 1 (20 x RÄH):

Malate	60	g
NH_4Cl	24	g
$MgSO_4$ x 7 H_2O	2	g
$CaCl_2$ x 2 H_2O	0.7	g
10 x trace element solution SL12	20	mL
H_2O_{demin}	ad 1000	mL

SL 12 (10 x trace element solution):

EDTA-Na_2 x 2 H_2O	3.0	g
$FeSO_4$ x 7 H_2O	1.1	g
$ZnCl_2$	42	mg
$MnCl_2$ x 4 H_2O	50	mg
H_3BO_3	300	mg
$CoCl_2$ x 6 H_2O	190	mg
$CuCl_2$ x 2 H_2O	2	mg
$NiCl_2$ x 6 H_2O	24	mg
Na_2MoO_4 x 2 H_2O	18	mg
H_2O_{demin}	ad 1000	mL

Solution 2 (20 x potassium phosphate buffer PPB):

K_2HPO_4	180	mM
KH_2PO_4	180	mM
	pH 7.0	

The unsterile solutions were stored at 4°C.

RCV-phytagel plates:

RCV-phytagel plates were used for cultivation of *A. vinosum* strains on solid medium. For solidification of the RCV medium 1 % (w/v) phytagel was added, as well as 0.5 % (w/v) NaCl to aid gelling and 0.02 % (w/v) $Na_2S_2O_3 \times 5\ H_2O$, 2 mM sodium acetate and 2.6 mL feeding solution for growth enhancement. The plates were used directly after solidification and were always freshly prepared.

Feeding solution:

HNaS x H_2O	3.1	g
$NaHCO_3$	5.0	g
H_2O_{demin}	ad 100	mL

The solution was sterilized and stored in the dark at RT.

4.1.2. Modified Pfennig's medium

Photolithoautotrophic growth was achieved by using a modified Pfennig's medium (Trüper and Pfennig, 1992; Dahl *et al.*, 2008b). The medium, also called 0 medium due to the lack of sulfide, was prepared in a 10 L container with three openings at the top and one at the bottom. Sterile solutions were added through an opening at the top that also served as gas-outlet. Through the other two openings, tubes led into the container: one short, N_2- and a longer CO_2-inlet tube, both with sterile cotton filters. The bottom outlet was connected to a rubber tube with a pinchcock and a bell for aseptic dispensing of the medium into bottles. The medium consisted of three solutions that were autoclaved separately. After cooling, solution 2 and 3 were added to solution 1 under stirring and nitrogen atmosphere. The medium was saturated with CO_2 by stirring under CO_2 atmosphere till the opaque medium cleared up. The pH value was adjusted to pH 6.6 to 6.7 to prevent the carbonate from precipitating. The medium was distributed aseptically into 1000 mL screw-capped bottles, using a positive N_2 gas pressure. The tightly sealed bottles could be stored for several weeks in the dark. Reduced sulfur compounds were added with the inoculum.

Modified Pfennig's medium:

Solution 1:

KCl	3.3	g
$MgCl_2$ x 6 H_2O	3.3	g
$CaCl_2$ x 2 H_2O	4.3	g
NH_4Cl	3.3	g
SL 12	10	mL
H_2O_{demin}	ad 8000	mL

Solution 2:

KH_2PO_4	3.3	g
H_2O_{demin}	ad 1000	mL

Solution 3:

$NaHCO_3$	15	g
H_2O_{demin}	ad 1000	mL

4.2. Conservation of *A. vinosum* strains

For long-term conservation, *A. vinosum* strains were stored in liquid nitrogen. 100 mL of a four days old, well-grown, photoorganoheterotrophic culture were harvested by centrifugation (4000 ***g***; 10 min). The supernatant was discarded and the cells were resuspended in 6 mL fresh medium. The cells were mixed with an equal volume of sterile 10 % (v/v) dimethylsulfoxide (DMSO), transferred to 2 mL cryo tubes (CryoTubes, Nunc) and placed in liquid nitrogen.

4.3. Cultivation of *E. coli* strains

E. coli strains were cultivated aerobically at 37°C if not mentioned otherwise. In case of liquid medium the cultures were agitated at 180 rpm (shaker-incubator HT I FORS AI 70, INFORS, Bottmingen, Germany) to guarantee sufficient aeration. Antibiotics were used at the following concentrations: ampicillin 100 µg mL^{-1}, kanamycin 50 µg mL^{-1}.

4.3.1. LB medium

LB (lysogeny broth) medium (Sambrook *et al.*, 1989; Bertani, 2004) was the main medium for *E. coli* cultivation. LB medium was solidified by the addition of 1.5 % (w/v) agar. 0.3 mM IPTG and 80 µg mL^{-1} X-gal (dissolved in N,N-dimethylformamide) were included in solid media to identify recombinant plasmids containing inserts in the α-portion of *lacZ* .

LB medium:

Tryptone	10	g
Yeast extract	5	g
NaCl	5	g
H_2O_{demin}	ad 1000	mL
	pH 7.5	

4.3.2. 2 x YT medium

E. coli cells intended to be made competent were cultivated in 2 x YT medium (Sambrook *et al.*, 1989).

2 x YT medium:

Tryptone	16	g
Yeast extract	10	g
NaCl	5	g
H_2O_{demin}	ad 1000	mL
	pH 7.0	

4.4. Preparation of competent *E. coli* cells

E. coli cells were prepared for the reception of plasmid DNA using the $CaCl_2$ method of Dagert and Ehrlich (1974). 5 mL of 2 x YT medium inoculated with *E. coli* were incubated over night in a shaker-incubator. 700 µL of this starting culture was used to inoculate 70 mL 2 x YT medium. The culture was incubated in a shaker-incubator until an optical density at 600 nm (OD_{600}) of 0.3-0.5 was reached. The cells were harvested in sterile tubes (4000 ***g***, 6 min, 4°C) and were resuspended in 21 mL 70 mM $CaCl_2$/20 mM $MgSO_4$ solution. Following a 30-45 min incubation on ice, the cells were sedimented by centrifugation (4000 ***g***, 10 min, 4°C) and resuspended in 7 mL 70 mM $CaCl_2$/20 mM $MgSO_4$ solution. After the cells were cooled on ice for 30-45 min, 1750 µL sterile glycerin was added and the cells were stored in 250 µL aliquots at -70°C.

4.5. Turnover of reduced sulfur compounds by *A. vinosum* wild-type and mutant strains

The turnover of reduced sulfur compounds by *A. vinosum* wild-type and mutant strains was examined in batch culture under continuous illumination in a medium containing sulfide as the sole sulfur compound. 250 mL of a photoheterotrophically grown stationary-phase culture were harvested (14000 ***g***, 10 min) and the sedimented cells were resuspended in a small amount of fresh modified Pfennig's medium (*cf.* II.4.1.2). The cell material was used to inoculate 1 L of modified Pfennig's medium in a thermostatted fermenter under constant positive N_2 gas pressure. The experiment was started by injecting 2 mM sulfide from a 1 M sterile stock solution (7.4 g HNaS x H_2O (Fluka, Taufkirchen, Germany) ad 100 mL H_2O_{demin}) through a septum into the culture. A nitrogen filled balloon with a sterile cotton filter was attached to the fermenter to provide anaerobic conditions throughout the experiment. A pH electrode (SteamLine SL 80-325pH, Schott, Mainz, Germany) attached to a controlling unit (pH-mV controlling unit M7832, Mostec, Liestal, Switzerland) constantly measured the pH value of the culture. The pH value was adjusted to pH 7.0 by the addition of appropriate amounts of sterile 1M HCl and 1M Na_2CO_3 solutions injected through a septum into the culture. Spotlight lamps (60 Watt, Osram) were positioned on each side of the fermenter at approx. 40 cm distance. A water bath (Lauda M3/MT, MWG, Laude-Königshofen, Germany) connected to the fermenter kept the temperature at a constant 30°C. Sedimentation of the cells was prevented by a magnetic stirring rod. A sampling tube reaching to the bottom of the fermenter enabled sterile sampling. During the course of the experiment samples were taken to determine the optical denstiy at 690 nm, the concentration of sulfur compounds, the β-galactosidase activity if applicable and the protein concentration of the culture. After completion of the experiment the culture was harvested by centrifugation (14000 ***g***, 30 min) and the sedimented cells were stored at -20°C until further use.

5. Methods in molecular biology: DNA

5.1. DNA preparation

5.1.1. Isolation of genomic DNA from *A. vinosum*

Genomic DNA from *A. vinosum* strains was isolated using the sarcosyl lysis method based on Bazaral and Helsinki (1968).

Solutions

TE buffer	10 mM Tris-HCl, 1mM EDTA pH 8
TES buffer	100 mM NaCl, 10 mM Tris-HCl, 1 mM EDTA pH 8
Sucrose-TES buffer	20 % (w/v) sucrose in TES buffer
Lysozyme-RNase solution	20 mg mL^{-1} lysozym, 1 mg mL^{-1} RNase
Sarcosine solution	10 % (w/v) laurylsarcosine, 250 mM EDTA

Cells of a well-grown *A. vinosum* liquid culture were harvested by centrifugation (2500 ***g***, 10 min). The supernatant was discarded and the sedimented cells were washed in 50 mM Tris-HCl (pH 8). The cell pellet was stored at -20°C until further use. 80-100 mg of the cell material were transferred into a sterile tube and resuspended in 2 mL ice-cold TES buffer. Following centrifugation (14000 ***g***, 10 min, 4°C) the supernatant was discarded and the pellet was resuspended in 250 µL sucrose-TES buffer. The mixture was cooled on ice for 30 min. After the addition of 250 µL lysozyme-RNase solution the preparation was incubated for 1 h at 37°C in a water bath. 100 µL sarcosine solution was added and the reaction tube was gently inverted several times to mix. Following shearing of the DNA by passing the preparation several times through a sterile cannula (1.2 x 40 mm), 300 µL sterile H_2O_{demin} was added. Proteins were removed by phenol-chloroform-isoamylalcohol extraction. An equal volume of phenol-chloroform-isoamylalcohol (25:24:1) was added and the tube was vortexed until the mixture was homogenous. The tube was centrifuged (14000 ***g***, 5 min) and the aqueous phase was carefully transferred to a new sterile tube. The process was repeated at least twice more before a chloroform-isoamylalcohol extraction was performed to remove traces of phenol. Chloroform-isoamylalcohol (24:1) was added in equal volume to the DNA containing solution. After centrifugation (14000 ***g***, 5 min) the aqueous phase was transferred into a dialysis tube (MWCO 12000, Serva, Heidelberg, Germany). The DNA solution was dialysed against 1 L TE buffer (3 h and 15 h, respectively) and against 1 L of sterile $H_2O_{ultra\text{-}pure}$ (2 h) before it was transferred in a sterile reaction tube. The DNA was stored at 4°C.

5.1.2. Isolation of genomic DNA from *E. coli*

Genomic DNA from *E. coli* was isolated using the First-DNA all-tissue Kit (GEN-IAL, Troisdorf, Germany) following the manufacture's instructions. The DNA was dissolved in 50 µL TE buffer (10 mM Tris-HCl, 1 mM EDTA, pH8.0) and stored at 4°C.

5.1.3. Isolation of plasmid DNA

Plasmid DNA from *E. coli* was isolated using the QIAprep Spin Miniprep Kit (Qiagen, Hilden, Germany) or PureLink Quick Plasmid Miniprep Kit (Invitrogen, Karlsruhe, Germany) following the manufacturers' instructions. 5 mL overnight cultures of plasmid-containing *E. coli* in LB medium were subjected to plasmid isolation. The DNA was eluted in 50 µL sterile water and stored at -20°C.

5.2. Photometric determination of DNA concentration and purity

The concentration and purity of DNA solutions was determined by UV-visible spectroscopy. Nucleic acids exhibit an absorption maximum at 260 nm. At this wavelength, an absorption value of 1.0 corresponds to 50 µg mL^{-1} double stranded DNA (Sambrook *et al.*, 1989). In order to determine the purity of the DNA solution, the absorption at 280 nm, the absorption maximum of proteins, was measured. The ratio of the two wavelengths (A_{260}/A_{280}) should be between 1.8 and 2.0. Higher values indicate a contamination with RNA, lower values hint at a contamination with proteins or phenol. The measurements were performed with UV/VIS spectrometer Lambda 11 (Perkin-Elmer, Düsseldorf, Germany).

5.3. *In vitro* amplification of DNA by PCR

The polymerase chain reaction (PCR) permits the specific enzymatic amplification of DNA *in vitro* (Saiki *et al.*, 1985; Mullis *et al.*, 1986; Saiki *et al.*, 1986; Embury *et al.*, 1987). Short, single-stranded DNA fragments serve as starting oligonucleotides for DNA replication by thermostable DNA polymerases. These primers are complementary to the 3'- and 5'-end of the DNA template, respectively, and the 3'-ends of the primers are oriented towards each other. The cyclic repetition of primer annealing to the DNA, primer elongation by DNA polymerase and denaturing of the product leads to an exponential increase in the amount of specific DNA. Optimal annealing of primers to the target sequence was achieved by considering following points: a primer should consist of 18 to 28 bp, the GC content should be within the range of 50-60 % or be adjusted to the GC content of the target sequence, primers should not contain palindromes and multiple base repeats should be avoided. In addition it is advantageous to choose a primer pair with comparable to identical melting temperatures (T_m). The T_m was calculated using the following formulas: sequences with 15 or less bases: T_m [°C] = 2 (n_A + n_T) + 4 (n_C + n_G), where n is the number of the respective bases; sequences with more than 15 bases: T_m [°C] = 69.3 + 41 (n_G + n_C)/s – 650/s, where s is the total number of bases. The optimal annealing temperature T_a should be 2-5°C below the lowest melting temperature (ideally between 55°C and 70°C). Restriction sites were introduced into PCR amplicons by modified primers. The restriction site sequence was added to the 5'-end of the primer and capped by 4-7 further bases. The thermostable DNA polymerases from *Thermococcus aquaticus* (*Taq*) or from *Pyrococcus furiosus* (*Pfu*) were

used to amplify DNA. Contrary to the *Taq* polymerase, the *Pfu* polymerase is able to proof-read the newly synthesized DNA sequence by 3'-5' exonuclease activity, decreasing the rate of falsely integrated nucleotides at the cost of a slower amplification rate. Sequences intended for cloning purposes were therefore amplified by *Pfu* polymerases, whereas all other PCRs were performed using the *Taq* polymerase.

5.3.1. Standard PCR protocol

A standard PCR was carried out in a total volume of 25 µL or 50 µL in 0.2 or 0.5 mL sterile PCR tubes. The PCRs were performed using an iCycler by Bio-Rad (Munich, Germany) or a Biometra TRIO-Thermoblock (Göttingen, Germany). In the latter case, the PCR mixture was overlaid with mineral oil to avoid evaporation. A standard reaction contained the following components:

Standard PCR:

Polymerase-specific buffer	1 x
Forward primer	12.5-50 pmol
Reverse primer	12.5-50 pmol
Nucleotides (dATP, dTTP, dCTP, dGTP)	200 µM each
DNA template	0.1-0.5 µg
Taq polymerase	2.5 U
or *Pfu* polymerase	1.25 U
Sterile $H_2O_{ultra\text{-}pure}$	ad 50 µL

$MgCl_2$ (0.5-2.5 mM) was added to preparations with *Taq* polymerase. In case of *Pfu* polymerase, $MgSO_4$ was already included in the polymerase specific buffer.

Standard PCR program:

1.	Initial denaturation	95°C	3 min
2.	Denaturation	95°C	30 s
3.	Primer annealing	T_a	30 s
4.	Elongation	72°C	*
5.	Repeat steps 2. to 4.		25-35 x
6.	Final elongation	72°C	5 min
7.	Storage	4°C	hold

*Elongation time is dependent on the size of the amplicon and the speed of the applied DNA polymerase. *Taq* polymase: 1 min kb^{-1}; *Pfu* polymerase: 2 min kb^{-1}.

5.3.2. Colony PCR

Colony PCR was used as a fast detection method for recombinant cells. The DNA of the cells was not purified prior to PCR but whole cells were added to the PCR mixture instead. 100 µL liquid culture was centrifuged (13000 ***g***, 3 min), the sedimented cells were washed in 100 µL sterile water and resuspended in 50 µL sterile $H_2O_{ultra\text{-}pure}$. Alternatively, the cell material of one colony was resuspended in 50 µL sterile $H_2O_{ultra\text{-}pure}$. The cell material was stored at -20°C. 1-2 µL of the thus prepared cell material was used as template in PCR. The initial denaturation time was increased to 10 min in order to ensure cell breakage. *Taq* polymerase was added after this step was completed.

5.3.3. Construction of digoxigenin-labelled DNA probes by PCR

DNA fragments to be utilized as probes in DNA-DNA hybridization experiments (Southern hybridization) were labelled for later detection. Digoxigenin-dUTP (20 µM) was added to the PCR mixture and was inserted into the amplicon instead of dTTP. The dTTP concentration was slightly reduced (160 µM). The PCR was otherwise performed as described for the standard PCR. Following agarose gel electrophoresis and gel staining, the DNA probe was excised from the gel and either used directly in Southern hybridizations or further purified as described in II.5.4.2.

5.3.4. Gene splicing by overlap extension

Gene splicing by overlap extension (gene SOEing) is a sequence-independent PCR method for site-directed mutagenesis and recombination of DNA molecules (Horton, 1995). It is based on the possibility of modifying PCR products by adding complementary sequences to the 5'-ends of primers so that the resulting PCR amplicons can serve as primers in a following overlap extension reaction. As the genome of *A. vinosum* is quite GC-rich (64.3 % GC-content (Pfennig and Trüper, 1989)), the GC-RICH PCR System by Roche (Mannheim, Germany) was used in gene SOEing PCRs. Two DNA polymerases were utilized: *Taq* polymerase and *Tgo* polymerase (from *Thermococcus gorgonarius*), the latter exhibiting 3'-5' exonuclease activity. The PCRs were performed following the manufacturer's instructions. 1 µL of purified modified PCR products were used as template in the overlap extension reaction. In the reaction, the modified products annealed and complemented each other. The annealing temperature was chosen in relation to the melting temperature of the overlapping region. Afterward, the joined PCR fragment was amplified utilizing the outer primers.

Overlap-extension PCR program:

1.	Initial denaturation	95°C	3 min
2.	Denaturation	95°C	30 s
3.	Overlap region annealing	T_a	30 s
4.	Elongation	72°C*	45 s kb^{-1}
5.	Repeat steps 2. to 4.		12 x
6.	Denaturation	95°C	30 s
7.	Primer annealing	T_a	30 s
8.	Elongation	72°C*	45 s kb^{-1}
9.	Repeat steps 2. to 4.		25 x
10.	Final elongation	72°C*	5 min
11.	Storage	4°C	hold

*Elongation temperature for fragments up to 3 kb was 72°C, > 3 kb 68°C.

5.4. Electrophoretic separation of DNA

5.4.1. Agarose gel electrophoresis

The separation of DNA fragments by size was achieved by electrophoresis in 1-2 % (w/v) agarose gels (Sambrook *et al.*, 1989). Higher percentage gels were used to separate smaller fragments.

Solutions:

10 x sample buffer	0.25 % bromophenol blue, 40 % sucrose
50 x TAE buffer	2 M Tris, 1 M acetic acid, 50 mM EDTA, pH 8.0
5 x TBE buffer	0.45 M Tris, 0.4 M boric acid, 10 mM EDTA, pH 8.0

Agarose was melted in an appropriate volume of 1 x TAE buffer, or 0.5 x TBE buffer in case of DNA mobility shift assays, and poured into a gel chamber (Horizon 58, Horizon 11·14, Gibco, Eggenstein, Germany). 1 x TAE buffer, or 0.5 x TBE buffer respectively, served as electrophoresis buffer. Before the samples and DNA size standards (1 kb or 100 bp DNA ladder, Invitrogen, Karlsruhe, Germany) were placed into wells at one end of the gel, a tenth of their volume was added in sample buffer. Voltages of 20-100 V were applied, resulting in running times of 16 to 1 h. The DNA fragments separated by agarose gel electrophoresis were visualized by staining them for 10 min with the fluorescent dye ethidium bromide (10 µg mL^{-1}) and viewing the gel under ultraviolet illumination. The stained gels were documented using the imaging instrument of the company INTAS (Göttingen, Germany).

5.4.2. Purification of DNA fragments from agarose gels

DNA fragments were excised from stained agarose gels with a clean scalpel and purified using the QIAquick Gel Extraction Kit (Qiagen, Hilden, Germany) or PureLink Gel Extraction Kit (Invitrogen, Karlsruhe, Germany) following the manufacturers' instructions. The DNA fragments were eluted in 50 µL sterile water and stored at -20°C.

5.5. Enzymatic modification of DNA

5.5.1. DNA restriction digestion

Restriction digestion of DNA was performed using type II restriction endonucleases by Invitrogen (Karlsruhe, Germany) or Fermentas (St. Leon-Rot, Germany), following the manufacturers' instructions. 0.5-10 µg DNA was incubated together with 3-5 U restriction enzyme per µg DNA and enzyme-specific buffer at 37°C or at another manufacturer-recommended temperature. In case of plasmid DNA or DNA fragments the digestion was performed for 1-3 h or for 4-16 h with genomic DNA. When the fragments were used for further DNA modifications, the restriction enzymes were inactivated by heat treatment following the manufacturers' instructions.

5.5.2. Dephosphorylation by alkaline phosphatase

Calf intestinal alkaline phosphatase (CIAP) removes the 5'-phosphate groups of linearized plasmids. This reduces the occurrence of undesired plasmid-recirculation during ligation. 1 U alkaline phosphatase was added to a restriction preparation and incubated for 1 h at 37°C. The phosphatase was subsequently inactivated by heat treatment at 65°C for 10 min.

5.5.3. Purification of DNA after PCR or restriction digestion

DNA fragments gained by PCR or digestion were purified using the QIAquick Gel Extraction Kit (Qiagen, Hilden, Germany) or PureLink PCR Purification Kit (Invitrogen, Karlsruhe, Germany) following the manufacturers' instructions. The DNA fragments were eluted in 50 µL sterile water and stored at -20°C.

5.5.4. Ligation

The conjoining of digested plasmid DNA and equally prepared DNA fragments (inserts) was catalyzed by the ligase of the T4 bacteriophage of *E. coli*. Plasmid DNA and insert-DNA (approx. ratio of 1 to 3) were mixed with 1 U of T4 ligase, the provided ligase buffer and 1 mM ATP (freshly prepared) in a volume of max. 20 µL. The ligation was carried out for 12-16 h at 16°C or for 3 h at RT.

5.6. Cloning

5.6.1. Transformation of competent *E. coli* cells

The transfer of plasmid DNA into competent *E. coli* cells was achieved by employing the transformation technique of Hanahan (1983). Competent cells were thawed on ice before use. A complete ligation preparation with heat-inactivated ligase (15 min at 65°C) or 1 µL of pure plasmid preparation was added to 100 µL of competent cells and the mixture was incubated on ice for 30 min. Following a heat-shock of 90 s at 42°C, the cells were immediately cooled on ice for 5 min. After the addition of 500 µL 2 x YT medium the cells were incubated at 37°C for 45 min to recover from the procedure. The cells were plated on selective LB plates (containing antibiotics and/or X-gal and IPTG) designed to encourage the growth of plasmid-containing *E. coli* cells and, if applicable, to enable the identification of positive clones via blue-white selection.

5.7. Conjugative transfer of plasmid DNA from *E. coli* to *A. vinosum*

The method of transferring plasmid DNA from *E. coli* to *A. vinosum* via conjugation has been established by Pattaragulwanit and Dahl (1995). *E. coli* S17-1 was used as donor and rifampicin-resistant *A. vinosum* strains served as recipient. The plasmid-carrying *E. coli* donor was grown over night on LB plates containing the appropriate antibiotic. The cells were resuspended in 3 mL RCV medium to an OD_{600} of 0.4. According to Sambrook *et al*. (1989) the optical density of OD_{600} 0.1 corresponds to 1 x 10^8 *E. coli* cells mL^{-1}. The *A. vinosum* strain was grown on RCV medium until the optical density reached OD_{690} 1.4, corresponding to the stationary phase. The cell count per mL culture was determined by measuring the optical density at 690 nm (Pattaragulwanit, 1994). Approximate 12 x 10^8 *A. vinosum* cells were harvested by centrifugation at 9300 ***g*** for 5 min. The supernatant was carefully removed

and the cells were washed twice in 0.5 mL RCV medium before they were resuspended in the same volume. Approx. 4 x 10^8 *E. coli* cells were added to the *A. vinosum* recipient strain and gently mixed, resulting in a three times higher cell number of *A. vinosum* compared to *E. coli*. The mixture was sedimented (93000 ***g***, 5 min) and the supernatant was removed. The cells were resupended in 100 µL RCV medium and the suspension was spread on a sterile cellulose-nitrate filter (Sartorius, Göttingen, Germany) that was positioned on a RCV agar plate without antibiotics. After incubating the cells for two days in the light under anaerobic conditions the filter was removed, transferred to a sterile tube and the cells were washed from the filter using 1 mL RCV medium. The cells were plated on selective RCV-phytagel plates containing a plasmid-appropiate antibiotic as well as rifampicin in order to select for transconjugants.

5.8. DNA-DNA hybridization

The detection of specific DNA sequences within genomic DNA was achieved utilizing the DNA-DNA hybridization technique established by Edwin Southern in the 1970s (Southern hybridization) (Southern, 1975; Southern, 1979).

5.8.1. Southern transfer

Genomic-DNA was cleaved by restriction endonucleases and the fragments were separated by agarose gel electrophoresis. The transfer of the DNA fragments onto a nylon membrane (Roth, Karlsruhe, Germany) was achieved by capillary blot.

Solutions

Depurination solution	0.25 M HCl
Transfer solution	0.4 M NaOH
20 x SSC	3 M NaCl, 0.3 M sodium citrate, pH 7.0
2 x SSC + 1 % SDS	10 % 20 x SSC, 1 % (w/v) SDS

The gel was washed twice with demineralized water and incubated in depurination solution for 10 min. Two sheets of Whatman 3MM paper (soaked in transfer solution) were placed on a stack of absorbent tissues. Onto these a soaked nylon membrane was positioned. The gel was placed gently on the membrane and two pieces of soaked Whatman paper were placed on top of the gel. The blot was connected by soaked Whatman paper stripes to a container filled with transfer solution. The blot was disassembled after 2 h and the membrane was briefly washed in 2 x SSC + 1 % SDS. The transferred DNA was covalently linked to the membrane by UV cross-linking (Stratalinker 1800, Stratagene, La Jolla, USA).

5.8.2. Hybridization with digoxigenin-labelled DNA probes

The immobilized DNA was hybridized with a single-stranded digoxigenin-labelled DNA probe.

Solutions

Buffer 1	0.1 M maleic acid, 0.15 M NaCl, pH 7.5
Pre-hybridization solution	20 % (v/v) buffer 1, 25 % (v/v) 20 x SSC, 0.1 % N-lauroyl sarcosine, 0.02 % (w/v) SDS, 2 % (w/v) blocking reagent
0.1 x SSC + 1 % SDS	0.5 % (v/v) 20 x SSC, 1 % (w/v) SDS

To prevent unspecific binding, the membrane was incubated in 20 mL pre-hybridization solution for 4 h at 68°C in a hybridization oven (Biometra, Göttingen, Germany). The pre-hybridization solution contained a blocking reagent that saturated free binding sites on the membrane. The dig-labelled DNA probe was initially heated to 100°C for 20 min and added directly to the pre-hybridization solution. After over-night incubation at 68°C the probe-containing solution was poured into a sterile tube and stored at -20°C. For repeated use the probe-containing solution was heated to 100°C for 10 min before exchanging it against the pre-hybridization solution. Unspecifically bound and unbound probe was removed by washing the membrane twice for 5 min at RT with 100 mL 2 x SSC, + 1 % SDS and twice for 15 min at 68°C with 100 mL 0.1 x SSC + 1 % SDS.

5.8.3. Chemiluminescence detection

A chemiluminescent reaction was used to localize the hybridized dig-labelled probe on the membrane.

Solutions

Buffer 2	1 % blocking reagent in buffer 1 (storage at 4°C)
Buffer 3	0.1 M Tris-HCl, 0.1 M NaCl, pH 9.5 (storage at 4°C)
Washing buffer	0.3 % Tween-20 in buffer 1

All steps were carried out at room temperature. Following a washing step (50 mL washing buffer for 5 min), the membrane was incubated in 50 mL buffer 2 for 30 min, saturating unspecific binding sites of the membrane. Afterwards, the membrane was incubated for 30 min with a digoxigenin-specific antibody coupled to an alkaline phosphatase (2 µL anti-digoxigenin-AP (Roche, Mannheim, Germany) in 15 mL buffer 2). The antibody bound to the dig-dUTP that was used in the labelling of the DNA probe. The membrane was washed twice with 50 mL washing buffer to remove unspecifically bound antibody. Following a 5 min equilibration with 20 mL buffer 3, the substrate solution (10 µL CDP-*Star* in 10 mL buffer 3) was added to the membrane. After 20 min, the membrane was placed on a Whatman 3MM paper and sealed in clear plastic film. The alkaline phosphatase coupled to the antibody degraded the substrate CDP-*Star* resulting in emission of visible light that was detectable by X-ray film. The film (X-OMAT AR, Kodak, Rochester, USA) was positioned directly on top of the membrane and exposed for 30 min up to 16 h, depending on signal strength. The development and fixing of the film was performed following the manufacturer's instructions (Kodak, Rochester, USA).

6. Methods in molecular biology: RNA

Due to the omnipresence and high stability of RNases, special precautionary measures had to be taken to prevent contaminations when working with RNA. All used solutions and buffers were RNase-free. They were mixed with 0.1 % (v/v) diethylpyrocarbonate (DEPC), a potent inhibitor of ribonuclease, stirred over night and autoclaved twice. Tris-containing buffers were prepared with RNase-free water (H_2O_{DEPC}). Glass blottles, flasks, measuring cylinder and metallic spatulas were baked at 160°C for at least 6 h. All work surfaces and work materials were cleaned with RNase AWAY (Roth, Karlsruhe, Germany).

6.1. Isolation of RNA from *A. vinosum*

The total RNA from *A. vinosum* strains was isolated according to a protocol established by Pott-Sperling (2000). The protocol is based on the method for rapid isolation of RNA from gram-negative bacteria by Ausubel *et al.* (1997).

Solutions

Protoplasting buffer	15 mM Tris-HCl, 0.45 M sucrose, 8 mM EDTA, pH 8.0; autoclaved for 10 min and stored at 4°C
Lysozyme solution	50 mg mL^{-1} lysozyme in sterile H_2O_{demin}
Lysing buffer	10 mM Tris-HCl, 10 mM NaCl, 1 mM sodium citrate, 1.5 % (w/v) SDS, pH 8.0; sterilized
Saturated NaCl	40 g NaCl in 100 mL H_2O_{demin}; stirred until saturated, incubated with DEPC and autoclaved

10 mL of an *A. vinosum* culture was filled into a sterile centrifugation tube and sedimented at 12000 ***g***, 4°C for 10 min. The pelleted cells were resuspended in 10 mL ice-cold protoplasting buffer. 80 µL lysozyme solution was added and the preparation was incubated on ice for 15 min. The resulting protoplasts were sedimented at 5900 ***g***, 4°C for 5 min and resuspended in 0.5 mL lysing buffer. 15 µL DEPC was added and the preparation was gently mixed. After transferring the lysate to a sterile microcentrifugation tube, it was incubated for 5 min at 37°C. Immediately afterwards, the preparation was cooled on ice. 250 µL saturated NaCl solution was added and the preparation was mixed by gentle inversion. Following a 10 min incubation on ice, the precipitate, containing SDS, protein and DNA, was sedimented by centrifugation at max. speed for 10 min. The RNA-containing supernatant was transferred to two sterile tubes and mixed with 1 mL ice-cold 100 % ethanol. The RNA precipitated over night at -20°C. The preparations were centrifuged at 13000 ***g*** for 15 min and the pellets were air dried. The sediments were resuspended in 50 µL RNase-free water. The reunited RNA preparations were further purified using the RNeasy Mini Kit by Qiagen (Hilden, Germany), following the manufacturer's instructions. During purification, the RNA was digested with RNase-free DNase (Qiagen, Hilden, Germany) as specified by the manufacturer. The RNA was eluted in 2 x 30 µL H_2O_{DEPC}. After the addition of 1 U μL^{-1} recombinant RNasin ribonuclease inhibitor (Promega, Madison, USA), the RNA was stored at -70°C.

6.2. Photometric determination of RNA concentration and purity

The concentration and purity of RNA solutions was determined photometrically. At 260 nm an absorption value of A_{260} 1.0 corresponds to 40 µg mL^{-1} RNA (Sambrook *et al.*, 1989). The ratio between the absorption values at 260 nm and 280 nm gives an estimate of RNA purity. Pure RNA has an A_{260}/A_{280} ratio of 1.9-2.0. Lower ratios indicate the presence of contaminants such as proteins. The measurements were performed with the UV/VIS spectrometer Lambda 11 (Perkin-Elmer, Düsseldorf, Germany).

6.3. Denaturating formaldehyde agarose gel electrophoresis

The separation of RNA fragments by size was achieved by denaturating formaldehyde agarose gel electrophoresis (Sambrook *et al.*, 1989).

Solutions:

5 x RNA electrophoresis buffer	200 mM MOPS, 50 mM sodium acetate, 10 mM EDTA, pH 7.0; incubated with DEPC and autoclaved

The RNA samples and the RNA size standard (RiboRuler RNA Ladder High Range, Fermentas, St. Leon-Rot, Germany) were mixed with equal volumes of 2 x RNA Loading Dye solution (Fermentas, St. Leon-Rot, Germany), heated at 70°C for 10 min and chilled on ice. A 6.5 % formaldehyde 1 % agarose gel in 1 x RNA electrophoresis buffer (formaldehyde was added after the agarose was melted), was poured into a Horizon 58 gel chamber (Gibco, Eggenstein, Germany) and pre-run at 80 V for 10 min before the samples were loaded into the wells. The duration of the electrophoresis was 2 h at 80 V. The gel was stained with 10 µg mL^{-1} ethidium bromide solution prepared with RNase-free water and documented as described for DNA agarose gels.

6.4. Quantitative real-time RT-PCR

The expression of several *dsr* genes (*dsrA, dsrE, dsrC, dsrL, dsrR* and *dsrS*) was examined by absolute quantitative real-time RT-PCR utilizing the QuantiTect SYBR Green RT-PCR kit (Qiagen, Hilden, Germany) and the iCycler iQ real-time detection system (Bio-Rad, Munich, Germany) as specified by the manufacturers. The QuantiTect SYBR Green RT-PCR kit allows transcription, amplification and quantification of specific RNAs in one-step, thereby minimizing the risk of contamination. The fluorescent dye SYBR Green I binds all double-stranded DNA molecules, emitting a fluorescent signal on binding (excitation at 494 nm; emission at 521 nm). The signal is detected during the elongation step of each PCR cycle. Using the iCycler iQ software, the detected fluorescence is plotted against the cycle number. After an initial low baseline, the fluorescence increases exponentially before stagnating. The cycle number at which the signal intensity increases is depended on the initial concentration of PCR target. A threshold is set above the fluorescence baseline and within the linear region of the amplification plot that represents the exponential phase of the reaction. In this phase,

the fluorescence intensity is directly proportional to the amount of PCR product. The cycle at which the exponentially increasing fluorescence crosses this threshold (C_T) is used to calculate the initial target amount. A standard curve was generated by plotting the C_T values of different RNA standard dilutions against the logarithm of their copy numbers. Comparing the C_T of the target with the standard curve allowed the calculation of the initial amount of target. By using external RNA standards that contained the target sequence, the variable efficiency of the reverse transcription was taken into account. All template RNAs were isolated from cultures of the same growth phase. The RNAs were isolated and purified following the same protocol and the concentration was carefully determined in order to guarantee comparability between the different samples.

6.4.1. Generation of RNA standards

RNA standards were generated as described in Fey *et al.* (2004). The RNA standard primers were located up- and downstream of the RT-PCR target and the T7 promoter sequence was added to the forward primer. The primers were used to amplify DNA fragments of approx. 800 bp using a standard PCR protocol with *Pfu* DNA polymerase and *A. vinosum* genomic DNA as template. The PCR products were purified and subsequently transcribed *in vitro* with T7 polymerase by using the Riboprobe in vitro Transcription Systems (Promega, Madison, USA). Following a digestion with RNase-free DNase RQ1 (15 min, 37°C), the RNA standards were purified using the RNeasy Mini Kit (Qiagen, Hilden, Germany) as specified by the manufacturer. A second RNase-free DNase (Qiagen, Hilden, Germany) digestion was performed on column during the purification (15 min, RT). The transcripts were analyzed using denaturating formaldehyde agarose gels. RNA standards were quantified spectrophotometrically and the copy number was calculated. The standards were diluted in RNase-free water and stored at -70°C.

6.4.2. Standard real-time RT-PCR protocol

Based on the protocol recommended by Qiagen for the use of the QuantiTect SYBR Green RT-PCR kit, an optimized PCR protocol was created for the transcription and amplification of *dsr* genes. The optimal concentration of RNA template, $MgCl_2$, and primer as well as the optimal primer annealing temperature was determined empirically. DNA fragments of approx. 200 bp were amplified. Control reactions without the QuantiTect RT Mix that contains the reverse transcriptases, were performed for each RNA sample to detect potential DNA contaminations. The reactions were carried out in triplicate.

Standard real-time RT-PCR:

2 x QuantiTect SYBR Green RT-PCR Master Mix	12.5 µL
Forward primer (12.5 µM)	1.0 µL
Reverse primer (12.5 µM)	1.0 µL
RNA template (250 ng μL^{-1})	1.0 µL
QuantiTect RT Mix	0.25 µL
RNase-free $H_2O_{ultra\text{-}pure}$	ad 25 µL

The program for the quantitative RT-PCR consisted of seven steps: transcription of RNA to cDNA (reverse transcription), inactivation of the reverse transcriptase and activation of the HotStarTaq DNA polymerase, denaturation of the template, amplification, melting curve analysis and cooling. The depicted program was used for absolute quantitative real-time RT-PCR with iCycler iQ real-time detection system.

Standard real-time RT-PCR program:

1.	Reverse transcription	50°C	30 min
2.	Initial activation	95°C	15 min
3.	Denaturation	94°C	15 s
4.	Primer annealing	T_a*	30 s
5.	Elongation	72°C	30 s
	Repeat steps 3. to 5.		40 x
6.	Melting curve analysis	40-100°C	0.5°C $(30\ s)^{-1}$
7.	Storage	4°C	hold

*T_a: *dsrA*: 59°C, *dsrE*: 56°C, *dsrC*: 55°C, *dsrL*: 57°C, *dsrR*: 60°C, *dsrS*: 58°C

6.4.3. Analysis of the melting temperature

The absence of non-specific PCR products and primer-dimers that would otherwise contribute to the fluorescence signal was confirmed by melting curve analysis. Every double-stranded DNA has a characteristic melting temperature that is defined as the temperature at which 50 % of the DNA is single-stranded. The length of the DNA fragment and the GC-content are significant factors influencing the melting temperature. The PCR products were analysed by increasing the temperature every 30 s by 0.5°C starting at 40°C up to 100°C. At low temperatures the PCR products are double-stranded and the fluorescent dye SYBR Green I binds to them. With rising temperature the PCR products denature resulting in a decrease in fluorescence. The fluorescence is measured continuously as the temperature is increased and plotted against the temperature. The iCycler iQ software calculates the first derivative of the resulting curve, yielding curves with peaks at the respective melting temperatures. Peaks at a lower melting temperature than that of the specific RT-PCR product indicate the formation of primer-dimers, while diverse peaks with different melting temperatures indicate the production of non-specific products. The PCR products were furthermore analysed by agarose gel electrophoresis.

7. Protein techniques

7.1. Production of recombinant protein in *E. coli*

The *E. coli* strain BL21(DE3) was used for the heterologous production of recombinant protein. The genes of the respective proteins were amplified via PCR, utilizing primers that introduced restriction sites to the 5' and 3' ends of the resulting amplicons. The fragments were ligated into expression plasmids based on the pET series (Novagen) thereby adding a C-terminal (pET-22b) or N-terminal (pET-15b) oligo-histidine tag (His tag) to the protein. 5 mL LB medium inoculated with plasmid-containing *E. coli* cells was incubated over night in a shaker-incubator at 180 rpm. This starting culture was added to 495 mL LB medium in a shaking flask. In general, the culture was incubated at 37°C and 180 rpm in a shaker-incubator. After reaching an optical density of OD_{600} 0.5, 100 µM IPTG was added to induce gene expression. Two hours later, the cells were harvested (4°C, 10000 ***g***, 30 min) and the pellet was stored at -20°C until further use.

In case of DsrR and IscA production the LB medium contained 200 µM $Fe(NH_4)_2(SO_4)_2$. The incubation temperature during DsrS production was lowered to 25°C and the IPTG concentration was reduced to 2 µM in an effort to achieve a higher yield of soluble protein.

7.2. Cell harvesting and disruption

Harvested *E. coli* cells were resupended in 3 mL disruption buffer (50 mM NaH_2PO_4, 300 mM NaCl, 10 mM imidazole, pH 7.5) per 1 g wet weight. 1 mg lysozyme mL^{-1} was added and the cells were incubated for 30 min on ice. Following cell disruption by sonication (2 min mL^{-1}, 50 % intensity, 4°C, CeII Disruptor B15, Banson, Danbury, USA) the crude extract was centrifuged at 25000 ***g*** and 4°C for 30 min to sediment whole cells and larger cell fragments. When the preparation was too viscous, a small amount of RNase and DNase was added. The supernatant, also named soluble fraction, and the pellet, also referred to as insoluble fraction, were stored at 4°C until further use.

A. vinosum cultures were harvested by centrifugation at 10000 ***g*** at 4°C for 45 min. The pellets were either utilized directly or stored at -20°C until further use. The cells were resuspended in 3 mL 50 mM Tris-HCl pH 7.5 per 1 g wet weight. The resuspended and homogenized cells were disrupted by sonication (see above) and whole cells and larger cell fragments were pelleted by centrifugation (30 min, 4°C, 25000 ***g***). The supernatant was separated in a soluble fraction and membrane fraction by ultracentrifugation (145000 ***g***, 2.5 h, 4°C). The membranes were resuspended in a buffer volume equal to that of the soluble fraction and the fractions were stored at -20°C until further use.

7.3. Determination of protein concentration

7.3.1. BCA Protein Assay Reagent Kit

The concentration of purified protein solutions was determined utilizing the BCA Protein Assay Reagent Kit (Pierce, Rockford, USA). The measurements were performed in a 96-well plate following the manufacturer's instructions. 25 µL of the protein sample was mixed with 200 µL working reagent and incubated for 30 min at 37°C. The absorption was measured at 550 nm against a chemical blank using the plate reader SLT 340 ATTC (SLT Labinstruments, Crailsheim, Germany). BSA concentrations in the rage of 0-500 µg mL^{-1} were used as standards.

7.3.2. Modified Bradford method

The protein concentration of culture samples was determined essentially as described by Bradford (1976). 1 mL of the culture was centrifuged at 13000 ***g*** for 3 min and the pellet was stored at -20°C. The thawed cells were resuspended in 1 mL 1 M NaOH, heated to 95°C for 5 min and immediately cooled on ice. Following centrifugation (3 min, 13000 ***g***), 25 µL of the supernatant were mixed with 750 µL Bradford reagent (Sigma-Aldrich, Steinheim, Germany) and incubated in the dark for 10 min. The absorption at 595 nm was measured against a chemical blank. BSA concentrations in the rage of 0 to 1.4 mg mL^{-1} served as standards

7.4. Electrophoretic separation of proteins

7.4.1. SDS-PAGE

The separation of proteins by molecular mass was achieved by discontinuous SDS polyacrylamide gel electrophoresis (PAGE) (Laemmli, 1970).

Solutions

Solution A	1.5 M Tris-HCl, pH 8.8, 0.3 % SDS
Solution B	0.5 M Tris-HCl, pH 6.8, 0.4 % SDS
APS solution	10 % (w/v) ammonium peroxodisulfate
5 x Electrophoresis buffer	15 g Tris, 72 g glycine, 5 g SDS ad 1 L $H_2O_{ultra\text{-}pure}$
30 % Acrylamide/bisacryl-amide solution	Roth (Karlsruhe, Germany)
4 x Rotiload 1	Roth (Karlsruhe, Germany)
TEMED	Roth (Karlsruhe, Germany)

A polyacrylamide gel consisted of a stacking and running gel. The stacking gel had a lower acrylamide concentration and pH value than the running gel, thereby focussing the protein samples into a thin band before they entered the running gel. The acrylamide concentration of the running gel varied, depending on the molecular mass of the proteins. Proteins of lower molecular mass were separated in higher percentage gels. The composition of the gels was as follows:

	Running gel 12.5 %*	Running gel 15 %*	Stacking gel 4.5 %*
ultra-pure water	4 mL	3 mL	3 mL
Solution A	3 mL	3 mL	-
Solution B	-	-	1.25 mL
Acrylamide/bisacrylamide	5 mL	6 mL	0.75 mL
TEMED	5 µL	5 µL	5 µL
APS solution	100 µL	100 µL	100 µL

* The given amounts yield two gels of 0.75 mm thickness.

The addition of APS solution started the polymerization process. The running gel mixture was poured between two glass plates separated by a 0.75 mm spacer and water was gently placed on top of it. After the gel was polymerized (~45 min), the water was removed. The stacking gel mixture was poured on top of the running gel and a well comb was inserted. The protein samples were mixed with 0.25 x volume of 4 x Rotiload 1 and heated to 100°C for 5 min. The polymerized gels were placed into a Mini-PROTEAN 3 gel chamber (Bio-Rad, Munich, Germany) and the chamber was filled with 1 x electrophoresis buffer. The protein samples were placed into the wells next to a protein molecular mass marker (PageRuler Prestained Protein Ladder, Fermentas, St. Leon-Rot, Germany). The focussing of the samples was carried out at 60 V, the separation at 100 V. After completion of the electrophoretic separation, the running gel was carefully removed from the glass plates and either stained or blotted.

7.4.2. Coomassie staining

The electrophoretically separated proteins were visualized by staining with Coomassie Brilliant Blue.

Solution

Coomassie solution	0.25 % Coomassie Blue R-250, 50 % methanol, 10 % acetic acid, 40 % $H_2O_{ultra\text{-}pure}$
Dye remover/fixer	10 % acetic acid, 20 % methanol, 70 % $H_2O_{ultra\text{-}pure}$

The gel was incubated for 1-2 h in Coomassie solution. Excess dye was removed by rinsing the gel several times with dye remover/fixer solution until the protein bands were clearly visible (sensitivity: 100 ng protein per band). The stained gel was scanned into the computer and/or placed onto a water soaked Whatman 3MM paper and vacuum dried at 70°C for 2 h (Aldo-Xer gel dryer, Schütt, Göttingen, Germany).

7.4.3. Silver staining

Silver staining was used for sensitive detection of proteins of low concentrations in polyacrylamide gels (sensitivity: 1 ng protein per band).

Solutions*

Fixation solution	50 % methanol, 5 % acetic acid, 45 % $H_2O_{ultra\text{-}pure}$
Wash solution	50 % methanol, 50 % $H_2O_{ultra\text{-}pure}$
Thiosulfate reagent	0.02 % $Na_2S_2O_3$ in $H_2O_{ultra\text{-}pure}$
Silver nitrate reagent	0.1 % $AgNO_3$ in $H_2O_{ultra\text{-}pure}$
Developer solution	3 % Na_2CO_3, 0.04 % formaldehyde in $H_2O_{ultra\text{-}pure}$
Stop reagent	5 % acetic acid in $H_2O_{ultra\text{-}pure}$

* All solutions were freshly prepared.

The gels were incubated for 20 min in 50 mL fixation solution. When the gels were stained with Coomassie beforehand, they were rigorously washed with dye remover/fixer solution instead. Following a 10 min incubation in wash solution and 10 min rinsing in ultra-pure water, the gel was sensitized by soaking in 50 mL thiosulfate reagent for 1 min. A short washing step (rinsed twice for 1 min with ultra-pure water) preceded the incubation in chilled 50 mL silver nitrate reagent (20 min, 4°C). The protein gel was developed by transferring it to 50 mL developer solution until the protein bands were clearly discernible. The staining was terminated by the addition of 50 mL stop reagent. The stained gel was rinsed several times with ultra-pure water and documented as described above.

7.5. Western blot

Proteins separated by SDS-PAGE were transferred to a cellulose nitrate membrane by electroblotting (Western blot) with Towbin blot buffer (Towbin *et al.*, 1979).

Solutions

Towbin blot buffer	25 mM Tris, 192 mM glycine, 20 % methanol, pH 8.3

The polyacrylamide gel and a gel-sized cellulose nitrate membrane (Protran BA 85, Schleicher & Schuell, Dassel, Germany) were equilibrated in Towbin buffer for 15-20 min. Three pieces of Towbin buffer-soaked Whatman 3MM paper, the membrane, gel, and three further pieces of gel-sized soaked Whatman paper were placed in this order onto the anode of the Transblot SD Semi-Dry transfer cell (Bio-Rad, Munich, Germany). The cathode was placed on top, thereby closing the cell. The transfer was carried out at 15 V for 25-45 min depending on the size of the protein (DsrE, DsrC, DsrR: 25 min, DsrK, DsrL, DsrS: 45 min).

7.6. Immunological detection methods

The immunological detection of proteins transferred to a cellulose nitrate membrane was essentially performed as described by Sambrook *et al.* (1989). Dsr protein-specific antibodies, except for DsrC, were raised in rabbits against peptides encompassing highly immunogenic epitopes deduced from the nucleotide sequence. The Dsr protein-specific antisera were created by Eurogentec (Seraing, Belgium). DsrC-specific antibodies were raised in rabbits against recombinant DsrC protein purified from *E. coli* (Pott-Sperling, 2000). His-tagged proteins were detected by a pentahistidine-specific antibody raised in mice

(Novagen, Madison, USA). As secondary antibodies Goat Anti-Rabbit IgG horseradish-peroxidase (HRP) conjugate (Sigma-Aldrich, Steinheim, Germany) or Goat Anti-Mouse IgG HRP conjugate (Novagen, Madison, USA) were used. Depending on the expected strength of the signal, colorimetric or the more sensitive chemiluminescence detection method was utilized.

7.6.1. Colorimetric detection method

Solutions

10 x PBS*	80 g NaCl, 2 g KCl, 11.5 g Na_2HPO_4 x 7 H_2O, 2 g KH_2PO_4 ad 1 L $H_2O_{ultra\text{-}pure}$
20 x TBS†	3 M NaCl, 200 mM Tris-HCl, pH 7.5
10 x TBSTT	5 M NaCl, 200 mM Tris-HCl, 2 % (v/v) Triton X-100, 0.5 % (v/v) Tween-20, pH 7.5
Staining solution	30 mg 4-chloro-1-naphthol ad 7 mL ethanol (ice cold)

* Phosphate Buffered Saline †Tris Buffered Saline

For the colorimetric protein detection with Dsr protein-specific antisera, the free binding sites of the membrane were saturated by incubation in 100 mL 1 x PBS with 5 % (w/v) skim milk for 12-16 h at 4°C. The membrane was washed five times with 50 mL 1 x PBS and incubated for 3 h in 20 mL 1 x PBS with 0.5 % BSA and the appropriate antibody at a 1:500 dilution (DsrE-antiserum: 1:1000 dilution). After the membrane had been rinsed three times with 50 mL 1 x PBS for 5 min, the secondary antibody (Goat Anti-Rabbit IgG HRP conjugate), diluted at 1:5000 in 20 mL 1 x PBS buffer with 0.5 % BSA, was added to the membrane. After 1 h the membrane was washed twice with 1 x PBS for 5 min and transferred to a clean container with 43 mL ultra-pure water and 7 mL staining solution. The reaction was started by the addition of 20 µL H_2O_2. As soon as a signal was clearly perceived the reaction was stopped by rigorous washing with demineralized water.

The detection of histidine-tagged proteins was performed following the antibody manufacturer's instructions. After the proteins were transferred to the membrane, it was washed twice with 1 x TBS and incubated in 50 mL 1 x TBS buffer with 5 % skim milk for 12-16 h at 4°C, saturating the free binding sites. After washing the membrane twice with 20 mL 1 x TBSTT for 10 min and rinsing it for 10 min with 1 x TBS buffer, the His-tag monoclonal antibody was added to the membrane at a dilution of 1:1000 in 10 mL 1 x TBS buffer with 0.3 g BSA. One hour later, the membrane was washed twice with 20 mL 1 x TBSTT for 10 min and once with 15 mL 1 x TBS for 10 min. The secondary antibody (Goat Anti-Mouse IgG HRP conjugate) was diluted at 1:5000 in 10 mL 1 x TBS, 0.3 g BSA and applied for 1 h. Afterward, the membrane was washed five times for 5 min with 20 mL 1 x TBSTT, before staining was commenced as described above.

7.6.2. Chemiluminescent detection method

A more sensitive detection of proteins with antibodies was achieved utilizing the SuperSignal West Pico Chemiluminescent Substrate (Pierce, Rockford, USA).

Solutions

20 x TBS	3 M NaCl, 200 mM Tris-HCl, pH 7.5
1 x TBST	1 x TBS, 0.05 % (w/v) Tween-20, pH 7.5

After the proteins were blotted onto the membrane, free binding sites were saturated by incubation in 100 mL 1 x TBST with 5 % skim milk for 1 h. The primary antibody, diluted at 1:1000 (Dsr protein-specific) or 1:2000 (His-tag-specific) in 20 mL 1 x TBST, 0.1 g BSA was applied to the membrane for 1 h at RT or over night at 4°C. After washing the membrane five times with 1 x TBST for 5 min, the secondary antibody, diluted at 1:5000 in 20 mL 1 x TBST, 0.1 g BSA, was applied to the membrane. After one hour, the membrane was washed five times with 1 x TBST for 5 min and incubated for 5 min in 5 mL SuperSignal West Substrate Working Solution that was prepared as specified by the manufacturer. The membrane was placed on a piece of Whatman 3 MM paper and sealed in clear plastic film. The peroxidase coupled to the secondary antibody degraded the substrate, resulting in emission of visible light that was detectable by X-ray film. The film (X-OMAT AR, Kodak, Rochester, USA) was positioned directly on top of the membrane and exposed for 1 min up to 16 h, dependent on signal strength. The development and fixing of the film was performed following the manufacturer's instructions.

7.7. Desalting of protein solutions

7.7.1. Desalting of protein solutions by dialysis

In order to desalt or change the protein solution's buffer, the protein solutions were dialysed against 4 L of the desired buffer for 16 h at 4°C. Dialysis tubes (molecular weight cut off (MWCO) 6000-8000 Da, Serva, Heidelberg, Germany) of 10 to 20 cm length were prepared as follows: the tubes were boiled for 10 min in 1 L of 2 % (w/v) $NaHCO_3$, 1 mM EDTA (pH 8), washed with sterile H_2O_{demin}, autoclaved for 10 min in 1 mM EDTA (pH 8) and rinsed with sterile H_2O_{demin} before use.

7.7.2. Desalting of protein solutions by HiTrap Desalting Column

Protein solutions with a small volume were desalted by passage through a HiTrap Desalting Column (GE Healthcare, Munich, Germany). The HiTrap Desalting Column is prepacked with 5 mL Sephadex G-25 Superfine and fractionates molecules in the range of 1000-5000 relative molecular weight. Proteins with a molecular weight more than 5000 are therefore separated from molecules with a molecular weight less than 1000. The separation was performed with a syringe, following the manufacturer's instructions.

7.8. Concentration of protein solutions

Protein solutions were concentrated by ultrafiltration using Centriplus Centrifugal Filter Devices (Millipore, Schwalbach, Germany) of appropriate molecular weight cut off. The protein solutions were centrifuged following the manufacturer's instructions until the desired volume was achieved.

7.9. Chromatography methods

The chromatographic separation of proteins was performed using a HiLoad System (Pharmacia, Uppsala, Sweden). All buffers and solutions were degassed and filtrated (cellulose nitrate filter, 0.45 µm pore size, Sartorius, Göttingen, Germany) before use. The chromatography columns were cooled to 4°C. Before the protein samples were applied to the column, they were centrifuged (15000 ***g***,10 min, 4°C) in order to sediment potential blockage-causing material. All columns were handled as specified by the manufacturers.

7.9.1. Nickel-chelate affinity chromatography

The nickel-chelate affinity chromatography enables the specific purification of proteins carrying an oligo-histidine tag (His-tag). The histidin residues bind to nickel ions immobilized by NTA (nitrilotriacetic acid) groups on the agarose matrix. The His-tagged protein is thus retained on the column. The protein can be eluted by increasing imidazole concentrations, as the imidazole ring is part of the histidine structure and binds to nickel ions as well. Imidazole competes with the histidine residues for binding sites on the Ni-NTA resin, causing the His-tagged protein to dissociate.

Column	Ni-NTA agarose in polypropylene column (Qiagen, Hilden, Germany)
Column volume	5 mL
Disruption buffer	50 mM NaH_2PO_4, 300 mM NaCl, 10 mM imidazole, pH 7.5
Buffer A	50 mM NaH_2PO_4, 300 mM NaCl, pH 7.5
Buffer B	50 mM NaH_2PO_4, 300 mM NaCl, 1 M imidazole, pH 7.5

Loose Ni-NTA agarose matrix was packed into polypropylene columns according to the manufacturer's instructions and equilibrated with disruption buffer. The soluble fraction containing the tagged protein was subsequently applied. The column was washed with four column volumes (CV) 1 % buffer B and 3 CV 2 % buffer B, before the protein was eluted by a stepwise increase of imidazole concentrations (40 mM, 60 mM, 80 mM, 100 mM, 150 mM, 200 mM and 250 mM). The column was washed with two column volumes of each step. After the protein eluted, the column was washed with 5 CV 0.5 NaOH, 2 CV demineralized water and 2 CV 30 % EtOH, before the column was stored in 30 % EtOH at 4°C.

To increase the purity of proteins, a second passage through a Ni-NTA agarose column could be beneficial. The protein-containing fractions of the first chromatography were

combined and dialyzed against 5 L 50 mM NaH_2PO_4, 300 mM NaCl, pH 7.5 over night at 4°C, before they were applied to a second column.

7.9.2. Gel filtration chromatography

The molecular mass and state of oligomerization of a protein was determined by gel filtration chromatography.

Column	HiLoad 16/60 Superdex-75 (GE Healthcare, Munich, Germany)
Separation range	3000-70000 Da
Column volume	126 mL
Buffer	50 mM Tris-HCl, 500 mM NaCl, pH 8.0
Standard proteins	Aprotinin (bovine lung) 6.5 kDa, cytochrome *c* (horse heart) 12.4 kDa, carbonic anhydrase (bovine erythrocytes) 29 kDa, ovalbumin (chicken egg) 45 kDa, albumin (bovine serum) 66 kDa (Sigma-Aldrich, Steinheim, Germany)

Column	HiLoad 16/60 Superdex-200 (GE Healthcare, Munich, Germany)
Separation range	10000-600000 Da
Column volume	126 mL
Buffer	50 mM Tris-HCl, 300 mM NaCl, pH 7.5
Standard proteins	Cytochrome *c* (horse heart) 12.4 kDa, carbonic anhydrase (bovine erythrocytes) 29 kDa, albumin (bovine serum) 66 kDa, aldolase (rabbit muscle) 158 kDa, catalase (bovine liver) 232 kDa, ferritin (horse spleen) 440 kDa (Sigma-Aldrich, Steinheim, Germany)

Gel filtration separates molecules according to differences in size as they pass through a porous column matrix. Smaller proteins were applied to the column Superdex-75. The molecular mass of bigger proteins was determined using the column Superdex-200. The columns were calibrated with standard proteins. The logarithm of the molecular mass of proteins correlates to the partition coefficient K_{av}. K_{av} is determined by the elution volume of the protein (V_e), the void volume of the column (V_o) and the total volume of the column (V_t) and can be calculated using following formula: $K_{av} = (V_e - V_o)/(V_t - V_o)$. Plotting the K_{av} values against the logarithms of the molecular mass of standard proteins, a column-specific standard curve can be generated. Using this standard curve the molecular mass of protein samples could be calculated, if their elution volume was determined on the same column. The columns were equilibrated with two column volumes of the respective buffer before the protein sample was applied with a 0.2 mL min^{-1} flow rate. The isocratic elution was performed with a flow rate of 0.5 mL min^{-1}. The absorption of the eluate was measured at 280 nm and fractions of 1 mL volume were collected. After use, the column was stored in 20 % ethanol at 4°C.

7.10. UV-visible absorption spectra

UV-visible absorption spectra of protein solutions were recorded using a 1 mL quartz cuvette and the UV/VIS spectrometer Lambda 11 (Perkin-Elmer, Düsseldorf, Germany).

7.11. Removal of the His-tag by thrombin digestion

The plasmid pET-15b encodes a thrombin cleavage site between the His-tag sequence and the cloning site into which protein sequences were inserted. Following purification, the N-terminal His-tag could be removed from the recombinant protein by digestion with thrombin. The Thrombin Cleavage Capture Kit (Novagen, Madison, USA) provided biotinylated thrombin that could easily be removed from the cleavage reaction using streptavidin agarose. The proteolytic digestion and removal of thrombin was performed according to the manufacturer's instructions. The success of the cleavage was verified by the failure of the protein to bind to nickel agarose and by SDS-PAGE.

7.12. Iron- and iron-sulfur cluster-binding assay of DsrR

The iron-binding ability of DsrR was tested based on a protocol by Ding and Clark (2004). The assay was carried out in an anaerobic chamber (flexible glove box, Toepfer Lab Systems, Goeppingen, Germany), maintaining anoxic conditions throughout the experiment. 50 µM purified recombinant protein solution without N-terminal His-tag was incubated in 50 mM Tris-HCl, 500 mM NaCl, pH 8.0 with 2.5 mM dithiothreitol for 10 min at 10°C. After the addition of no or 400 µM $Fe(NH_4)_2(SO_4)_2$, the preparations were incubated for 16 h at 10°C. The samples were separated from unbound iron by passing them through a HiTrap Desalting Column. The UV-visible absorption spectra of the samples were recorded in a 1 mL quartz cuvette using a Lambda 11 UV/VIS spectrometer (Perkin Elmer). The spectra were calibrated to an absorbance at 260 nm of A_{260} 1.0. The ability to bind Fe-S clusters was tested by adding 400 µM Na_2S to the above-mentioned preparation. The iron- and iron-sulfur cluster-binding protein IscA was used for comparison.

7.13. Coprecipitation

The interaction of several Dsr proteins with each other was investigated by coprecipitation based on a protocol described in Coligen *et al*. (1997).

Solutions

Incubation buffer	5 mM HEPES, 20 mM KCl, 1 mM TCEP, 0.002% Tween-20, pH 7.8
Washing buffer	5 mM HEPES, 20 mM KCl, 20 mM imidazole, 1 mM TCEP, 0.002% Tween-20, pH 7.8

1.5 nmol of a purified His-tagged protein (DsrEFH (provided by Andrea Schulte), DsrC, DsrL (provided by Yvonne Lübbe) or IscS (provided by Yvonne Stockdreher)) was incubated together with 2 nmol of a non-tagged protein (DsrC or DsrR) in incubation buffer for 90 min at RT. The preparations were continuously inverted. The sample was centrifuged at 10000 ***g*** for 1 min at RT and the supernatant was transferred to a new microcentrifuge tube. 30 µL Ni-NTA agarose resin (Qiagen, Hilden Germany) was added and the sample was rotated for 1 h

at RT. After centrifugation (1000 ***g***, 30 s), the supernatant was carefully removed using a cannula and syringe and the resin was washed with washing buffer. The sample was centrifuged (1000 ***g***, 30 s) and after careful and thorough removal of the supernatant, the resin was resuspended in 15 µL 4 x Rotiload 1 (Roth, Karlsruhe, Germany) and boiled for 5 min. 7 µL of the sample was loaded on a 15 % (w/v) SDS-polyacrylamide gel. Following electrophoresis the proteins were silver stained.

7.14. Electrophoretic mobility shift assay

Protein-DNA interactions were investigated by electrophoretic mobility shift assays (EMSA). This method is based on the observation that binding of a protein to a DNA fragment leads to a reduction in electrophoretic mobility of the fragment (Lane *et al.*, 1992). The protein is incubated together with a potential protein-binding site containing, linear, double-stranded DNA fragment in an appropriate incubation buffer. The protein-DNA compex and free DNA are separated by gel electrophoresis and visualized by staining with ethidium bromide.

Solutions

Incubation buffer	5 mM HEPES, 20 mM KCl, 0.02 ‰ (v/v) Tween-20, 1 mM TCEP, pH 7.8

A 923 bp fragment of the *dsrA* promoter region was obtained by PCR utilizing *Pfu* DNA polymerase, GfdsrPromf1 and TLGfdsrPromr1 as primers, and *A. vinosum* Rif50 genomic DNA as template. The amplicon was digested with *Xho*I and *Eco*RV. The *dsr* promoter region or fragments (200 fmol) were incubated with purified recombinant DsrC (0-500 pmol) in incubation buffer for 15 min at RT. The samples were transferred to a 2 % agarose gel in 0.5 x TBE buffer. Following electrophoresis (90 V) the gel was stained with ethidium bromide and documented. A fragment of the kanamycin resistance gene (200 fmol), amplified with Kmfor1 and Kmrev2 as primers and pK18*mobsacB* as template, was incubated together with the promoter region and DsrC as non-specific competitor.

7.15. β-Galactosidase assays

Reporter gene fusion plasmid carrying strains were grown on 12 mL modified Pfennig's medium with 2 mM thiosulfate, sulfide, and/or sulfite, and/or malate for 24 h before β-galactosidase activity was tested as described by Miller (1972).

Solutions

Phosphate buffer	100 mM sodium phosphate buffer pH 7.0
Z buffer	10 mM KCl, 1 mM $MgSO_4$, 50 mM β-mercaptoethanol in phosphate buffer; prepared just before use
SDS solution	0.1 % (w/v) SDS
Substrate solution	4 mg mL^{-1} ONPG in phosphate buffer; prepared just before use; preheated to 30°C
Stop solution	1M Na_2CO_3

1 mL culture was pelleted (13000 ***g***, 3 min, 4°C) and resuspended in 1 mL Z buffer. The cells were lysed by the addition of 100 µL chloroform and 50 µL SDS solution and vigorous vortexing for 10 s at maximum speed. After incubation at 30°C for 10 min, 200 µL preheated substrate solution was added. The β-galactosidase hydrolyzed the colorless ONPG to yield yellow-colored *o*-nitrophenol. As soon as the yellow color could be discerned, the reaction was stopped by adding 500 µL stop solution which shifted the pH to 11. After centrifugation (15000 ***g***, 5 min), the absorption of the supernatant was measured in a 1 mL quartz cuvette at 460 nm against a chemical blank in a Genesys 20 spectrometer (Thermo Spectronic, Dreieich, Germany). The specific β-galactosidase activity was calculated by using the following formula: [nmol *o*-nitrophenol (min mg)$^{-1}$] = ((A_{420} x k^{-1}) x V_{assay} [mL]) / (t_{assay} [min] x protein [mg mL^{-1}] x $V_{culture}$ [mL]). Under the above conditions 1 µM *o*-nitrophenol had an aborbance A_{420} of 0.0044 (*k*). The protein concentration for each sample was determined by modified Bradford assay.

8. Analytical determination of sulfur compounds

The concentration of sulfur compounds, like sulfide, sulfite, thiosulfate, and sulfate in culture samples of *A. vinosum* was determined by high performance liquid chromatography (HPLC). The HPLC apparatus (Thermo Separation Products, Dreieich, Germany) consisted of a vacuum degasser (SCM1000), a pump (P4000), an UV-detector (UV150) or fluorescence detector (FL3000), a column thermostat (Jetstream 2) and an autosampler (AS3000), all connected to a PC via a communication unit (SN4000). Chromatograms were analyzed using the software PC100 provided by Thermo Seperation Products. The HPLC columns were handled according to manufacturers' instructions. All utilized solutions were filtrated (polypropylene filter, 0.2 µm pore-size, PALL Life Science, Dreieich, Germany). The determination of elemental sulfur was performed using a colorimetric method based on Bartlett and Skoog (1954).

8.1. Determination of thiols using HPLC

Thiol compounds like sulfide, polysulfide, thiosulfate and sulfite were labelled with the fluorescent dye monobromobimane and separated by reverse-phase HPLC. The derivatized sulfur compounds were detected by their fluorescence emission at 480 nm (Rethmeier *et al.*, 1997).

Sample derivatization

HEPES buffer	50 mM HEPES, 5 mM EDTA, pH 8.0 (titrated with NaOH)
Monobromobimane (MBB)	48 mM MBB in acetonitrile, storage at -20°C

50 µL culture sample was mixed with 50 µL HEPES buffer, 55 µL acetonitrile and 5 µL MBB. The preparation was incubated for 30 min in the dark. The derivatization was stopped by the

addition of 100 µL 65 mM methanesulfonic acid. The sample was stored at -20°C before quantification. Thawed samples were centrifuged for 5 min at maximum speed sedimenting cell components. The supernatant was diluted twenty-fold with solvent mixture (85 % acetic acid pH 4, 15 % methanol) and filled into an HPLC sample vial.

Sample separation and detection:

Solvent A	0.25 % (v/v) acetic acid, pH 4 (titrated with NaOH)
Solvent B	HPLC-grade methanol (Roth, Karlsruhe, Germany)

50 µL of the derivatized sample were injected by the autosampler into the sample loop and directed to the column LiChrospher 100 RP-18e (250-4.5 µm) by Merck (Darmstadt, Germany) that was protected by a guard column of the same material. The column was heated to 35°C in the column oven. The optimal separation of the sulfur compounds was achieved using a binary gradient, consisting of solvent A and solvent B.

Time [min]	Solvent A [%]	Solvent B [%]
0	85	15
5	85	15
50	55	45
55	0	100
58	0	100
61	85	15
76	85	15

The flow rate was 1 mL min^{-1}. The derivatized thiols were detected by fluorescence detector FL3000 (excitation at 380 nm, emission at 480 nm). The retention times of the compounds were as follows: sulfite ~4.8 min, thiosulfate ~9 min, polysulfide I ~39 min, sulfide: ~40 min and polysulfide II ~44 min. The standards were in the ranges of 50-1000 µM for all compounds except polysulfides. As no standards were available for polysulfides, the concentration of these compounds remained relative.

8.2. Determination of sulfate using HPLC

The concentration of sulfate in culture samples of *A. vinosum* was determined by anion excange HPLC with indirect UV-detection based on the method by Rethmeier *et al.* (1997).

Solutions

Solvent A	4 mM *p*-hydroxybenzoic acid pH 10
Solvent B	HPLC-grade methanol (Roth, Karlsruhe, Germany)

1 mL culture sample was centrifuged for 3 min at 13000 ***g***. The supernatant was transferred to a fresh tube and stored at -20°C until quantification. 200 µL of the thawed and once more centrifuged supernatant (5 min, max. speed) were filled into an HPLC vial and 100 µL were injected by the autosampler into the sample loop. As column served the anion exchanger PRP-X100 (4.1 x 150 mm) (Hamilton, Bonaduz, Switzerland) protected by a guard column of the same material. The column was kept at a temperature of 25°C. The separation of the

sample was achieved by isocratic elution using 97.5% solvent A and 2.5% solvent B (flow rate 2 mL min^{-1}). The decrease in UV absorbance as sulfate eluted was detected at 310 nm by UV detector UV150. The retention time of sulfate was ~9 min. Standards were used in the range of 0.5-5 mM sulfate in ultra-pure water.

8.3. Determination of elemental sulfur

The concentration of elemental sulfur in culture samples of *A. vinosum* was determined by a modified cyanolysis based on Bartlett and Skoog (1954).

Solutions

Ferric nitrate reagent	30 g $Fe(NO_3)_3$ x 9 H_2O in 34 mL 65 % HNO_3 ad 100 mL H_2O_{demin}

A culture sample containing up to 200 nmol of elemental sulfur was centrifuged at 13000 ***g*** for 3 min. The supernatant was discarded and the sedimented cells were stored at -20°C. The thawed pellet was resuspended in 200 µL demineralized water, mixed with 100 µL 0.2 M sodium cyanide solution and incubated for 10 min at 100°C. After cooling, 650 µL H_2O_{demin} and 50 µL ferric nitrate reagent were added and the preparation was centrifuged for 2 min at full speed. The supernatant was poured into a quartz cuvette and the absorption was measured at 460 nm against a chemical blank. Sodium thiocyanate was used to create standards in the range of 0-300 nmol per preparation (200 µL).

III. Results

1. Insights into the regulation of the *dsr* operon

The regulation of *dsr* gene expression has so far not been investigated and almost nothing is known about it. Northern blot analyses showed an enhanced transcription of the *dsr* genes under sulfide-oxidizing conditions and implicated a secondary promoter for *dsrC* probably located in the *dsrF* gene region (Pott and Dahl, 1998; Pott-Sperling, 2000). An enhanced production of the Dsr proteins under sulfur-oxidizing conditions was previously shown by Western blot analyses (Dahl *et al.*, 2005). Further investigations were not performed and a more detailed survey had been missing until now.

In the course of this work, *dsr* promoter activity was investigated under various growth conditions by transcriptional and translational reporter gene fusions. Furthermore, the transcription pattern of several *dsr* genes was examined under photoorganoheterotrophic and photolithoautotrophic growth conditions by performing absolute quantitative real-time RT-PCR using RNA isolated from *A. vinosum* wild-type and interposon mutants 21D and 34D (Pott and Dahl, 1998; Dahl *et al.*, 2005). Additionally, the possible DNA-binding capability of the DsrC protein was investigated by electrophoretic mobility shift assays (EMSA). Earlier structural analyses had indicated the presence of a helix-turn-helix (HTH)-like motif in the protein (Cort *et al.*, 2001; Cort *et al.*, 2008), making DsrC a possible candidate for a regulatory protein.

1.1. Expression studies with reporter gene fusions

The examination of the *dsr* promoter activity under various growth conditions was performed by utilizing transcriptional and translational reporter gene fusions with *lacZ*. The gene *lacZ* from *E. coli* encodes for β-galactosidase, an enzyme that hydrolyzes β-D-galactosides. The enzyme activity can easily be measured using chromogenic substrates, like the colorless synthetic compound *o*-nitrophenyl-β-D-galactoside (ONPG) that is hydrolyzed to yield yellow-colored *o*-nitrophenol. If the ONPG concentration is in excess, the amount of *o*-nitrophenol produced is proportional to the amount of enzyme present (Miller, 1972), thus allowing conclusions to be drawn concerning the promoter activity. The transcriptional fusion joins the *dsr* promoter $dsrA_P$ to a promoterless *lacZ* gene that contains its own translational start codon and *rbs*. The β-galactosidase expression is proportional to the rate of transcription of the *dsrA* gene. In the translational fusion, *dsr* promoter region and the first 12 bp of the *dsrA* gene are joined in frame to the eighth codon of the *lacZ* gene that lacks its transcriptional and translational start site. Thus, the specific activity of the resulting β-galactosidase fusion protein reflects the rates of both transcription and translation of the *dsrA* gene.

1.1.1. Construction of reporter gene fusion plasmids

In order to create the transcriptional gene fusion, a 908 bp DNA fragment, encompassing the *dsr* promoter $dsrA_P$, was amplified by standard PCR using *Pfu* polymerase, introducing *Eco*RI and *Pst*I restriction sites via modified primers (GfdsrPromf2, GfTKdsrProm2). *A. vinosum* Rif50 genomic-DNA served as template. The *Eco*RI/*Pst*I digested fragment was inserted into pK18*mobsacB*, yielding pKdsrProm. The *lacZ* gene, including its *rbs*, was amplified using lacZrbsf1 and lacZrbsr1 as primers and *Escherichia coli* K-12 genomic-DNA as template. *Pst*I and *Hin*dIII restriction sites were introduced via the modified primers. The amplicon was digested and ligated to the 6560 bp *Pst*I/*Hin*dIII fragment of pKdsrProm, resulting in the $dsrA_P$-*lacZ* transcriptional fusion plasmid pTS (Figure III.1).

The translational gene fusion was generated by amplifying the *dsr* promoter region, including the first 12 bp of the *dsrA* coding region, using the primers GfdsrPromf1 and TLGfdsrPromr1 that introduced *Pst*I and *Hin*dIII restriction sites, respectively. The fragment was inserted into the plasmid pK235 (Franz, 2010), a pK18*mobsacB* plasmid containing the promoterless *lacZ* gene from the translational *lacZ* fusion vector pPHU235 (Hübner *et al.*, 1991), resulting in the *dsrA'-lacZ* translational fusion plasmid pTL (Figure III.1).

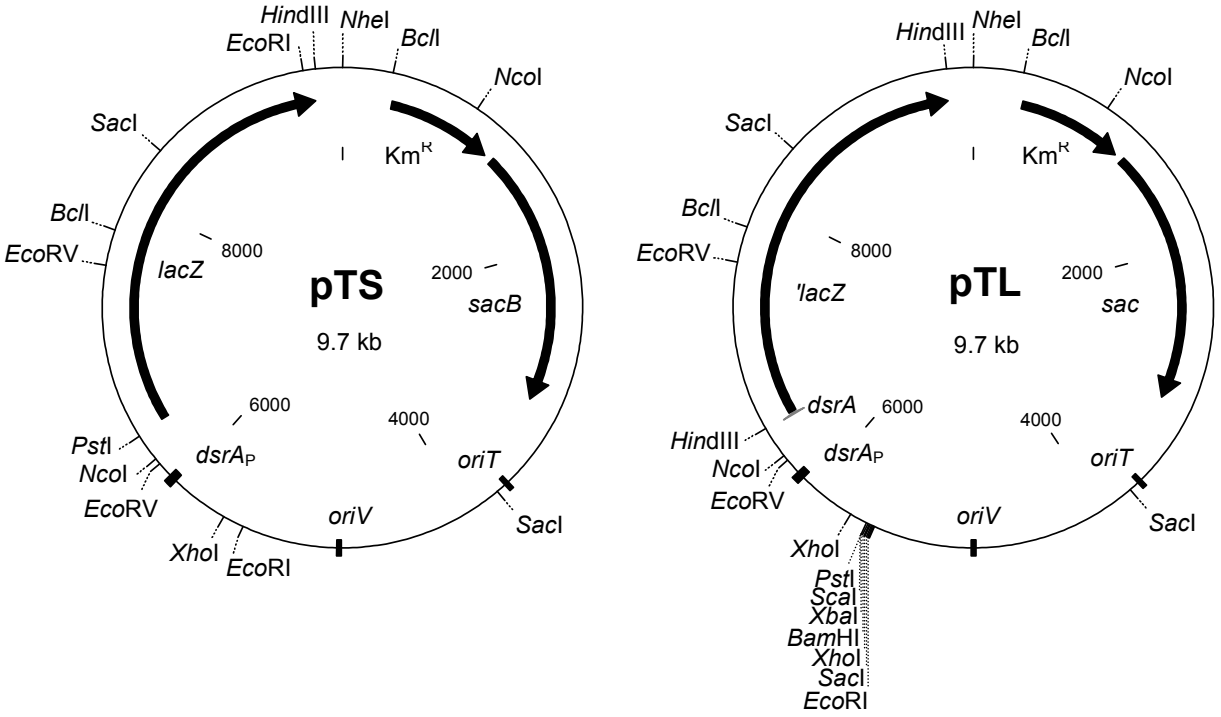

Figure III.1. Maps of the transcriptional and translational gene fusion plasmids pTS and pTL.

The gene fusion plasmids were transferred into *A. vinosum* Rif50 using conjugation and were stably integrated into the genome via single-crossover under antibiotic stress as the plasmids cannot replicate in *A. vinosum*. This ensures that only a single copy of the gene fusion

construct is present in the cell. The measured β-galactosidase activity is therefore directly proportional to the *in vivo* expression level of *dsrA*.

1.1.2. Expression of *dsrA* under sulfur-oxidizing conditions

The expression of the *dsrA* gene was examined in *A. vinosum* wild-type grown under photoorganoheterotrophic conditions and compared to the expression under photolitho-autotrophic growth conditions. The reporter gene fusion plasmid-carrying strains were grown on modified Pfennig's medium with 2 mM sulfide, thiosulfate or malate as electron donors for 24 h before β-galactosidase activity was tested. *A. vinosum* wild-type itself did not exhibit any β-galactosidase activity. As expected, the specific β-galactosidase activity was significantly raised under sulfur-oxidizing conditions. In case of the transcriptional gene fusion, the β-galactosidase activities were at a low level in malate-grown cells and three times higher under sulfur-oxidizing conditions (Table III.1). A similar level of increase was observed for the activities of the translational fusion. This increase was also observed when thiosulfate instead of sulfide was used as electron donor by the pTL carrying strain. The regulation of the *dsrA* gene expression is sensitive to the presence of reduced sulfur compounds.

Table III.1. Expression of transcriptional and translational gene fusions. Photoorganoheterotrophically grown cultures containing transcriptional (*dsrA*$_P$-*lacZ*) or translational (*dsrA'-lacZ*) gene fusion plasmids were used to inoculate modified Pfennig's medium containing 2 mM of the indicated electron source. The specific β-galactosidase activity is given in nmol *o*-nitrophenol min^{-1} (mg protein)$^{-1}$. The average protein content was 500 µg mL^{-1}. The results represent the means and standard deviations of three independent measurements. ND, not determined.

	Specific β-galactosidase activity	
Electron source	*dsrA*$_P$-*lacZ*	*dsrA'-lacZ*
Malate	2.9 ± 0.7	42.6 ± 1.7
Sulfide	9.1 ± 0.9	96.2 ± 27.1
Thiosulfate	ND	89.5 ± 9.4

As essentially the same expression pattern was observed for the translational gene fusion as for the transcriptional fusion, regulation on the post-transcriptional level appears not to have a major influence on the production of DsrA under the tested conditions. Nevertheless, the β-galactosidase activities were roughly ten times higher for the translational fusion than for the transcriptional fusion, demonstrating the importance of the native ribosome binding site for the expression of *dsrA* in *A. vinosum*. All subsequent experiments were performed with the DsrA'-LacZ fusion.

The influence of the initial concentration of sulfide on the expression level of *dsrA* was examined by determining the β-galactosidase activites of the *dsrA'-lacZ* fusion carrying strain

grown on media containing various sulfide concentrations. As can be seen in Table III.2 and Figure III.2, the higher the initial sulfide concentration, the higher the measured β-galactosidase activity. Apparently, the expression level of *dsrA* is dependent on the strength of the inducing signal.

Table III.2. Influence of the concentration of sulfide on the expression level of *dsrA'-lacZ*. Photoorganoheterotrophically grown culture containing translational (*dsrA'-lacZ*) gene fusion plasmid was used to inoculate modified Pfennig's medium with the indicated sulfide concentrations. The specific β-galactosidase activity is given in nmol *o*-nitrophenol min^{-1} (mg protein)$^{-1}$. The average protein content was 500 µg mL^{-1}. The results represent the means and standard deviations of three independent measurements.

Sulfide	Specific β-galactosidase activity
0.0 mM	36.7 ± 3.8
0.2 mM	44.0 ± 0.2
0.5 mM	57.0 ± 8.6
2.0 mM	85.1 ± 10.5
6.0 mM	110.7 ± 8.0

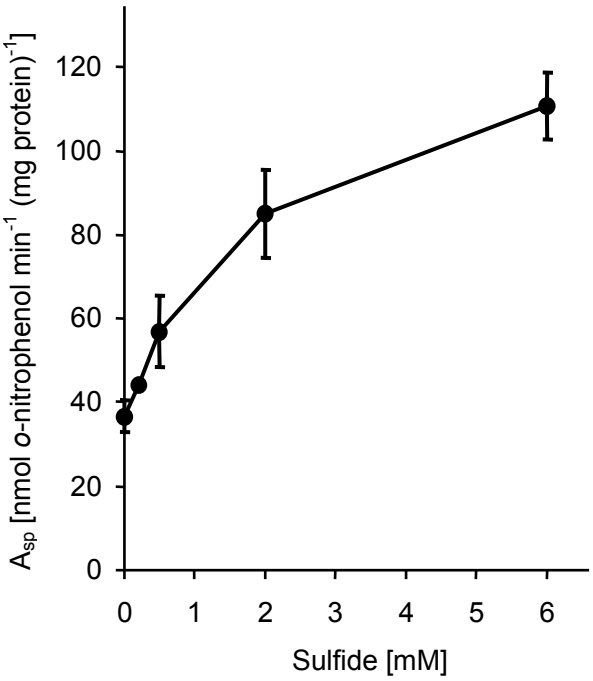

Figure III.2. Influence of the initial concentration of sulfide on the expression level of *dsrA'-lacZ*. Photoorganoheterotrophically grown *A. vinosum* cultures containing the translational gene fusion plasmid were incubated for 24 h in modified Pfennig's medium with different concentrations of sulfide before the β-galactosidase activities were determined (*cf*. Table III.2).

1.1.3. The time-course of *dsrA* expression under sulfur-oxidizing conditions

The time-course of the *dsrA* expression during sulfide oxidation was examined using the translational gene fusion-carrying strain and incubating it in a 1 L batch culture with 2 mM sulfide under controlled conditions (Figure III.3). As expected for the purple sulfur bacterium *A. vinosum*, sulfide was immediately metabolized and intracellular sulfur globules were

formed. The stored sulfur was further oxidized to the end product sulfate. Sulfite was not detected during sulfur oxidation. The β-galactosidase activity started at a low level and increased significantly after sulfide had been almost completely oxidized and sulfur globules had been formed. The activity increased simultaneously to the sulfate production. The high specific β-galactosidase activities observed were due to the optimized conditions under which the culture was grown. Apparently, sulfide itself does not directly induce *dsrA* expression and the oxidation of stored sulfur to sulfite is the rate-limiting step during the oxidation of sulfur to sulfate.

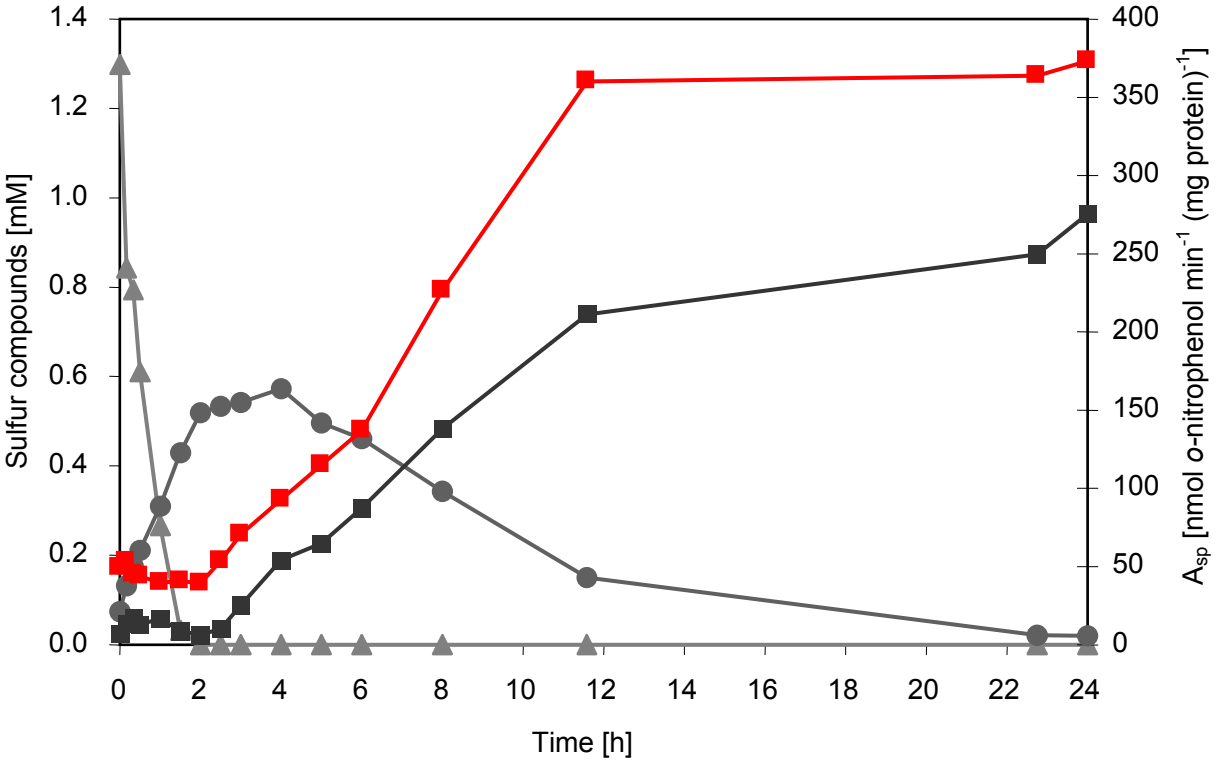

Figure III.3. Time-course of *dsrA'-lacZ* expression under sulfur-oxidizing conditions. The oxidation of sulfide (▲), formation and degradation of sulfur (●), production of sulfate (■) and expression of *dsrA'-lacZ* (■) were examined in a thermostatted fermenter with modified Pfennig's medium containing 2 mM sulfide. Sulfide could not be completely recovered as sulfate due to loss of gaseous H_2S during sampling. The high specific β-galactosidase activities were due to the optimized conditions under which the culture was grown. The protein content was 84 µg mL^{-1} at the onset of the experiment and amounted to 106 µg mL^{-1} at the end. A representative of two independent experiments is shown.

1.1.4. Inhibition of *dsrA* expression by malate and sulfite

A. vinosum is able to utilize organic compounds as alternative photosynthetic electron donors (Fuller *et al.*, 1961; Pfennig and Trüper, 1989). Therefore, the question arose whether the expression of *dsrA* would be inhibited by the presence of an organic electron donor like malate. The translational reporter strain was incubated on malate + sulfide-containing medium and the β-galactosidase activity was examined in comparison to cultures grown on either malate or sulfide (Table III.3). The malate + sulfide-grown cells showed the same level

of activity as sulfide-grown cells, showing that the presence of malate had no influence on the expression of *dsrA*.

Table III.3. Influence of malate or sulfite on the expression of *dsrA'-lacZ*. Photoorgano-heterotrophically grown culture containing translational (*dsrA'-lacZ*) gene fusion plasmid was used to inoculate modified Pfennig's medium containing 2 mM of the indicated electron source. The specific β-galactosidase activity is given in nmol *o*-nitrophenol min^{-1} (mg protein)$^{-1}$. The average protein content amounted to 500 µg mL^{-1}. The results represent the means and standard deviations of three independent measurements.

Electron source	Specific β-galactosidase activity
Sulfide	96.2 ± 27.1
Malate	42.6 ± 1.7
Malate + sulfide	96.4 ± 10.5
Sulfite	39.0 ± 7.4
Sulfite + sulfide	94.3 ± 30.9

Sulfite is the proposed product of the reaction catalyzed by reverse-acting sulfite reductase (Schedel *et al.*, 1979; Frigaard and Dahl, 2009). As such, sulfite could affect the expression of the sulfite reductase-encoding genes *dsrAB*. However, when sulfite was added to the medium, the β-galactosidase activity did not decrease compared to the activity exhibited under photoorganotrophic conditions (Table III.3). Comparison of the specific β-galactosidase activities of cells grown on sulfite + sulfide to cells grown on sulfide alone showed the activities to be virtually identical. Clearly, sulfite does not inhibit the expression of *dsrA* in *A. vinosum*.

1.2. Expression studies using real-time RT-PCR

The examination and comparison of the transcription patterns of several *dsr* genes was performed using absolute quantitative real-time reverse transcriptase (RT)-PCR. Real-time RT-PCR is a highly sensitive technique that enables the amplification and quantification of a specific RNA sequence. The reverse transcription of the RNA and specific amplification of cDNA with simultaneous quantification were performed in a one-step reaction. The dye SYBR Green I bound all double-stranded DNA molecules and emitted a fluorescent signal of a defined wavelength upon binding. The fluorescence generated was directly proportional to the amount of PCR product, provided the reaction was in the exponential phase. The initial amount of target RNA was determined using absolute quantification with external gene-specific RNA standards. By using RNA standards that contained the target sequence the variable efficiency of reverse transcription was taken into account, thus guaranteeing comparability between the samples and the standards. Absolute quantification determines the absolute amount of target contrary to relative quantification which determines the ratio

between the amount of target and an endogenous reference molecule (*e. g.* housekeeping gene). The latter requires the expression of the reference gene to be known under all tested conditions. As even so-called housekeeping genes show dramatic changes in their expression levels under different conditions (Gourse *et al.*, 1996; Vandecasteele *et al.*, 2001) and the expression level of a housekeeping gene in *A. vinosum* has so far not been studied, the absolute quantification was the method of choice.

The expression of the genes *dsrA*, *dsrE, dsrC, dsrL, dsrR,* and *dsrS* was investigated under photoorganoheterotrophic and photolithoautotrophic conditions. With the exception of *dsrA*, encoding the α-subunit of the dissimilatory sulfite reductase, these genes encode for proteins of uncertain function. Photoorganoheterotrophically grown *A. vinosum* cultures of the wild-type and the mutants 21D and 34D were incubated for 3 h in modified Pfennig's medium with either 2 mM malate or 2 mM sulfide before total RNA was isolated. Three hours after induction, *A. vinosum* usually has completely metabolized the added sulfide, the maximum content of stored sulfur globules has been reached and the oxidation of sulfur globules has started. The 21D mutant carries an insertion of a kanamycin Ω interposon in *dsrB* thereby prematurely terminating the transcription that started at the *dsrA* promoter (Pott and Dahl, 1998; Dahl *et al.*, 2005). In the mutant 34D, the Ω cassette had been inserted into the gene region of *dsrH* (Pott and Dahl, 1998; Pott-Sperling, 2000).

1.2.1. Construction of gene-specific RNA standards

The external RNA standards for each target sequence were constructed following the protocol of Fey *et al.* (2004). A DNA fragment was generated using primers that were located approximately 300 bp up- and downstream of the RT-PCR target. The T7 promoter sequence was added to the forward primer, enabling the subsequent transcription of the PCR product (Figure III.4). The resulting RNA fragments were sequentially diluted to yield six RNA standards in the range of 10^4 – 10^9 copy numbers for each target.

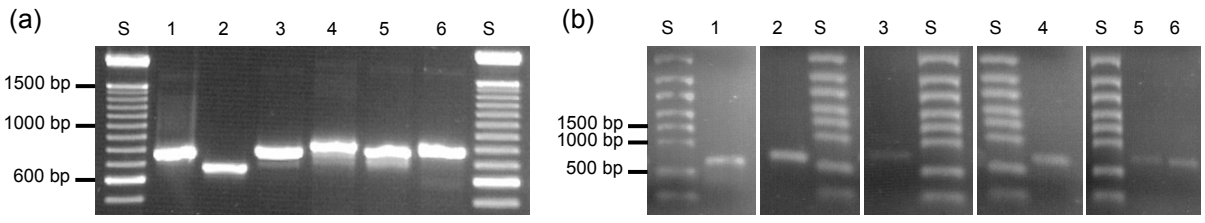

Figure III.4. Construction of gene-specific RNA standards. (a) DNA fragments used in the creation of the RNA standards (approx. 800 bp). S: 100 bp DNA ladder; 1: *dsrA*; 2: *dsrE*; 3: *dsrC*; 4: *dsrL*; 5: *dsr*; 6: *dsrS*. **(b)** RNA standards. S: RNA ladder; 1: *dsrA*; 2: *dsrE*; 3: *dsrC*; 4: *dsrL*; 5: *dsr*; 6: *dsrS*.

In all cases the gene-specific RNA standards yielded calibration curves of high linearity (correlation coefficient >0.990). Melting curve analyses and gel electrophoresis following the RT-PCR revealed no unspecific products.

1.2.2. Expression of *dsr* genes in the wild-type and the mutants 21D and 34D

In the wild-type, the transcript level of *dsrA* was very low under organoheterotrophic growth conditions and clearly increased during sulfur oxidation (Figure III.5). In light of the results of the transcriptional gene fusion experiments, this outcome was to be expected. The same pattern was observed for the genes *dsrE, dsrC, dsrL, dsrR,* and *dsrS*, indicating that all of the encoded gene products are indeed involved in sulfur oxidation (Figure III.5). The transcript levels of the genes *dsrL* and *dsrR* were very similar to that of *dsrA*. In contrast to this, the transcript level of *dsrE* was similar to *dsrA* under heterotrophic conditions but six times higher than that of *dsrA* under sulfur-oxidizing conditions. The genes *dsrC* and *dsrS* exhibited 18 times higher transcript levels under heterotrophic conditions compared to *dsrA* but only five times higher transcript levels when *A. vinosum* was grown on sulfide.

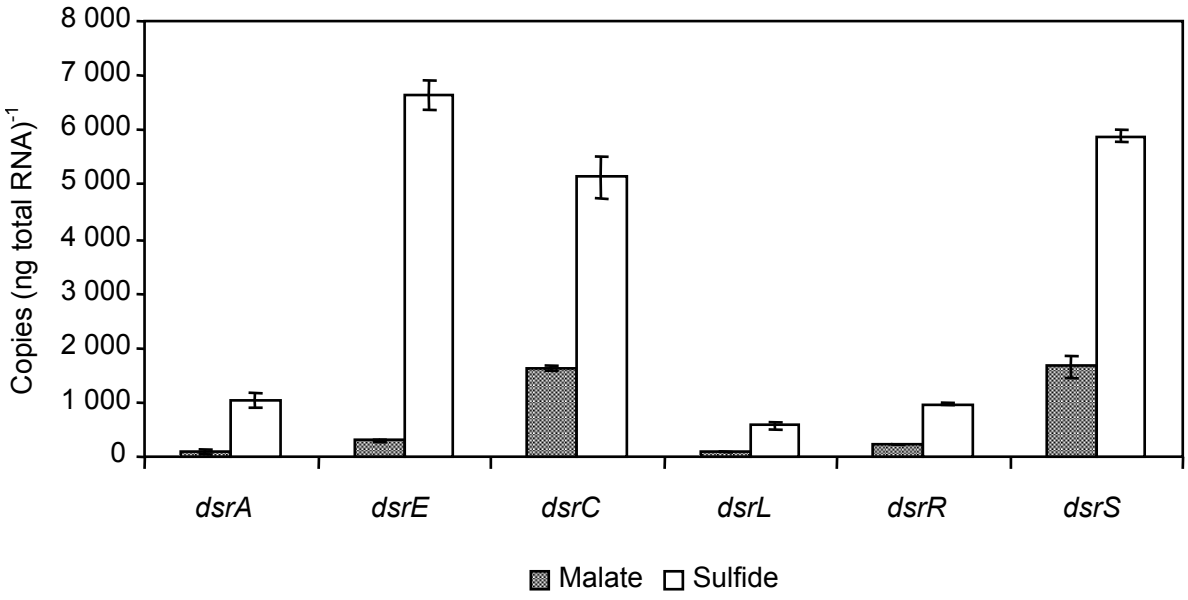

Figure III.5. Expression levels of six *dsr* genes in the *A. vinosum* wild-type under photoorganoheterotrophic (malate) and photolithoautotropic (sulfide) conditions determined by real-time RT-PCR. 250 ng of total RNA were used as template. Quantified external RNA fragments containing the target sequence served as standards.

The interposon mutant 21D showed unchanged transcript levels for *dsrA* compared to the wild-type (Figure III.6). As the Ω-fragment had been inserted in the gene *dsrB,* which is located downstream of *dsrA*, this was to be expected. The upregulation of the transcription of *dsr* genes located downstream of the interposon insertion site did not occur under sulfur-oxidizing conditions and the mRNA levels of *dsrE*, *dsrL* and *dsrR* were found to be severely

reduced due to this transcriptional block. The low amount of mRNA that was detected despite the block might be due to a spurious transcriptional initiation site located downstream of the interposon. The genes *dsrC* and *dsrS*, on the other hand, were still expressed at a high level, although the mRNA levels were reduced under photolithoautotrophic conditions when compared to the levels in malate-grown 21D cells. These findings might indicate that *dsrC* and *dsrS* are additionally expressed by secondary promoters.

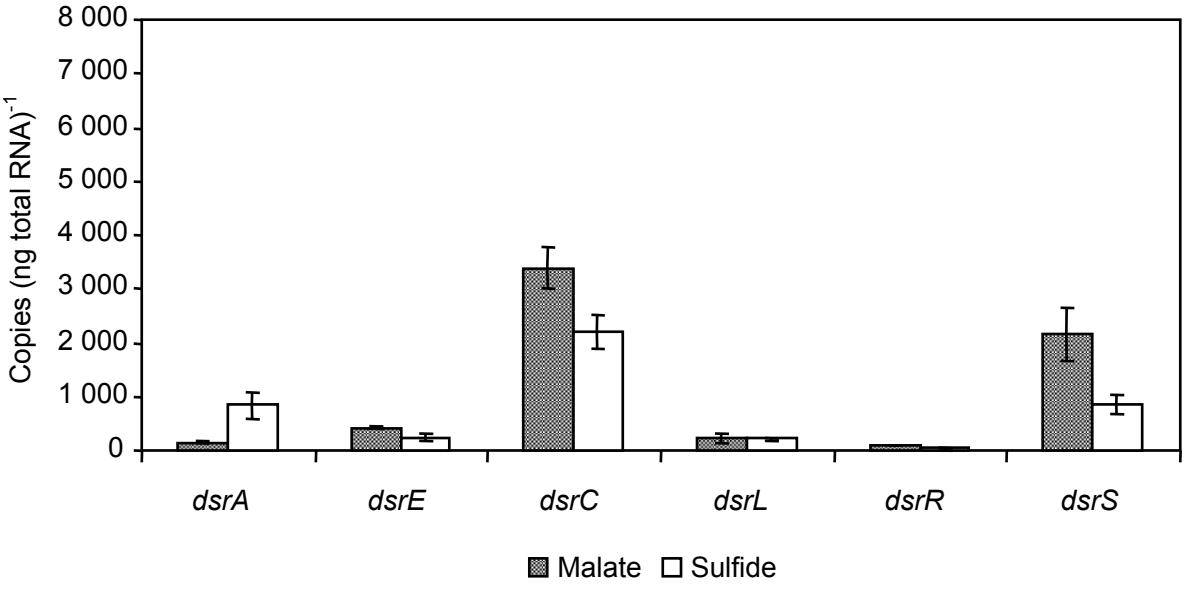

Figure III.6. Expression levels of six *dsr* genes in the *A. vinosum* 21D mutant under photoorganoheterotrophic (malate) and photolithoautotropic (sulfide) conditions determined by real-time RT-PCR. 250 ng of total RNA were used as template. Quantified external RNA fragments containing the target sequence served as standards.

Indeed, *in silico* analyses of the respective upstream gene regions using the online tools Neural Network Promoter Prediction (NNPP) and BPROM revealed potential promoter sequences in the region of *dsrHC* for *dsrC* (Figure III.7a) and *dsrNR* for *dsrS* (Figure III.7b). As typical for secondary promoters, the identified potential promoters were located in the intergenic region or at the end of a gene (Wek and Hatfield, 1986).

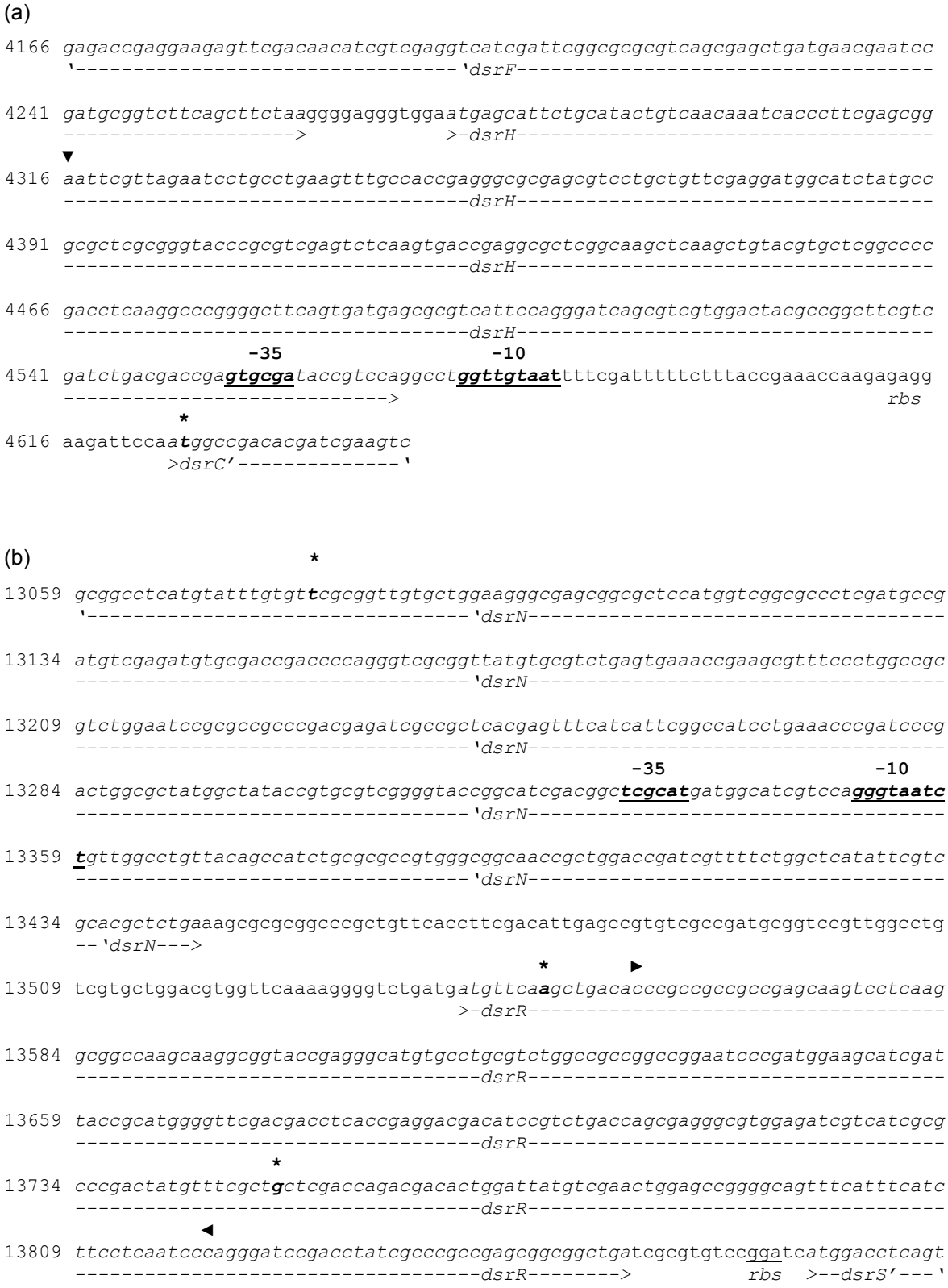

Figure III.7. The location of potential secondary promoters for (a) *dsrC* and (b) *dsrS* as determined by BPROM and Neural Network Promoter Prediction. The BPROM-predicted -35 and -10 boxes are marked bold and underlined. The NNPP-predicted transcription start points are marked bold and by an asterisk. The insertion site of the Ω-fragment of the 34D mutant is marked by a filled triangle. The borders of the deletion of the *dsrR* gene (*cf.* III.2.3) are indicated by filled triangles. Only promoters with a score of above 2.0 in case of BPROM and 0.60 in case of NNPP were considered. The sequences can be found under the GenBank acc. no. U84760.4.

Northern blot experiments by Pott-Sperling (2000) resulted in the conclusion that the potential *dsrC* promoter might be located in the *dsrF* gene region. Indeed, both promoter prediction programs predicted potential promoters in the *dsrFH* gene region, but the likelihood of them being false positives was significantly higher than for those of the *dsrHC* gene region (Figure III.8).

(a)

```
Promoter Pos:   4590                  LDF-   2.39
-10 box at pos.   4575 ggttgtaat      Score    52
-35 box at pos.   4555 gtgcga         Score     5

Promoter Pos:   4282                  LDF-   0.69
-10 box at pos.   4267 gggtggaat      Score    36
-35 box at pos.   4242 atgcgg         Score     2
```

(b)

Start	Promoter Sequence	End	Score
4157	gaggacatggagaccgaggaagagttcgacaacatcgtcg**a**ggtcatcga	4206	0.48
4551	ccgagtgcgataccgtccaggcctggttgtaattttcgat**t**tttctttac	4600	0.42
4586	tcgatttttctttaccgaaaccaagagaggaagattccaa**t**ggccgacac	4635	0.73

Figure III.8. Promoter prediction for the coding strand of the region upstream of *dsrC* (nt 3446-4625, GenBank acc. no. U84760.4) using the (a) BPROM and (b) Neural Network Promoter Prediction software (score cutoff 0.30). The NNPP-predicted transcriptional start points are marked bold and underlined.

The mutant 34D contains an Ω interposon in *dsrH* that should result in the termination of the transcription of *dsrC* if the transcription is initiated at the originally proposed promoter in the *dsrFH* gene region.

The interposon mutant 34D exhibits a similar transcription pattern for *dsrA* and *dsrE* to the wild-type, though the transcript level of *dsrE* under sulfur-oxidizing conditions is three times lower (Figure III.9). Interestingly, the transcription pattern and levels of the downstream encoded genes are quite similar to that of the 21D mutant. The transcription of *dsrC* appears not to be negatively influenced by the insertion of the Ω interposon when compared to the 21D mutant. This result corroborates the conclusion that the *dsrC* promoter is located in the *dsrHC* region.

It should be noted that the intergenetic region between *dsrH* and *dsrC* exhibits a conspicuously low GC content of only 35.7 mol% (the overall GC content of the *dsr* operon is 63.4 mol%). A GC content that low is another indicator for a function in transcription initiation (Pott and Dahl, 1998).

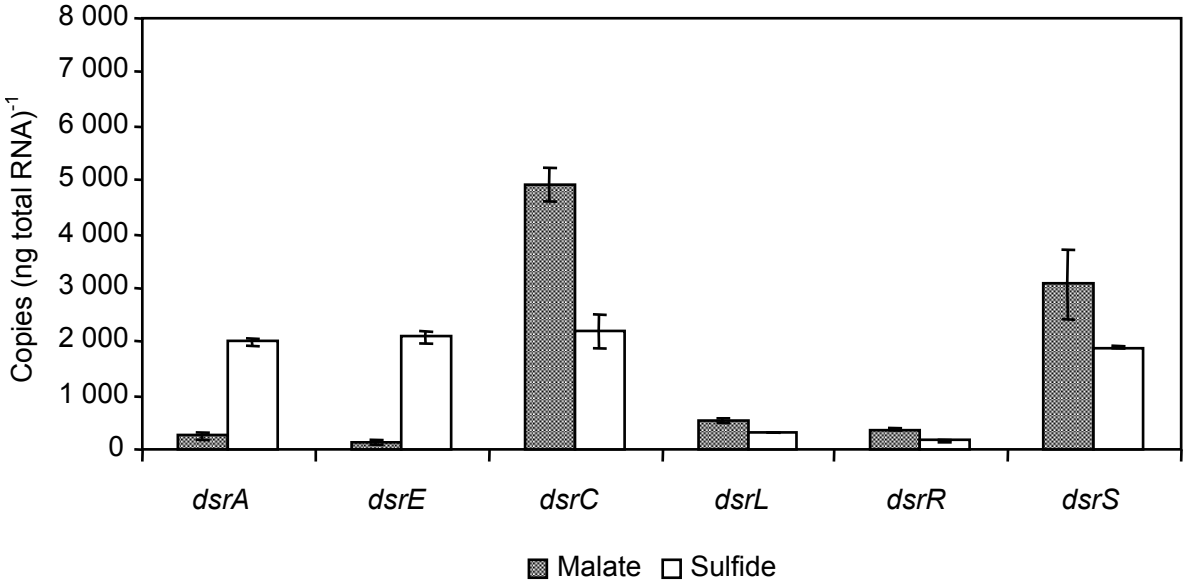

Figure III.9. Expression levels of six *dsr* genes in the *A. vinosum* 34D mutant under photoorganoheterotrophic (malate) and photolithoautotropic (sulfide) conditions determined by real-time RT-PCR. 250 ng of total RNA were used as template. Quantified external RNA fragments containing the target sequence served as standards.

The high transcript level of *dsrE* under sulfur-oxidizing conditions in the wild-type cannot be explained at the moment. But considering that secondary promoters are usually located in the intergenic region or at the end of a gene (Wek and Hatfield, 1986) and that the Ω-fragment was inserted in the first part of *dsrB* in the 21D mutant, it appears unlikely that the insertion disrupted a potential secondary promoter for *dsrE* and thus that the expression initiated at a secondary promoter is responsible for the observed transcript level. Furthermore, potential promoters in the *dsrBE* gene region were not identified using the online tools BPROM and NNPP. A possible explanation could be that the *dsrE* transcript is stabilized under sulfur-oxidizing conditions by a Dsr protein encoded downstream of *dsrE* or a protein influenced by a downstream encoded Dsr protein (*e.g.* DsrF or DsrH, the other subunits of the heterohexameric protein complex DsrEFH). These proteins are absent or reduced in the interposon mutants and could thus cause a reduced *dsrE* transcript level.

1.3. Electrophoretic mobility shift assays with the *dsrA* promoter region and DsrC

A potential helix–turn–helix (HTH) DNA-binding domain has been found in the NMR structure of *A. vinosum* DsrC (Cort *et al.*, 2008) and in the structure of the archaeal *Pyrobaculum aerophilum* DsrC (Cort *et al.*, 2001). The domains are comparable to that of bacterial transcriptional regulatory proteins. DsrC could therefore be a possible candidate for a regulatory protein of the *dsr* operon. Electrophoretic mobility shift assays (EMSA) were used to investigate a potential protein-DNA interaction. The binding of a protein to a DNA fragment leads to a reduction of its electrophoretic mobility (Lane *et al.*, 1992), thus resulting in a

retardation of the protein-bound DNA fragment in comparison to the free DNA. In this case, recombinant DsrC carrying an N-terminal His-tag was incubated with 923 bp of the *dsrA* promoter region. A 683 bp PCR-amplified fragment of the kanamycin-resistance gene served as non-specific competitor. The separation of free and bound DNA fragments was achieved using agarose gel electrophoresis.

As seen in Figure III.10a, DsrC could bind to the *dsrA* promoter fragment but not to the competitor DNA, thus demonstrating that DsrC interacts with the *dsrA* promoter region. In order to narrow down the DsrC binding site within the promoter region, the DNA fragment was cleaved with *Eco*RV or *Xho*I restriction enzymes and subsequently incubated with DsrC (Figure III.10b). In both cases only the larger of the two fragments shifted, narrowing down the potential DsrC binding region from 923 bp to a 538 bp fragment.

(a)

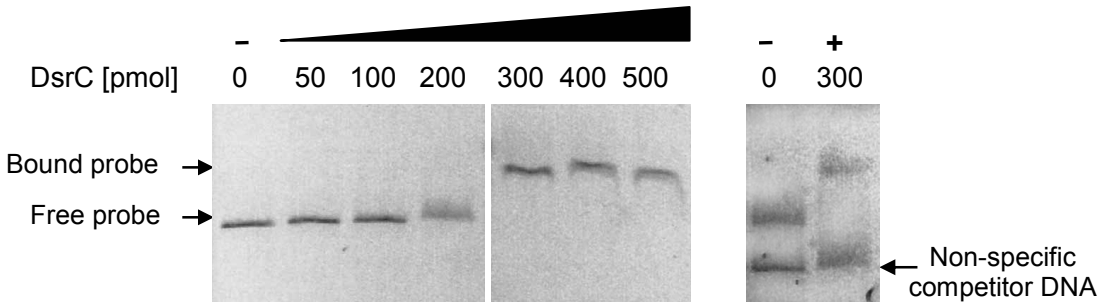

(b)

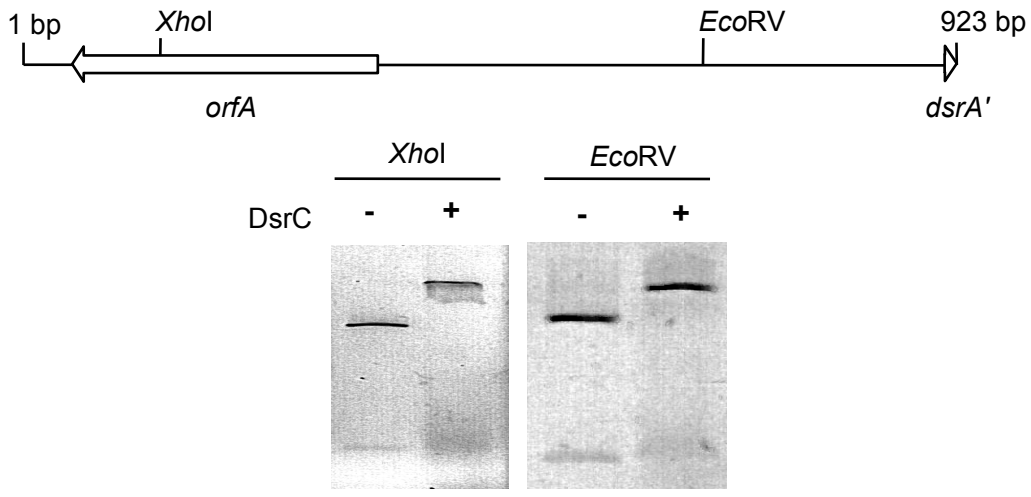

Figure III.10. DNA mobility shift assay of DsrC and the *dsrA* promoter region. (a) The 923 bp fragment of the *dsrA* promoter region was mixed with 0 – 500 pmol recombinant DsrC. A fragment of the kanamycin-resistance gene served as non-specific competitor and was incubated together with the *dsr* promoter region with (+) and without (-) 300 pmol DsrC. **(b)** Narrowing down the DsrC binding site within the *dsr* promoter region. The subfragments of the promoter region were achieved by digestion with the indicated restriction enzymes. The DNA fragments were incubated with or without 300 pmol DsrC prior to agarose gel electrophoresis.

According to Pott-Sperling (2000) the potential promoter for *dsrA* is located in a region 420 – 320 nucleotides upstream of the *dsrA* coding region (Figure III.11) and thus within the 538 bp fragment that interacts with DsrC. *In silico* analysis of the DNA fragment used in the DNA mobility shift assays utilizing the online tool REPuter revealed several noticeable sequence patterns (palindromic and reverse repeats) within the DNA fragment. Especially conspicuous is a nearly perfect 20 bp palindrome, aaactgtaat-attagagttt, that is located 391 nucleotides upstream of the *dsrA* gene and situated immediately upstream of the potential promoter. Such motifs with pronounced dyad symmetry are typically bound by symmetrical transcription factor homodimers where each subunit binds to one half of the motif via a helix–turn–helix motif. It is interesting to note in this respect that DsrC has been reported to form homodimers (Cort *et al.*, 2008).

```
  17 ttgaagacggaatcggcggcagtgtccggcagtcggatggcgaaggggtcgaatgacttcatggtgttcatggcg

                                                                        XhoI
  92 tgagaaaccctgctggtcgttaggatcgtggaatcagcgcagcaggccgctgaaggcggcctcgagtcggtcctc
                                    <---------orfA----------------------------

 167 ccagttctccggcgtgtccgggtagggcggcttgacgtccatgcggaagaaccgctcgccggaacgcgccacggc
     ----------------------------------orfA-------------------------------------

 242 ctggacgagcgggatgagttcgtcgaaggattcgaggtcttggttggcaaccaggatttcgctgagcttgagcat
     ----------------------------------orfA-------------------------------------

 317 ctgagtctgagtgtctgtatggatcgaagggttcggagcatgccacgtcatcggtatccatgcgaatcatccgtc
     ----------------------------------orfA-----------<

 392 gcgagaggcgagcgccggtacctgggtgtggttgaatgtgcaggcgtccggacccgaaaacaacagcgcccgacc

 467 agcccgcgccctgatgcgtcggcgatcatggaaacttaggtggagtattctgatgaccctgaattttagaaaact

          *          *-35                  -10    *
 542 gtaatattagagtttattgactttctggtgagctggcttgtaggatttttcgccaatccggccgctgtctttgat

                                                                        EcoRV
 617 cgctgggccacatcacctgcggaaggctccaggcactggcgtatatctccaaagggatagaggtcgaggaggata

 692 tccccccccgatcgtggaatgggcgcgcatcctgtccatgggtatattagaaaacgccgatggggttgagggtcc

 767 ggctcgatacgcacgccgagcgtgtcggtaccaccggctccacacacagacccgacgcgatgcagcgatccgcgc

 842 tgtcccggccaagcggtcgagacaggttcgtgcacgcgcacaaaccatatccgttcctggttatatcgataggag
                                                                          rbs

 917 agaccgcgcaatggctatcgaca
               >---dsrA'---'
```

Figure III.11. The location of potential promoters for *dsrA* as determined by BPROM and Neural Network Promoter Prediction and the potential binding site for DsrC. The BPROM-predicted -35 and -10 boxes are marked bold and underlined. The NNPP-predicted transcription start points are in bold face and marked by an asterisk. The potential binding site for DsrC is in red bold face. Only promoters with a score of above 2.0 in case of BPROM and 0.90 in case of NNPP were considered. The sequence can be found under the GenBank acc. no. U84760.4.

2. Characterization of the DsrR protein

The penultimate gene of the *dsr* operon in *A. vinosum* encodes the soluble cytoplasmic protein DsrR (Dahl *et al.*, 2005). Earlier sequence similarity searches revealed a homologous gene in the chemotrophic sulfur oxidizer *Thiobacillus denitrificans* (Beller *et al.*, 2006a) and showed DsrR to be very distantly related to the A-type scaffold IscA (E value 0.17) that partakes in the maturation of protein-bound iron-sulfur clusters (Pott-Sperling, 2000; Dahl *et al.*, 2005). However, DsrR lacks the three highly conserved cysteine residues of the IscA-like scaffolds that are involved in iron-sulfur cluster coordination or iron-binding (Wollenberg *et al.*, 2003; Cupp-Vickery *et al.*, 2004; Ding *et al.*, 2004). An *A. vinosum dsrR* deletion mutant exhibited a severely affected oxidation of stored sulfur, implicating DsrR to be involved in the process (Grimm, 2004), but nothing further is known about the protein.

In order to gain insights on the DsrR protein and to elucidate the function of DsrR in sulfur oxidation, the effect of the deletion of *dsrR* on the expression of other *dsr* genes was examined in depth by immunoblot analyses, RT-PCR and transcriptional and translational gene fusion experiments. The formation of the protein in the *A. vinosum* cell was verified using a DsrR-specific antiserum and the interaction of DsrR with other Dsr proteins was investigated utilizing a recombinant DsrR protein. The similarities between IscA and DsrR were studied more closely using gel filtration chromatography and iron-sulfur cluster- and iron-binding assays as well as nuclear magnetic resonance (NMR) methods.

2.1. Sequence analyses

In *A. vinosum*, the *dsrR* gene is the penultimate gene of the *dsr* operon and located between *dsrN* and *dsrS* (Figure III.12) (Dahl *et al.*, 2005). Only one copy of the gene occurs in the *A. vinosum* genome sequence (locus tag Alvin_1264, genome accession no. NC_013851). Updated similarity searches revealed homologues of the *dsrR* gene in free-living chemotrophic sulfur oxidizers, like *Thiobacillus denitrificans* (Tbd_2472, NC_007404) (Beller *et al.*, 2006a), *Thioalkalivibrio* sp. HL-EbGR7 (Tgr7_2198, NC_011901) and *Beggiatoa* sp. PS (BGP_1732, NZ_ABBZ01001151), as well as in the endosymbiotic sulfur oxidizers Candidatus *Ruthia magnifica* (Rmag_0858, NC_008610) (Newton *et al.*, 2007) and Candidatus *Vesicomyosocius okutanii* (COSY_0782, NC_009465) (Kuwahara *et al.*, 2007). The gene *dsrR* is absent from the genome of the green sulfur bacterium *Chlorobaculum tepidum* (formerly *Chlorobium tepidum* (Imhoff, 2003)) (NC_002932) (Eisen *et al.*, 2002), *Chlorobium limicola* (NC_010803), and *Chlorobaculum parvum* (NC_011027), and the purple sulfur bacterium *Halorhodospira halophila* (NC_008789). The *dsrR* gene is therefore not part of the core *dsr* genes present in all sulfur-oxidizing bacteria that form sulfur globules as an intermediate (*dsrABEFHCMKLJOPN*) (Sander *et al.*, 2006).

Table III.4. Abbreviated results of Ψ-BLAST analysis (Altschul *et al.*, 1997) with *A. vinosum* DsrR protein sequence (accession no. YP_003443235.1) as query. Results with E values greater than 0.001 were discarded.

Accession	Description	Query coverage	E value
YP_002514265.1	DsrR [*Thioalkalivibrio* sp. HL-EbGR7]	100%	4e-24
ZP_02002202.1	DsrR [*Beggiatoa* sp. PS]	98%	4e-23
AAY89956.1	DsrR [uncultured bacterium BAC13K9BAC]	97%	9e-12
YP_001219612.1	DsrR [Candidatus *Vesicomyosocius okutanii* HA]	97%	1e-11
YP_904045.1	DsrNR [Candidatus *Ruthia magnifica* str. Cm (*Calyptogena magnifica*)]	93%	9e-11
YP_316230.1	DsrR [*Thiobacillus denitrificans* ATCC 25259]	67%	3e-09
YP_553873.1	IscA (HesB/YadR/YfhF family) [*Burkholderia xenovorans* LB400]	87%	6e-05
ZP_03725748.1	HesB/YadR/YfhF family protein [*Opitutaceae bacterium* TAV2]	75%	8e-05
ZP_06838992.1	IscA (HesB/YadR/YfhF family) [*Burkholderia* sp. Ch1-1]	87%	2e-04
YP_566425.1	HesB/YadR/YfhF family protein [*Methanococcoides burtonii* DSM 6242]	89%	2e-04
YP_001995885.1	HesB/YadR/YfhF family protein [*Chloroherpeton thalassium* ATCC 35110]	87%	7e-04
ZP_03227516.1	hypothetical protein Bcoam_16845 [*Bacillus coahuilensis* m4-4]	72%	7e-04
NP_615857.1	HesB/YadR/YfhF family protein [*Methanosarcina acetivorans* C2A]	90%	9e-04
YP_981801.1	IscA (HesB/YadR/YfhF family) [*Polaromonas naphthalenivorans* CJ2]	86%	0.001

The *dsrR* gene homologues are generally located immediately downstream of *dsrN* which encodes a siro(heme)amidase (Lübbe *et al.*, 2006). In fact, in the *dsr* operon of the endosymbiont Candidatus *Ruthia magnifica* the *dsrN* gene appears to be fused to *dsrR* (Figure III.12). The intergenic region is severely abbreviated compared to *A. vinosum*, no stop codon can been identified in the coding sequence of *dsrN*, and a *dsrR*-specific ribosome binding site is missing. The *dsrS* gene, encoding a protein of unknown function, which is located downstream of *dsrR* in *A. vinosum*, is absent in the other *dsrR* containing *dsr* operons. In most cases *dsrR* represents the last gene of the operon (Figure III.12). In *Thioalkalivibrio* the *dsrR* gene is followed by Tgr7_2199, an open reading frame that encodes an uncharacterized protein of the 2-oxoglutarate (2OG) and Fe(II)-dependent oxygenase superfamily. In *T. denitrificans* a *cysG* homologue and an open reading frame encoding a hypothetical protein (Tbd_2470) are located downstream of the *dsrR* gene. *cysG* encodes an uroporphyrinogen-III-synthase, an enzyme that is involved in siroheme biosynthesis (Stroupe *et al.*, 2003).

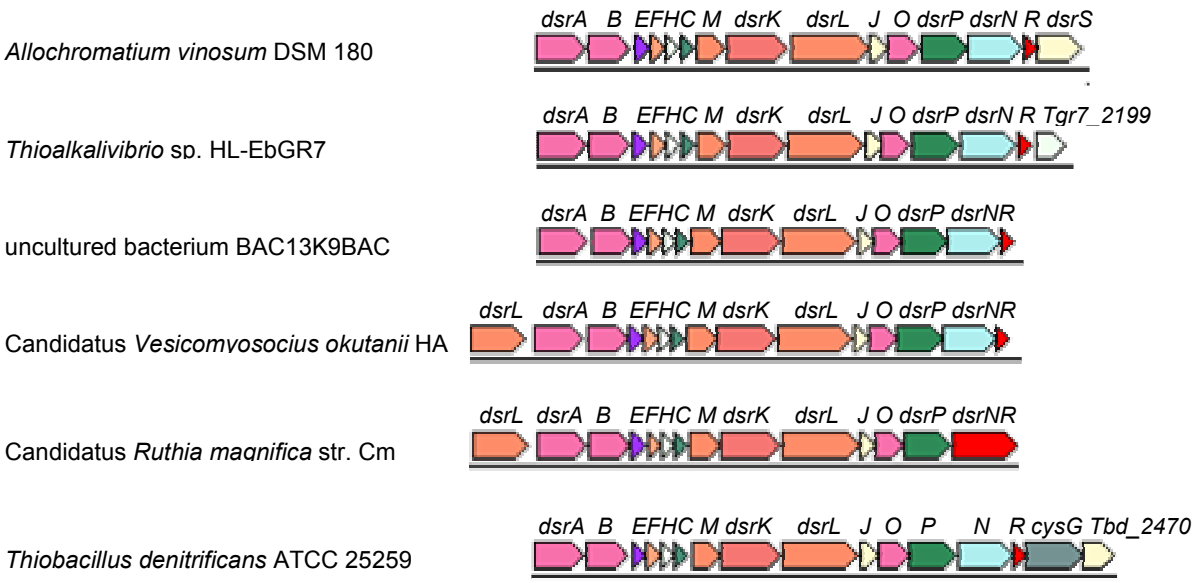

Figure III.12. The *dsr* gene regions of *dsrR*-containing organisms. The schematic representations of the *dsr* gene regions were created using the genome neighborhood tool of the IMG homepage. Sabehi *et al*. (2005) identified an entire *dsr* operon on a bacterial artificial chromosom (BAC) from an environmental sample (BAC113K9BAC) from the mediterranean sea (accession no. DQ068067). Predictions concerning the gene neighborhood in *Beggiatoa* sp. PS could not be made as only fragmented shotgun sequences were available. Underlining denotes fused genes.

The updated BLAST analysis (Table III.4) revealed the similarity of DsrR to IscA-like proteins to be much higher than previously recognized. Sequence alignments of several DsrR homologues of sulfur-oxidizing bacteria with IscA homologues of non-sulfur-oxidizing bacteria illustrate the sequence similarity between these proteins but also highlight the differences (Figure III.13). The overall sequence identity between *A. vinosum* DsrR and IscA is around 30%, while identity with the alternative A-type scaffolds SufA and ErpA is somewhat lower. Sequence identity among DsrR homologues varies but can be as low as 30%. All DsrR homologues lack the three invariant cysteine residues of the IscA protein family that are involved in iron-sulfur cluster coordination or iron binding (Wollenberg *et al.*, 2003; Cupp-Vickery *et al.*, 2004; Ding *et al.*, 2004). But sequence comparison also revealed a number of conserved acidic amino acid residues in DsrR-like proteins (*A. vinosum* DsrR Asp35, Asp45, Asp50, and Asp95). As acidic amino acids may in principle be able to bind iron, the possibility that DsrR retained a reduced iron-binding capability could not be entirely dismissed based merely on sequence data. The sequence alignment further revealed two motifs that appear to be typical for DsrR-like proteins. The first motive, Met42-Gly43-Phe44-Asp45 of *A. vinosum* DsrR, is fully conserved throughout all known DsrR proteins. The second motif, Ile89-Phe90-Leu91 of *A. vinosum* DsrR, consist of hydrophobic amino acid residues. The hydophobicity of this motif is fully conserved.

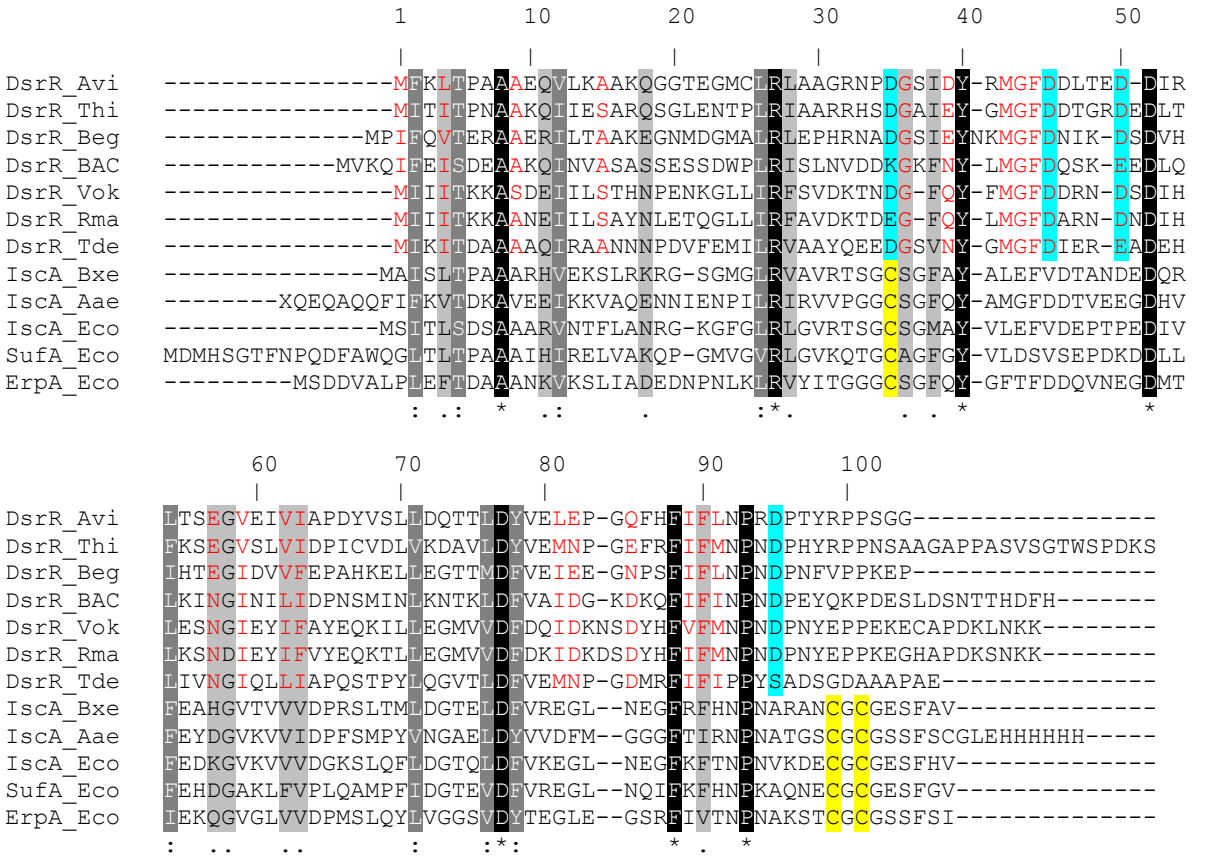

Figure III.13. Multiple sequence aligments of DsrR and IscA sequences. The alignments were generated using the program ClustalW (Chenna *et al.*, 2003). Fully conserved residues in both DsrR and IscA-like proteins are indicated by an asterisk (*) and are shaded black. Positions in which one of the strong groups (STA, NEQK, NHQK, NDEQ, QHRK, MILV, MILF, HY, FYW) is fully conserved are marked by a colon (:) and shaded gray and positions in which one of the weaker groups (CSA, ATV, SAG, STNK, STPA, SGND, SNDEQK, NDEQHK, NEQHRK, FVLIM, HFY) is fully conserved are indicated by a dot (.) and shaded light gray. Residues highly conserved only in DsrR proteins are in red and conserved acidic amino acid residues are shaded blue. Cysteine residues characteristic for IscA-like proteins are shaded yellow.
Avi, *Allochromatium vinosum* DSM 180; Thi, *Thioalkalivibrio* sp. HL-EbGR7; Beg, *Beggiatoa* sp. PS; BAC, uncultured bacterium BAC13K9BAC; Vok, Candidatus *Vesicomyosocius okutanii* HA; Rma, Candidatus *Ruthia magnifica* str. Cm; Tde, *Thiobacillus denitrificans* ATCC 25259; Bxe, *Burkholderia xenovorans* LB400 ; Aae, *Aquifex aeolicus* VF5; Eco, *Escherichia coli* K-12.

2.2. Biochemical characterization of DsrR

Sequence analyses suggest that DsrR is a soluble cytoplasmic protein of 11.4 kDa with a certain similarity to A-type scaffolds (Pott-Sperling, 2000; Dahl *et al.*, 2005). However, these postulations have not been experimentally investigated until now.

2.2.1. Production and purification of recombinant DsrR protein

In order to study the biochemical characteristics of DsrR, large amounts of the protein were necessary. A recombinant DsrR protein was produced in the *E. coli* strain BL21(DE3) under aerobic conditions. The purification of the protein was simplified by the addition of an N-

terminal oligo-histidine tag (His-tag) to the protein sequence. This was achieved by cloning the *A. vinosum dsrR* gene into the expression plasmid pET-15b, yielding the *dsrR* expression plasmid pREX.

As can be seen in Figure III.14, large amounts of the recombinant protein were produced and isolated. The protein occurred in the soluble (supernatant after centrifugation of the disrupted cells) as well as insoluble fraction (resuspended pellet). Nickel-chelate affinity chromatography was used to isolate the protein from the soluble fraction. The histidine residues of the protein bind to nickel ions immobilized by nitrilotriacetic acid groups on the agarose matrix and the His-tagged protein is thus retained on the column. The protein was eluted by step-wise increasing concentrations of imidazole that competes with the histidin residues for binding sites on the Ni-NTA resin.

The observed size of the protein of ~13 kDa in the SDS polyacrylamide gel is in accordance with the sequence deduced molecular mass of 13.6 kDa for the recombinant protein. The additional 2.2 kDa are due to the His-tag.

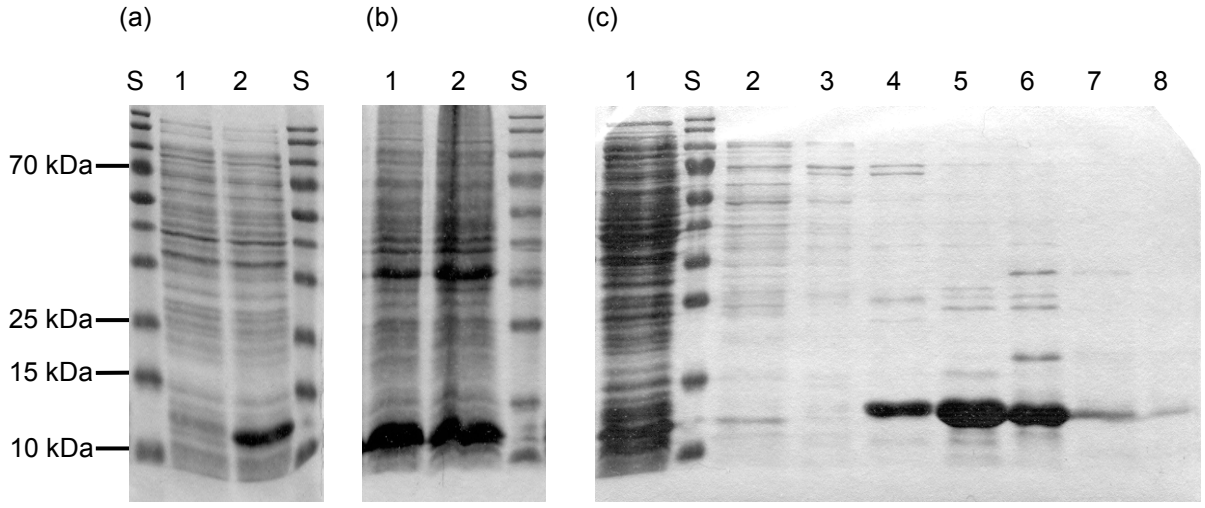

Figure III.14. Coomassie-stained SDS polyacrylamide gels documenting the production and purification of recombinant DsrR. (a) *E. coli* BL21(DE3) cells carrying pREX. 1: non-induced cells, 2: cells induced with IPTG. **(b)** Fractions after centrifugation of the disrupted cells. 1: soluble fraction, 2: resuspended insoluble fraction **(c)** Purification of recombinant DsrR by Ni-NTA chromatography. 1: wash (20 mM imidazole), 2-8: eluates (40, 60, 80, 100, 150, 200 and 250 mM imidazole). S: PageRuler Prestained Protein Ladder.

2.2.2. Testing of DsrR-specific antiserum and detection of DsrR in *A. vinosum*

The formation of the DsrR protein within the *A. vinosum* cell was investigated utilizing a DsrR-specific antiserum. The antiserum was raised against a potentially highly immunogenic synthetic peptide derived from the *A. vinosum dsrR* nucleotide sequence (Grimm, 2004). The functionality of the antiserum was tested using the recombinant DsrR protein.

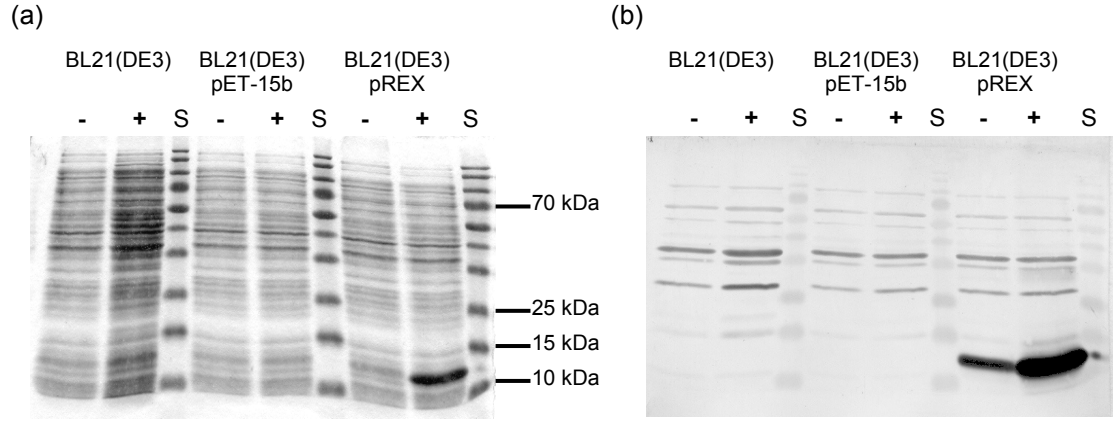

Figure III.15. Testing of DsrR-specific antiserum. (a) Coomassie-stained SDS polyacrylamide gel. **(b)** Western blot with antiserum against DsrR. The cell samples were take before (-) or after (+) induction with IPTG. S: PageRuler Prestained Protein Ladder.

The strongest signal was detected for the ~13 kDa band of the recombinant DsrR protein produced in the pREX-carrying *E. coli* BL21(DE3) cells, demonstrating that the antiserum binds to DsrR. The background signals are due to crossreactivity of the antiserum with *E. coli* BL21(DE3) specific proteins, as the same signals were detected in the BL21(DE3) samples.

The formation of DsrR in *A. vinosum* was investigated using photolithoautotrophically grown cells that were disrupted by sonication. The membrane fraction was separated from the soluble fraction by ultra-centrifugation. The presence of DsrR was detected in both fractions (Figure III.16). The signal appeared at approximately 10 kDa which is very close to the predicted molecular mass of 11.4 kDa for the native DsrR protein. In accordance with the predicted cytoplasmic location of the protein, the strongest signal was detected in the soluble fraction. The weaker signal in the membrane fraction might indicate an interaction of DsrR with membrane bound or associated proteins.

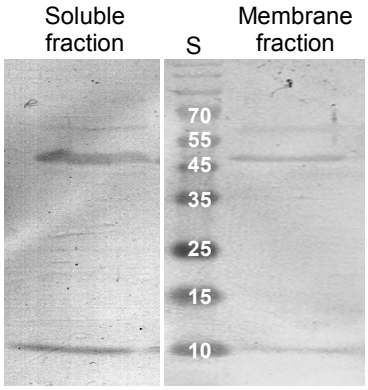

Figure III.16. Western blot analysis of the soluble and membrane fraction of *A. vinosum* with antiserum against DsrR. Each lane contained 95 µg of protein. S: PageRuler Prestained Protein Ladder [kDa].

2.2.3. State of oligomerization of DsrR

The molecular mass and state of oligomerization of DsrR was determined by gel filtration chromatography. Gel filtration separates molecules according to differences in size as they pass through the porous column matrix. By calibrating the columns with proteins of known molecular mass, the unknown mass of another protein can be determined.

The calculated molecular mass of the recombinant DsrR monomer is 13.6 kDa. The protein was loaded onto a precalibrated Superdex-75 column and the elution of the protein was monitored by absorption at 280 nm. DsrR eluted in one clear peak at an elution volume of 81 mL (Figure III.17). This volume corresponds to a molecular mass of 13.6 kDa. Recombinant DsrR does not oligomerize and occurs as a monomer.

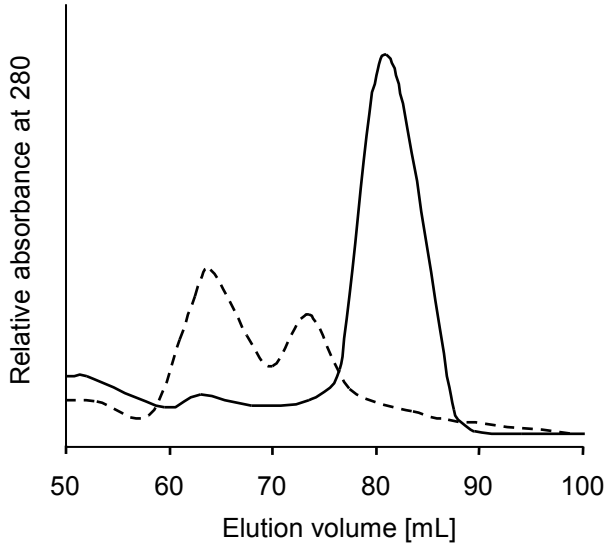

Figure III.17. Gel filtration chromatogram of recombinant DsrR (solid line) and IscA (dashed line). The proteins were loaded onto a Superdex-75 column. The elution was monitored by absorption at 280 nm. The column had been calibrated with several proteins of known molecular mass.

A recombinant IscA from *E. coli*, with a sequence deduced mass of 13.7 kDa per monomer, was loaded onto the Superdex-75 column under the same conditions as the DsrR protein. Contrary to DsrR, IscA eluted in two peaks at elution volumes of 64 mL and 73.5 mL (Figure III.17). These volumes correspond to molecular masses of 54.8 kDa and 27.4 kDa. IscA exists as tetramer and dimer.

2.2.4. Iron and iron-sulfur cluster binding of DsrR

The similarity to the iron-binding A-type scaffold IscA suggests a comparable activity for the DsrR protein. Even though the iron- or Fe-S cluster-binding cysteine residues present in the IscA-like proteins are missing, the conserved acidic amino acid residues in DsrR might facilitate a diminished iron-binding ability in the protein.

To examine this assumption, DsrR was incubated in the presence of a reducing agent with Fe^{2+} ions under anoxic conditions. The recombinant DsrR protein was divested of its N-terminal His-tag beforehand, as histidines have a low iron-binding capability by themselves. The UV-visible absorption spectra of the samples were recorded and calibrated to an absorbance at 260 nm of 1.0 (Figure III.18). The recombinant *E. coli* IscA protein without His-tag was used for comparison.

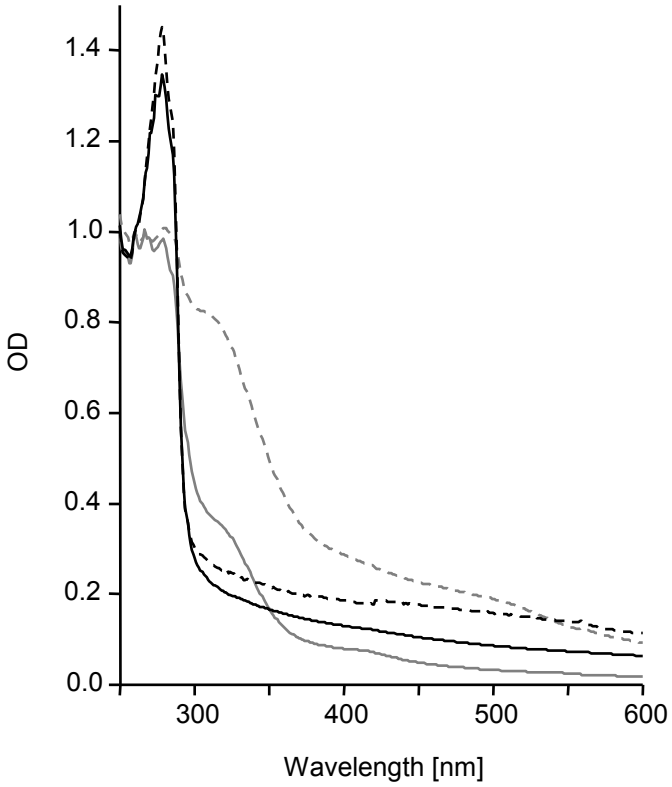

Figure III.18. Iron-binding assay of DsrR in comparison to IscA. Shown are UV-visible absorption spectra of DsrR (black) and IscA (gray) after incubation with 0 or 400 µM $Fe(NH_4)_2(SO_4)_2$ (solid and dashed lines) in the presence of 2.5 mM DTT. The proteins were repurified by passing them through a HiTrap desalting column. The spectra were calibrated to an absorbance at 260 nm of 1.0.

The IscA sample that had been incubated without iron ions nevertheless contained a small amount of bound iron, visible as an absorption peak at 315 nm, due to the presence of $Fe(NH_4)_2(SO_4)_2$ in the *E. coli* growth medium. The amplitude of the absorption peak at 315 nm dramatically increased after the protein was incubated with Fe^{2+} ions and dithiothreitol under anoxic conditions. The absorption spectrum of freshly purified recombinant DsrR did not indicate any bound iron ions, even though $Fe(NH_4)_2(SO_4)_2$ was present in the medium as well. The reconstitution of DsrR with iron ions did not lead to an increase of the amplitude at 315 nm, demonstrating that DsrR does not bind iron.

In order to also exclude a potential Fe-S cluster binding function of DsrR, Na_2S was added to the above-mentioned preparation. Following incubation with ferrous iron and sulfide, the IscA spectrum displayed a pronounced shoulder centered at 320 nm and an absorption peak at 415 nm that indicate bound iron-sulfur cluster (Krebs *et al.*, 2001; Yang *et al.*, 2006) (Figure III.19). Contrary to IscA, changes in the DsrR spectrum that would indicate bound iron-sulfur cluster were not detected. It is unlikely that DsrR serves as an alternative iron-sulfur cluster scaffold or iron-donor.

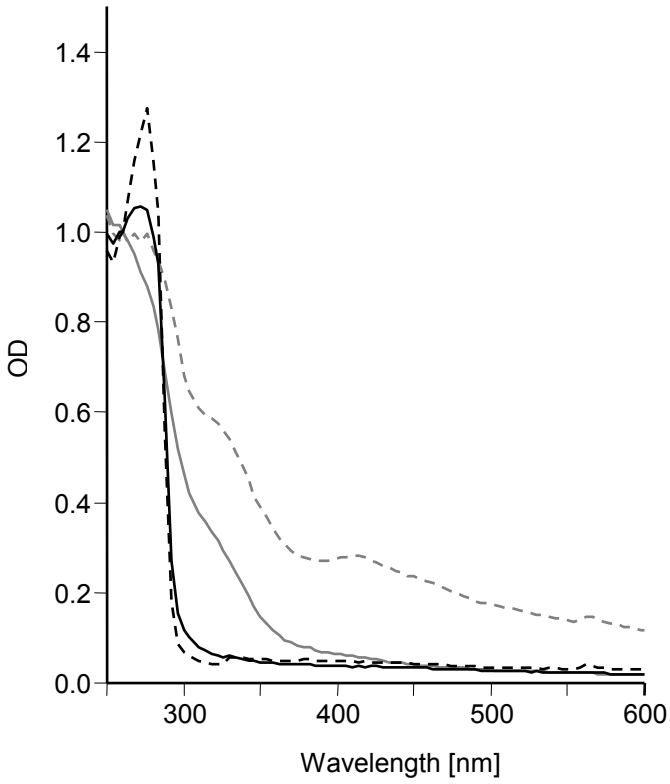

Figure III.19. Iron-sulfur cluster-binding assay of DsrR in comparison to IscA. Shown are UV-visible absorption spectra of DsrR (black) and IscA (gray) after incubation with 0 or 400 µM $Fe(NH_4)_2(SO_4)_2$ and 400 µM Na_2S (solid and dashed lines) in the presence of 2.5 mM DTT. The proteins were repurified by passing them through a HiTrap desalting column. The spectra were calibrated to an absorbance at 260 nm of 1.0.

2.2.5. Solution structure of DsrR

The structure of DsrR in aqueous solution was determined in cooperation with John R. Cort of the Washington State University who kindly performed the solution state NMR (nuclear magnetic resonance) analyses. The NMR structure clearly demonstrated that the DsrR protein displays the same fold as seen in several NMR and X-ray structures of A-type scaffolds like IscA (Bilder *et al.*, 2004; Cupp-Vickery *et al.*, 2004; Xu *et al.*, 2004), SufA (Wada *et al.*, 2005) and ErpA (Figure III.20).

The IscA-like fold, also known as the HesB-like domain fold (Murzin *et al.*, 1995), is considered to be unique to the HesB/YadR/YfhF family (Bilder *et al.*, 2004; Xu *et al.*, 2004). It is characterized by two β-hairpins opposed in two-fold symmetry that form a deep cleft. The formation of an iron-sulfur cluster binding site by the conserved Cys residues occurs upon dimer and/or tetramer formation (Bilder *et al.*, 2004; Cupp-Vickery *et al.*, 2004; Wada *et al.*, 2005; Morimoto *et al.*, 2006).

DsrR could be superimposed over the structured portion of IscA-like proteins to between 2 and 3 Å r.m.s.d. for the backbone atoms, with the exception of the NMR structure of IscA-like protein aq_1857 from *Aquifex aeolicus* (3.6 Å backbone r.m.s.d. to DsrR). DsrR was disordered in the C-terminal region beginning around residue Pro93 while the N-terminus was ordered from the beginning of the DsrR sequence. IscA-like proteins without bound iron typically exhibit a similar lack of structure in the C-terminus beginning at the equivalent proline residue, which is conserved throughout all DsrR and IscA-like proteins (*cf*. Figure III.13). In

IscA-like proteins this disordered C-terminal region contains the conserved Cys-Gly-Cys residues that are part of the Fe-S cluster binding site. Several residues at the tips of the β2-β3 and β6-β7 hairpins of DsrR exhibited decreased convergence in the NMR ensemble, probably reflecting greater mobility in these regions, a characteristic also seen in the corresponding regions of IscA-like proteins.

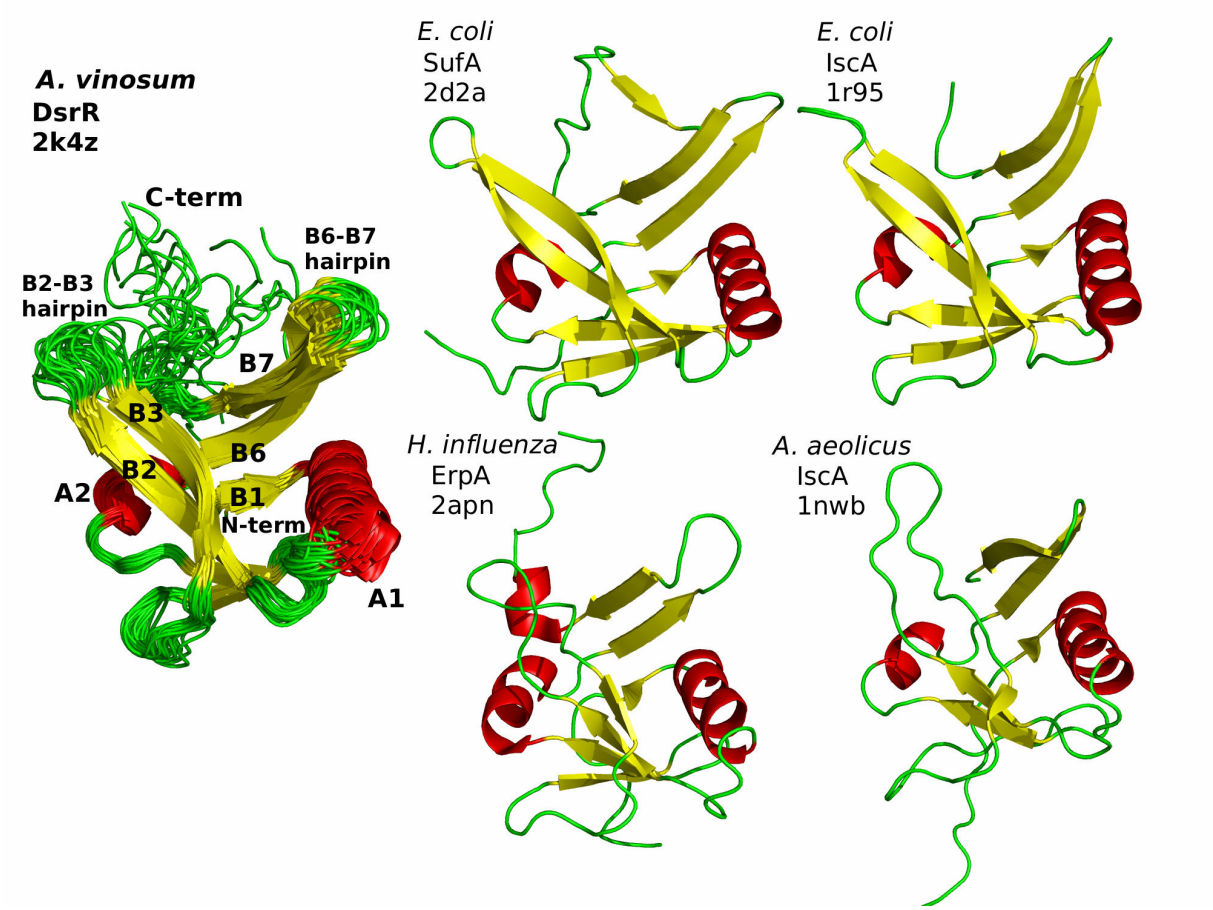

Figure III.20. Structural features of DsrR and comparison to IscA-like proteins. Left, structures of DsrR (overlaid ribbons for ensemble). Right, ribbon structures for *E. coli* IscA and SufA, *H. influenzae* ErpA, and *A. aeolicus* aq_1857, the only IscA-like protein found in this organism. The figure was provided by John R. Cort.

Contrary to various A-type scaffolds, the NMR spectra of the DsrR samples were not consistent with a multimeric species, further confirming the results of the gel filtration chromatographic analysis that DsrR occurs as monomer. Furthermore, the NMR spectra did not reveal any characteristics of a paramagnetic species and the UV-visible absorption spectra of the NMR sample did not show any absorption that was not due to the protein itself, thereby arguing against the presence of bound iron and corroborating the observations of the iron-binding assays.

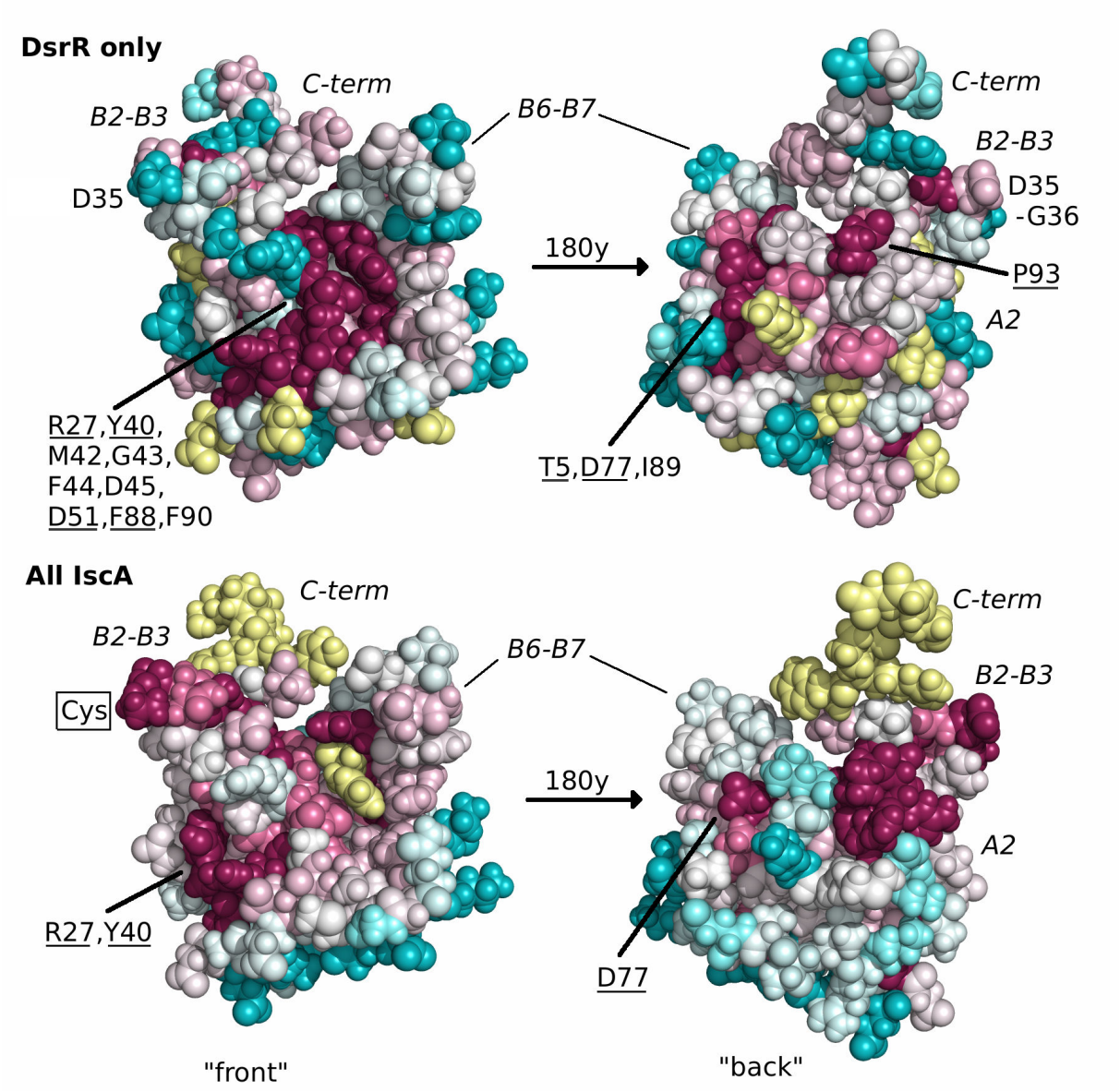

Figure III.21. Space filling structures of DsrR, colored according to conservation of residues in multiple sequence alignments of DsrR sequences only or all IscA-like sequences using ConSurf (Glaser *et al.*, 2003). Darker magenta colors indicate greater conservation, darker blue colors indicate lack of conservation, and lighter colors represent intermediate levels of residue conservation, while yellow indicates insufficient information, primarily in the C-terminus where the sequence alignment is uncertain. Residues that are particularly conserved in DsrR sequences are indicated, those also conserved in IscA are underlined. The position on the DsrR structure that is substituted with the conserved Cys residue in IscA on the β2-β3 hairpin is indicated. The other conserved IscA Cys residues are not indicated as they are align with the disordered portion of the C-terminus on DsrR. The figure is based on a picture provided by John R. Cort.

Marking the surface residues according to their conservation status in DsrR or in IscA-like proteins (*cf.* Figure III.13) revealed some interesting differences (Figure III.21). The most striking changes were found in the regions containing the conserved cysteine residues in IscA-like proteins. These regions are highly conserved in IscA-like proteins but are lacking

conservation in DsrR. On the other hand, several residues clustered in the cleft between the β2-β3 and β6-β7 hairpins are highly conserved in DsrR but not in IscA (Figure III.21), including the highly conserved Met42-Gly43-Phe44-Asp45 motif and the hydrophobic motif Ile89-Phe90-Leu91 of *A. vinosum* DsrR (*cf*. Figure III.13). Among all IscA-like proteins, conserved surface residues mainly cluster on the hairpins. However, the regions surrounding these sites in DsrR and IscA are structurally similar, despite the sequence differences. Other residues on the surface are conserved in both IscA and DsrR, including three charged residues and two partially buried aromatic residues (Arg27, Tyr40, Asp51, Asp77, and Phe88 in DsrR), most of which occur in the cleft formed by the twin β hairpins (Arg27, Tyr40, Asp51, and Phe88 in DsrR).

2.2.6. Interaction of DsrR with other Dsr proteins

To gain further information on the role of DsrR in sulfur oxidation, the interaction of DsrR with other Dsr proteins was investigated. To this purpose recombinant His-tagged DsrEFH, DsrC and DsrL were incubated with recombinant DsrR that was divested of its His-tag. Ni-NTA agarose was added so that the tagged protein and the potentially interacting protein were pulled down. The specificity of this method was confirmed by utilizing His-tagged DsrEFH and non-tagged DsrC as positive controls, while His-tagged IscS, a cysteine desulfurylase donating the sulfur during the maturation of iron-sulfur clusters, and non-tagged DsrC served as negative controls (Figure III.22a and b).

DsrR itself did not bind to nickel agarose, but in presence of the Dsr proteins DsrEFH, DsrC or DsrL, it was retained (Figure III.22c). In case of DsrEFH, the presence of DsrR was masked by DsrH in Coomassie-stained SDS gels as DsrR has roughly the same molecular mass (11.4 kDa) as the DsrEFH subunit DsrH (11.1 kDa). Therefore, immunoblot analysis with antiserum against DsrR was performed. Although the Western blot analysis revealed that a low amount of non-tagged DsrR appeared to interact with the Ni-NTA agarose on its own, the signal was much stronger when DsrEFH was present in the sample. Under the chosen conditions, DsrR appeared to interact with DsrEFH, DsrC and DsrL. All of these proteins are essential for the oxidation of stored sulfur in *A. vinosum*.

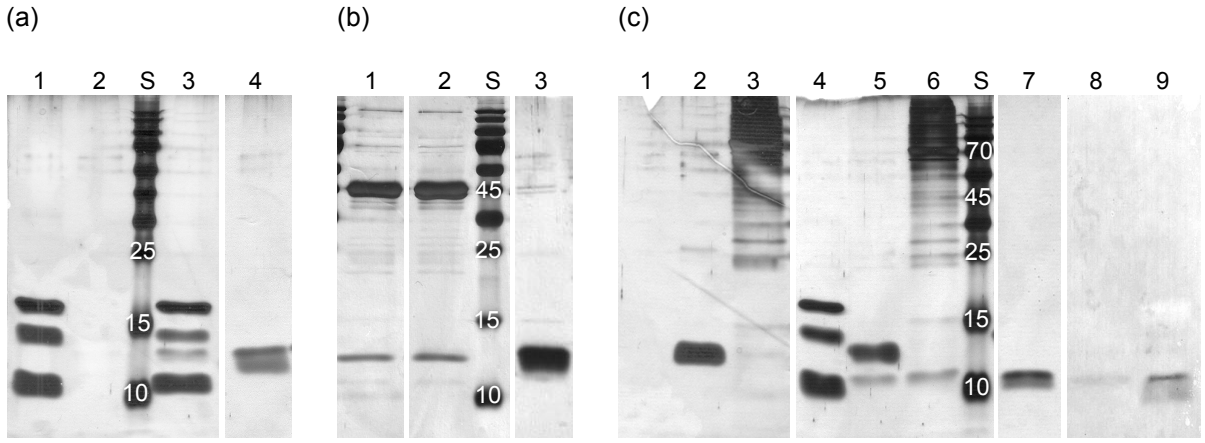

Figure III.22. Coprecipitation of several Dsr proteins with DsrR. Silver-stained SDS polyacrylamide gels. **(a)** Positive control. 1: His-tagged DsrEFH, 2: non-tagged DsrC, 3: non-tagged DsrC with His-tagged DsrEFH, 4: supernatant of 2. **(b)** Negative control. 1: His-tagged IscS, 2: non-tagged DsrC with His-tagged IscS, 3: supernatant of 2. **(c)** Coprecipitation of DsrR with other Dsr proteins. 1: non-tagged DsrR, 2: His-tagged DsrC, 3: His-tagged DsrL, 4: non-tagged DsrR with His-tagged DsrEFH, 5: non-tagged DsrR with His-tagged DsrC, 6: non-tagged DsrR with His-tagged DsrL, 7: supernatant of 1, 8-9: Western blot analysis of 1 and 4 with specific antibodies against DsrR. S: PageRuler Prestained Protein Ladder [kDa].

In Candidatus *Ruthia magnifica dsrR* appears to be fused to *dsrN* which could indicate DsrN and DsrR to be subunits of a heterooligomeric protein. In order to test this proposition, recombinant His-tagged DsrN was overproduced together with DsrR by introducing the *dsrNR* gene region of *A. vinosum* to the expression plasmid pET-15b, resulting in the plasmid pNREX. The plasmid was transferred to *E. coli* BL21(DE3) cells and the N-terminally His-tagged DsrN as well as DsrR were overproduced. In the subsequent purification using a Ni-NTA agarose column, the His-tagged DsrN bound to the column and was eluted with a step-wise increasing imidazole gradient (Figure III.23). DsrR was not retained and eluted in the flow-through instead. DsrR and DsrN do not interact as closely as for example the heterotrimeric protein complex DsrEFH where the interaction between the subunits is strong enough that by adding a His-tag to DsrE the complete complex can be isolated. A weaker, transient interaction of DsrN and DsrR cannot be excluded, but it appears unlikely that DsrR is a subunit of a DsrNR protein complex.

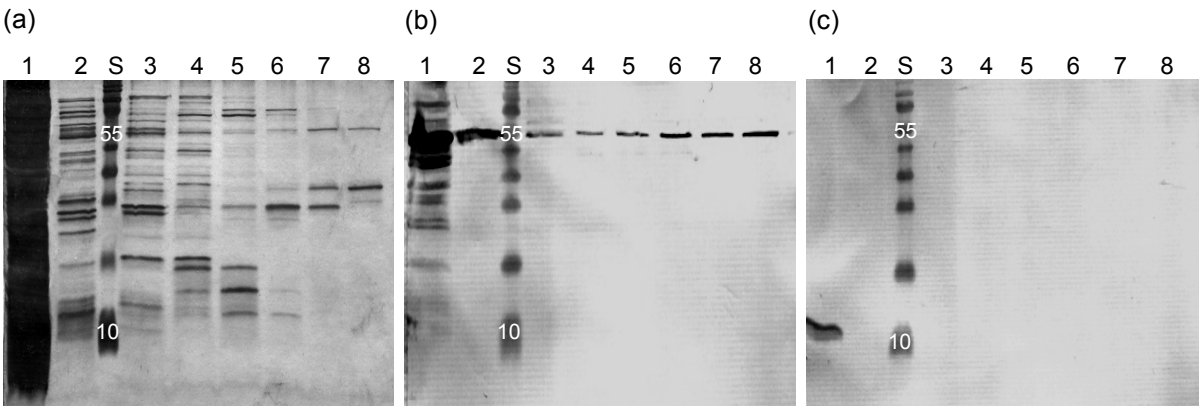

Figure III.23. Co-purification of recombinant DsrN (52.7 kDa) and DsrR (11.4 kDa) by Ni-NTA chromatography. (a) Silver-stained SDS polyacrylamide gel. **(b)** Western blot with DsrN specific antibodies**. (c)** Western blot with DsrR specific antibodies. 1: flow-through, 2: wash (20 mM imidazole), 3-8: eluates (40, 60, 80, 100, 150 and 200 mM imidazole). S: PageRuler Prestained Protein Ladder [kDa].

2.3. Physiological characterization of DsrR

The importance of DsrR for the oxidation of intracellularly stored sulfur in *A. vinosum* had been investigated by creating an in frame deletion mutant of *dsrR*. The oxidation of intermediary stored sulfur was severely affected in the Δ*dsrR* strain (Grimm, 2004). In order to confirm that the observed phenotype was due to the deletion of *dsrR*, the Δ*dsrR* mutant was complemented by reintroducing *dsrR in trans*. The oxidation rate of reduced sulfur compounds was quantified and compared between the *A. vinosum* mutant strains and the wild-type. Additionally, the effect of the deletion of *dsrR* on the formation of several Dsr proteins was investigated.

2.3.1. Complementation of a *dsrR* deletion mutant

The complementation of the Δ*dsrR* mutant was achieved by reintroducing *dsrR in trans* under control of the *dsrA* promoter. The *dsrA* promoter region of *A. vinosum* including the *rbs* of *dsrA* was amplified by standard PCR using *Pfu* polymerase, introducing *Hin*dIII and *Nhe*I restriction sites via modified primers (PromDsrHindf1, PromDsrNher1). The *dsr* terminator region (Dahl *et al.*, 2005) was amplified using the primer pair TermDsrXmaJf2 and TermDsrXbar1 that introduced *Xma*JI and *Xba*I restriction sites into the PCR fragment. The reverse primer PromDsrNher1 was elongated by the addition of a sequence complementary to the forward primer TermDsrXmaJf2 and vice versa, thus enabling the fusion of the two PCR fragments by a subsequent overlap extension reaction. The introduced *Nhe*I and *Xma*JI restriction sites were thus positioned between the fused *dsrA* promoter and *dsr* terminator region, enabling the in frame integration of any gene. The promoter and terminator fragment was digested and inserted into the *Hin*dIII and *Xba*I digested broad-host-range cloning vector pBBR1MCS-2 (Kovach *et al.*, 1995), resulting in the plasmid pBBR*dsr*PT1. The *A. vinosum*

DsrR coding region was amplified using the recombinant primer pair DsrRNhef1 and DsrRXmaJr1 that introduced *Nhe*I and *Xma*JI restriction sites respectively. The amplicon was digested and ligated to the *Nhe*I/*Xma*JI fragment of pBBR*dsr*PT1, resulting in the complementation plasmid pBBR*dsr*PT-*dsrR* (Figure III.24). The plasmid was transferred into *A. vinosum* Δ*dsrR* via conjugation, thereby producing the complementation strain Δ*dsrR*+*dsrR*.

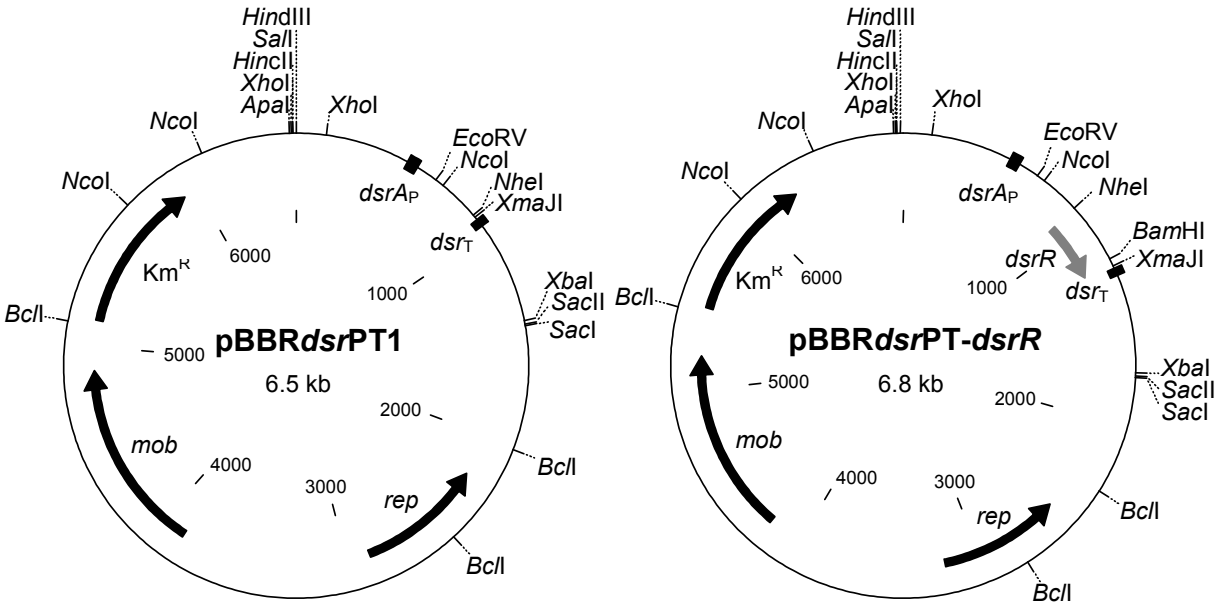

Figure III.24. Maps of pBBR*dsr*PT1 and the complementation plasmid pBBR*dsr*PT-*dsrR*.

2.3.2. Phenotypical characterization of the complementation mutant

The turnover of reduced sulfur compounds by *A. vinosum* mutant strains and wild-type was examined in a 1 L batch culture under continuous illumination in a medium containing 2 mM sulfide as sole sulfur compound. As expected for the purple sulfur bacterium *A. vinosum*, sulfide was immediately metabolized and intracellular sulfur globules were formed (Brune, 1995b). The stored sulfur was further oxidized to the end product sulfate. Sulfite was not detected during sulfur oxidation (Figure III.25).

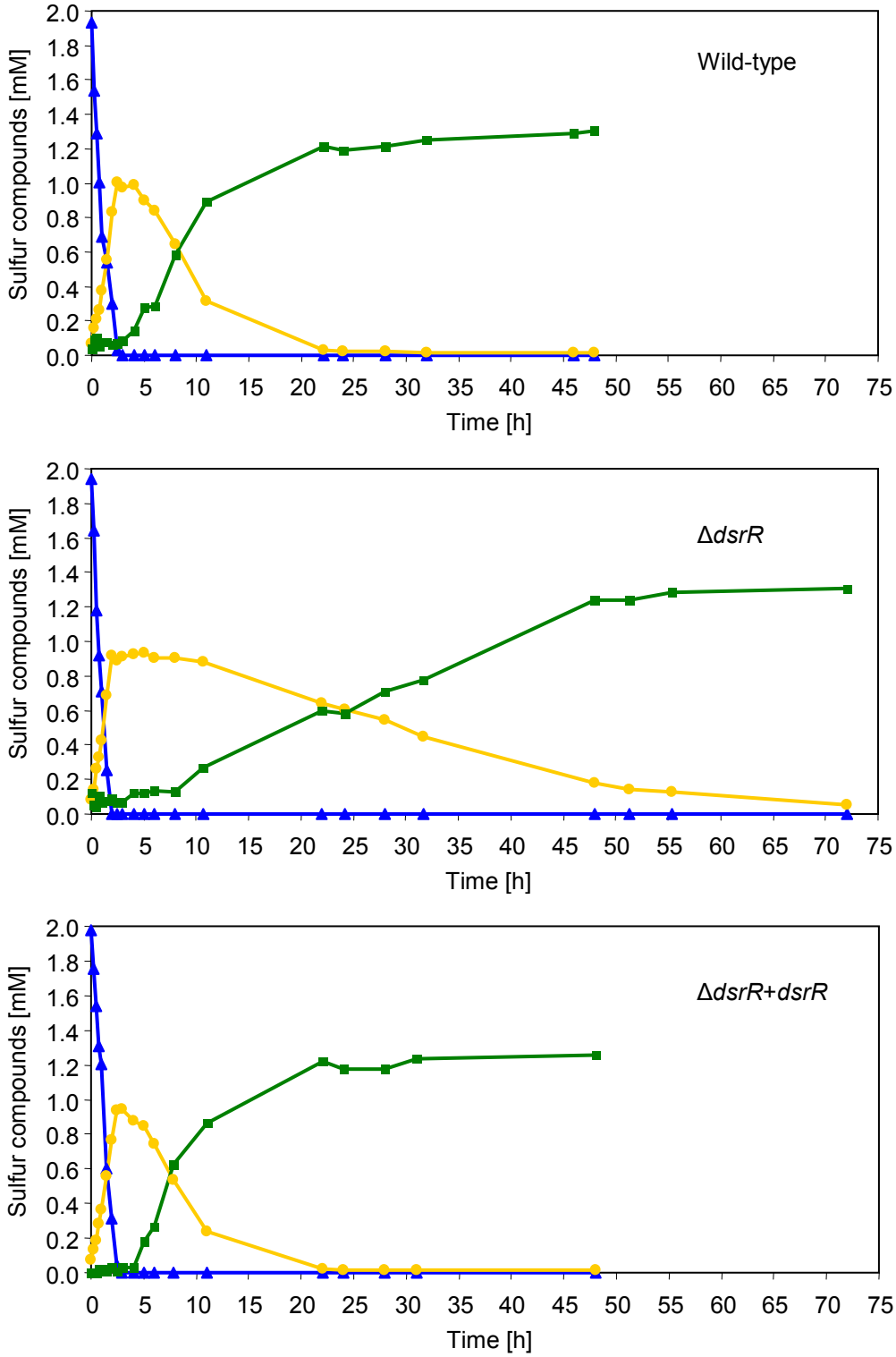

Figure III.25. Time-course of sulfide metabolization by *A. vinosum* Δ*dsrR* and *A. vinosum* Δ*dsrR*+*dsrR* compared to the wild-type. The oxidation of sulfide (▲), formation and degradation of sulfur (●) and production of sulfate (■) were examined in a thermostatted fermenter with modified Pfennig's medium containing 2 mM sulfide. Sulfide could not be completely recovered as sulfate due to loss of gaseous H_2S during sampling. The protein contents of the cultures were 49.7 µg mL^{-1} (wild-type), 91.0 µg mL^{-1} (Δ*dsrR*), and 62.7 µg mL^{-1} (Δ*dsrR*+*dsrR*) at the start of the experiment. Representatives of three independent growth experiments for each strain are shown.

Sulfide oxidation as well as the formation of sulfur globules was unchanged in the *dsrR* deletion mutant and in the Δ*dsrR*+*dsrR* complementation strain compared to the wild-type (Table III.5). The formation of polysulfides that occurs during the oxidation of sulfide (Gehrke, 2000; Prange *et al.*, 2004) was also not affected. For clarity reasons, the intermediary formation of these polysulfides is not depicted here. The oxidation of intracellularly stored sulfur is severely reduced in the Δ*dsrR* strain (Figure III.25, Table III.5). The *dsrR* deletion mutant exhibited a specific sulfur oxidation rate that was reduced by 88% compared to the wild-type. Complementation of the *dsrR* mutant restored the oxidation rate to the wild-type level (Figure III.25, Table III.5), thereby confirming that the observed phenotype was exclusively caused by the lack of *dsrR*. The growth yields of all three strains were in the same range (Table III.5). The lack of DsrR does not stop the oxidation of stored sulfur but leads to a severe slowing down of the process. DsrR is not absolutely essential for the oxidation of intermediary stored sulfur but it clearly plays an important role in ensuring an undisturbed process.

Table III.5. Characteristics of the *A. vinosum* Δ*dsrR* deletion mutant compared to the wild-type and the complementation mutant *A. vinosum* Δ*dsrR*+*dsrR*. The results represent the means and standard deviations of three independent growth experiments. Initial sulfide concentration was 2 mM. Oxidation and formation rates are given as nmol min^{-1} (mg protein)$^{-1}$. The growth yield is given as g protein (mol sulfide)$^{-1}$.

	A. vinosum strain		
	Wild-type	Δ*dsrR*	Δ*dsrR*+*dsrR*
Sulfide oxidation rate	199.0 ± 18.2	205.3 ± 0.4	200.0 ± 16.8
Sulfur globule formation rate	90.7 ± 0.6	90.7 ± 5.0	89.5 ± 2.1
Sulfur oxidation rate	24.1 ± 0.3	2.9 ± 0.5	23.9 ± 0.7
Growth yield	8.8 ± 0.9	9.0 ± 0.9	8.9 ± 0.5

2.3.3. Formation of Dsr proteins in the deletion and complementation mutant

The presence of several Dsr proteins was examined in the *A.vinosum* wild-type in comparison to the *dsrR* deletion mutant using protein-specific antisera. DsrR was detected in the soluble fraction of the wild-type but was absent in the *dsrR* deletion mutant (Figure III.26). The formation of DsrC and the membrane-associated cytoplasmic protein DsrK was not influenced by the deletion of *dsrR*. Surprisingly, the formation of DsrE, a subunit of the soluble cytoplasmic heterohexameric protein DsrEFH, was slightly reduced in the *dsrR* mutant, especially after stored sulfur had been completely metabolized. It should be noted that DsrE appears to be present in larger amounts after the completion of sulfur oxidation than in the phase of active degradation of sulfur globules. Furthermore, the formation of DsrL, a soluble cytoplasmic iron-sulfur flavoprotein with NADH:acceptor oxidoreductase

activity, was reduced in *A. vinosum* Δ*dsrR*. The formation of the affected proteins was checked in the complementation mutant using the same method. As expected, DsrR could be detected in the soluble fraction and the diminished formation of DsrE and DsrL, both proteins essential to the sulfur oxidation pathway (Lübbe *et al.*, 2006; Dahl *et al.*, 2008b), were restored approximately to wild-type level (Figure III.26).

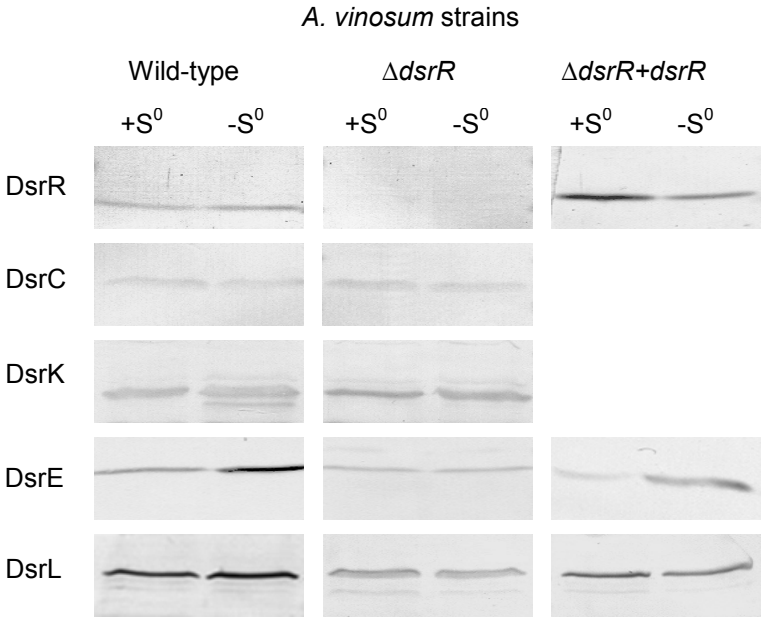

Figure III.26. Formation of several Dsr proteins in *A. vinosum* Δ*dsrR* and *A. vinosum* Δ*dsrR*+*dsrR* compared to the wild-type. Western blot analyses with antisera against DsrR (11.4 kDa), DsrC (12.6 kDa), DsrK (58.5 kDa), DsrE (14.6 kDa), and DsrL (71.4 kDa) were performed with soluble fractions of *A. vinosum* (96 µg protein), *A. vinosum* Δ*dsrR* (96 µg protein), and *A. vinosum* Δ*dsrR*+*dsrR* (68 µg) grown in batch culture on 2 mM sulfide and harvested either at the maximum content of intracellularly stored sulfur (+S^0) or after the sulfur had been completely metabolized (-S^0).

2.4. Influence of the *dsrR* deletion on the expression of other *dsr* genes

Balasubramanian *et al.* (2006) proposed an alternative function for IscA in the regulation of iron homeostasis and the sensing of redox stress in cyanobacteria.

In order to investigate if DsrR fulfills an analogous function in *A. vinosum*, the expression levels of six *dsr* genes were examined via RT-PCR under photoorganoheterotrophic and photolithoautotrophic conditions in the *dsrR* deletion mutant and compared to the wild-type.

Furthermore, the potential of DsrR to influence the regulation of *dsrA* expression on a translational level was examined by introducing a translational *dsrA*'-*lacZ* gene fusion into the *ΔdsrR* mutant and the wild-type. The β-galactosidase activities were compared to those achieved with a transcriptional *dsrA*p-*lacZ* fusion.

2.4.1. Expression studies by real-time RT-PCR

The deletion mutant *ΔdsrR* showed a nearly unchanged transcript pattern and levels for all investigated *dsr* genes compared to the wild-type (Figure III.27) with the exception of the *dsrR* transcript that, as expected, was not detected in the deletion mutant. The deletion of *dsrR* gene region appears not to have a detrimental effect on the expression of *dsrS*, implying that the *dsrS* promoter region is not affected by the deletion. As can be seen in Figure III.7, the predicted *dsrS* promoter region is located in the *dsrNR* gene region and not part of the deletion in the *ΔdsrR* mutant.

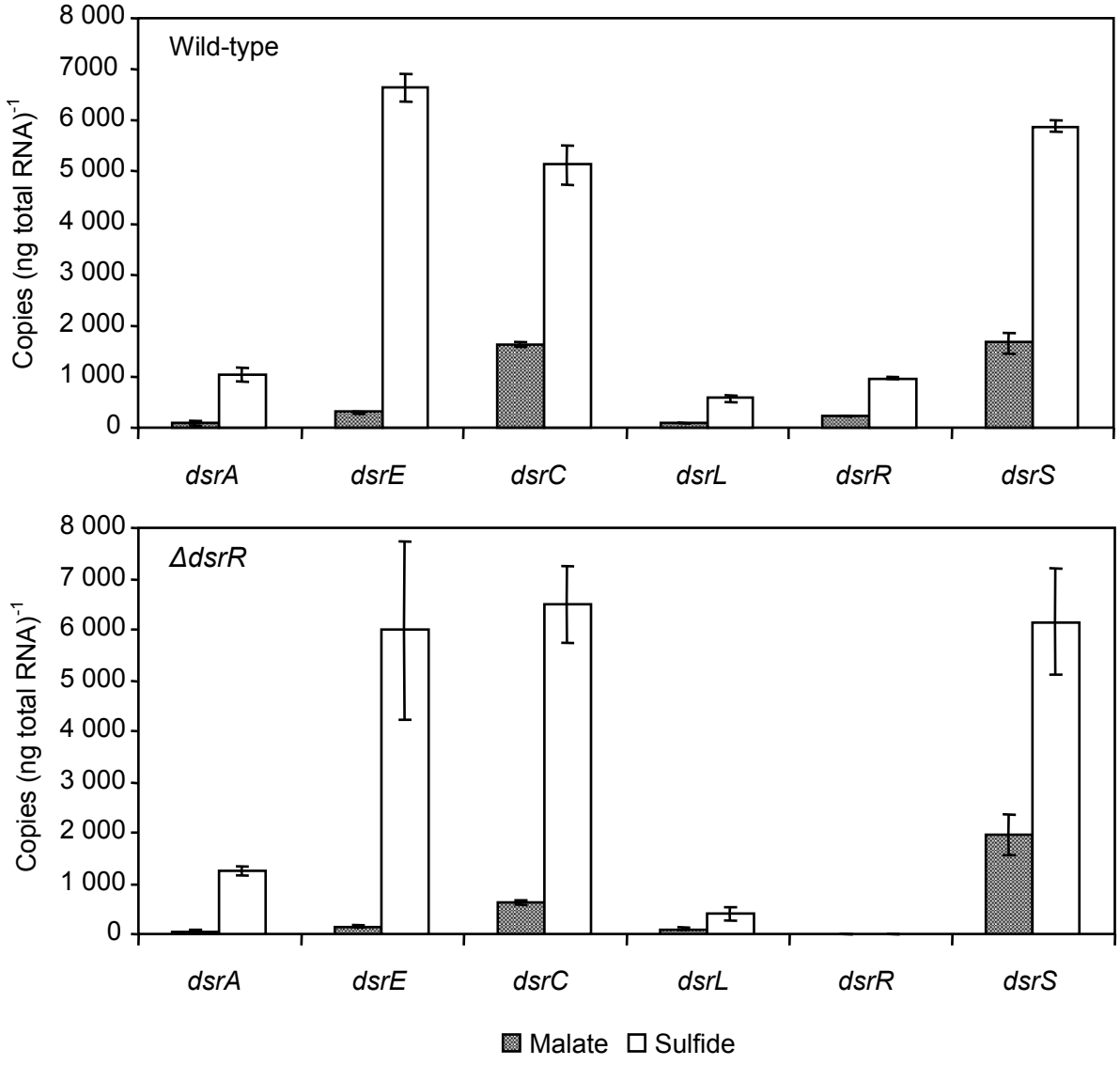

Figure III.27. Expression levels of six *dsr* genes in the *A. vinosum ΔdsrR* mutant compared to the wild-type under photoorganoheterotrophic (malate) and photolithoautotropic (sulfide) conditions determined by real-time RT-PCR. 250 ng of total RNA were used as template. Quantified external RNA fragments containing the target sequence served as standards.

2.4.2. Expression studies by reporter gene fusions

Plasmids in which the main *dsr* operon promoter $dsrA_P$ was fused to *lacZ*, a gene encoding for the β-galactosidase of *E. coli*, or in which $dsrA_P$ and a truncated *dsrA* gene were fused to a truncated *lacZ* gene, were introduced into the wild-type (*cf.* III.1.1) and the *dsrR* deletion mutant. The resulting strains were grown for 24 h on modified Pfennig's medium with 2 mM malate or sulfide before the *lacZ*-mediated β-galactosidase activity was determined.

As was expected in light of the RT-PCR results, no major differences between the β-galactosidase activity of the wild-type compared to the mutant could be detected with the transcriptional gene fusion (Table III.6, Figure III.28). The twofold higher LacZ activity in the malate grown culture of *ΔdsrR* cannot be explained at the moment. Surprisingly, the translation of *dsrA'-lacZ* in the *ΔdsrR* mutant is reduced by ~83 % under the tested growth condition.

Table III.6. Specific β-galactosidase activity in *A. vinosum ΔdsrR* and the wild-type carrying transcriptional or translational gene fusions. Photoorganoheterotrophically grown cultures containing transcriptional ($dsrA_P$-*lacZ*) or translational (*dsrA'-lacZ*) gene fusion plasmids were used to inoculate modified Pfennig's medium containing 2 mM of the indicated electron source. The specific β-galactosidase activity is given in nmol *o*-nitrophenol min^{-1} (mg protein)$^{-1}$. The average protein content amounted to 500 µg mL^{-1}. The results represent the means and standard deviations of three independent measurements.

	Specific β-galactosidase activity	
A. vinosum strain	Malate	Sulfide
Wild-type		
$dsrA_P$-*lacZ*	2.9 ± 0.7	9.1 ± 0.9
dsrA'-lacZ	42.6 ± 1.7	96.2 ± 27.1
ΔdsrR		
$dsrA_P$-*lacZ*	6.7 ± 0.8	11.3 ± 1.7
dsrA'-lacZ	6.4 ± 0.3	18.7 ± 1.0

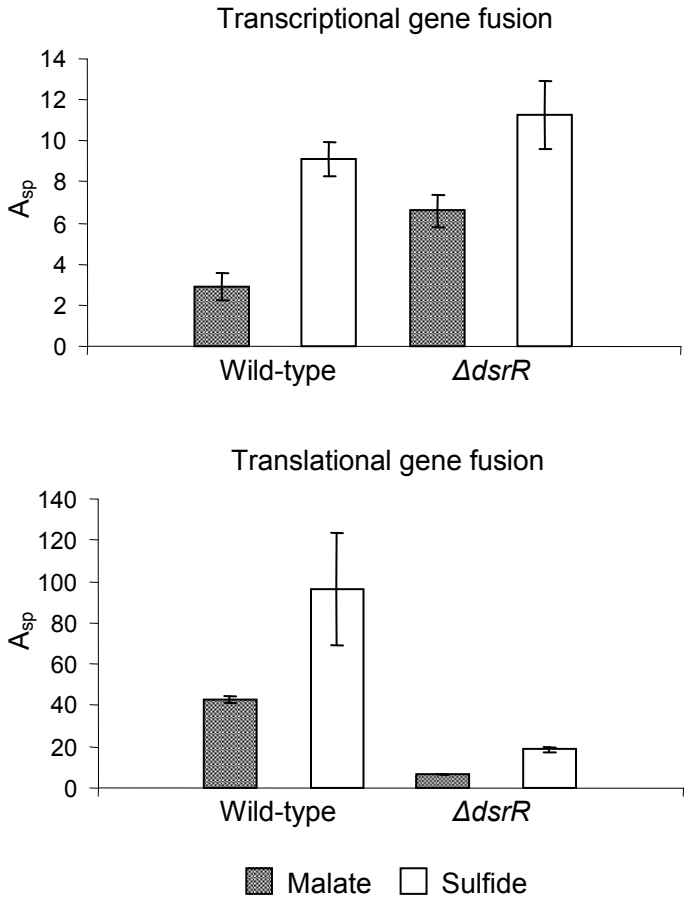

Figure III.28. Specific β-galactosidase activities in the *A. vinosum dsrR* deletion mutant and the wild-type carrying transcriptional or translational gene fusions. Photoorganoheterotrophically grown cultures containing transcriptional or translational gene fusion plasmids were used to inoculate modified Pfennig's medium containing 2 mM of the indicated electron source. The specific β-galactosidase activity A_{sp} is given in nmol *o*-nitrophenol min^{-1} (mg protein)$^{-1}$ (*cf*. Table III.6).

The same percentage of reduction was observed with sulfide of different concentrations (Table III.7, Figure III.29) and thiosulfate as electron source (Table III.8). The addition of malate or sulfite to sulfide as electron donor did not result in an additional inhibitory effect on the expression of DsrA'-LacZ in the *dsrR* deletion mutant (Table III.8, *cf.* III.1.1.4). These results implicate DsrR as a part of a post-transcriptional regulatory mechanism.

Table III.7. Influence of the concentration of sulfide on the expression level of DsrA'-LacZ in the *dsrR* deletion mutant. Photoorganoheterotrophically grown cultures containing translational (*dsrA'-lacZ*) gene fusion plasmid were used to inoculate modified Pfennig's medium with the indicated sulfide concentrations. The specific β-galactosidase activity is given in nmol *o*-nitrophenol min^{-1} (mg protein)$^{-1}$. The average protein content amounted to 500 µg mL^{-1}. The results represent the means and standard deviations of three independent measurements.

	Specific β-galactosidase activity	
Sulfide	Wild-type	*ΔdsrR*
0.0 mM	36.7 ± 3.8	6.6 ± 0.5
0.2 mM	44.0 ± 0.2	7.8 ± 0.4
0.5 mM	57.0 ± 8.6	8.2 ± 2.2
2.0 mM	85.1 ± 10.5	12.6 ± 4.1
6.0 mM	110.7 ± 8.0	21.9 ± 8.6

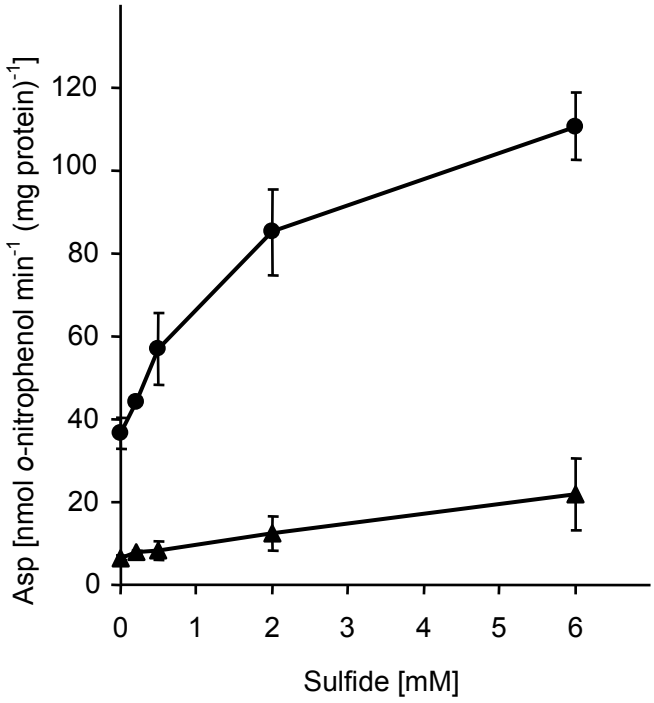

Figure III.29. Influence of the initial concentration of sulfide on the expression level of DsrA'-LacZ in the *dsrR* deletion mutant (triangles) compared to the wild-type (circles). Photoorganoheterotrophically grown cultures of the wild-type and the *dsrR* deletion mutant containing the translational gene fusion plasmid were incubated for 24 h in modified Pfennig's medium with different concentrations of sulfide before the β-galactosidase activities were determined (*cf.* Table III.7).

Table III.8. Influence of thiosulfate, malate or sulfite on the expression of DsrA'-LacZ in the *dsrR* deletion mutant. Photoorganoheterotrophically grown culture containing translational gene fusion plasmid was used to inoculate modified Pfennig's medium containing 2 mM of the indicated electron source. The specific β-galactosidase activity is given in nmol *o*-nitrophenol min^{-1} (mg protein)$^{-1}$. The average protein content amounted to 500 µg mL^{-1}. The results represent the means and standard deviations of three independent measurements.

	Specific β-galactosidase activity	
Electron source	Wild-type	*ΔdsrR*
Thiosulfate	89.5 ± 9.4	15.6 ± 2.5
Sulfide	96.2 ± 27.1	18.7 ± 1.0
Malate	42.6 ± 1.7	6.4 ± 0.3
Malate + sulfide	96.4 ± 10.5	22.5 ± 6.4
Sulfite	39.0 ± 7.4	7.6 ± 0.3
Sulfite + sulfide	94.3 ± 30.9	16.5 ± 4.9

3. Characterization of the DsrS protein

The protein DsrS is encoded by the last gene of the *A. vinosum dsr* operon. The protein is predicted to be a soluble cytoplasmic protein with a molecular mass of 41.1 kDa (Dahl *et al.*, 2005). Earlier sequence analyses revealed neither conserved domains nor motifs present in the sequence, and significant similarities to proteins of known function were not apparent (Dahl *et al.*, 2005). A homologous gene was found in the chemotrophic sulfur oxidizer *Thiobacillus denitrificans* (Beller *et al.*, 2006a). An *A. vinosum* Δ*dsrS* in frame deletion mutant appeared to be affected in the oxidation of stored sulfur, implicating DsrS to be involved in the process (Grimm, 2004), but nothing further is known about the protein.

In order to elucidate the function of DsrS in sulfur oxidation, the effect of the deletion of *dsrS* on the expression of other *dsr* genes was examined in depth by immunoblot analyses, RT-PCR and transcriptional and translational gene fusion experiments.

3.1. Sequence analyses

In *A. vinosum*, the *dsrS* gene is the last gene of the *dsr* operon and located downstream of *dsrR* (Figure III.31) (Dahl *et al.*, 2005). Only one copy of the gene occurs in the *A. vinosum* genome sequence (locus tag Alvin_1265, genome accession no. NC_013851). Updated similarity searches revealed homologues of the *dsrS* gene in several sulfur-oxidizing bacteria (*Thiobacillus denitrificans* (Tbd_2558, NC_007404) (Beller *et al.*, 2006a), *Thioalkalivibrio* sp. HL-EbGR7 (Tgr7_2284, NC_011901), *Beggiatoa* sp. PS (BGP_1012, NZ_ABBZ01001151), and endosymbionts Candidatus *Vesicomyosocius okutanii* (COSY_0120, NC_009465) (Kuwahara *et al.*, 2007) and Candidatus *Ruthia magnifica* (Rmag_0115 and Rmag_0114, NC_008610) (Newton *et al.*, 2007)) (Table III.9).

Table III.9. Abbreviated results of Ψ-BLAST analysis (Altschul *et al.*, 1997) with *A. vinosum* DsrS protein sequence (accession no. YP_003443236.1) as query. Results with E values greater than 1 were discarded.

Accession	Description	Query coverage	E value
ZP_02001652.1	DsrS [*Beggiatoa* sp. PS]	97%	1e-87
YP_002514351.1	DsrS [*Thioalkalivibrio* sp. HL-EbGR7]	98%	3e-71
YP_316316.1	DsrS [*Thiobacillus denitrificans* ATCC 25259]	95%	2e-54
EEZ80681.1	DsrS [uncultured SUP05 cluster bacterium]	98%	2e-40
YP_001218978.1	DsrS [Candidatus *Vesicomyosocius okutanii* HA]	95%	8e-31
YP_903382.1	hypothetical protein Rmag_0115 [Candidatus *Ruthia magnifica* str. Cm]	27%	2e-14
YP_903381.1	hypothetical protein Rmag_0114 [Candidatus *Ruthia magnifica* str. Cm]	20%	1e-04

In Candidatus *Ruthia magnifica* the two open reading frames Rmag_0115 and Rmag_0114 together encode for the N-terminal part of DsrS (*cf.* Figure III.30). The Rmag_0115 gene product corresponds to the first 120 amino acids of the 368 aa *A. vinosum* DsrS protein, whereas Rmag_0114 encodes a protein corresponding to the amino acids 115 to 199 of *A. vinosum* DsrS. The C-terminal part of the DsrS protein appears to be missing in *R. magnifica*.

The gene *dsrS* is absent from the genome of the green sulfur bacteria *Chlorobaculum tepidum* (formerly *Chlorobium tepidum* (Imhoff, 2003)) (NC_002932) (Eisen *et al.*, 2002), *Chlorobium limicola* (NC_010803), and *Chlorobaculum parvum* (NC_011027) and the purple sulfur bacterium *Halorhodospira halophila* (NC_008789). The *dsrS* gene, like *dsrR*, is therefore not part of the core *dsr* genes present in all sulfur-oxidizing bacteria that form sulfur globules as an intermediate (*dsrABEFHCMKLJOPN*) (Sander *et al.*, 2006).

Neither conserved domains nor motifs were revealed by this updated sequence analysis and significant similarities to proteins of known function were not found.

Sequence alignments of several DsrS homologues of sulfur-oxidizing bacteria illustrate the high sequence similarity in the N-terminal part of the protein, whereas the C-terminal region appears to be the least conserved part of the protein (Figure III.30). This is interesting to note in light of the missing sequence encoding the C-terminal part of DsrS in *R. magnifica*. The sequence identity among DsrS homologues varies and can be as low as 28%. Conserved cysteine residues were not identified.

(Next page) Figure III.30. Multiple sequence aligments of DsrS sequences. The alignments were generated using the program ClustalW (Chenna *et al.*, 2003). Fully conserved residues in DsrS proteins are indicated by an asterisk (*****) and are shaded black. Positions in which one of the strong groups (STA, NEQK, NHQK, NDEQ, QHRK, MILV, MILF, HY, FYW) is fully conserved are marked by a colon (**:**) and shaded gray and positions in which one of the weaker groups (CSA, ATV, SAG, STNK, STPA, SGND, SNDEQK, NDEQHK, NEQHRK, FVLIM, HFY) is fully conserved are indicated by a dot (**.**) and shaded light gray.

Avi, *Allochromatium vinosum* DSM 180; Beg, *Beggiatoa* sp. PS; Thi, *Thioalkalivibrio* sp. HL-EbGR7; Tde, *Thiobacillus denitrificans* ATCC 25259; Sup, uncultured SUP05 cluster bacterium; Vok, Candidatus *Vesicomyosocius okutanii* HA; Rma, Candidatus *Ruthia magnifica* str. Cm.

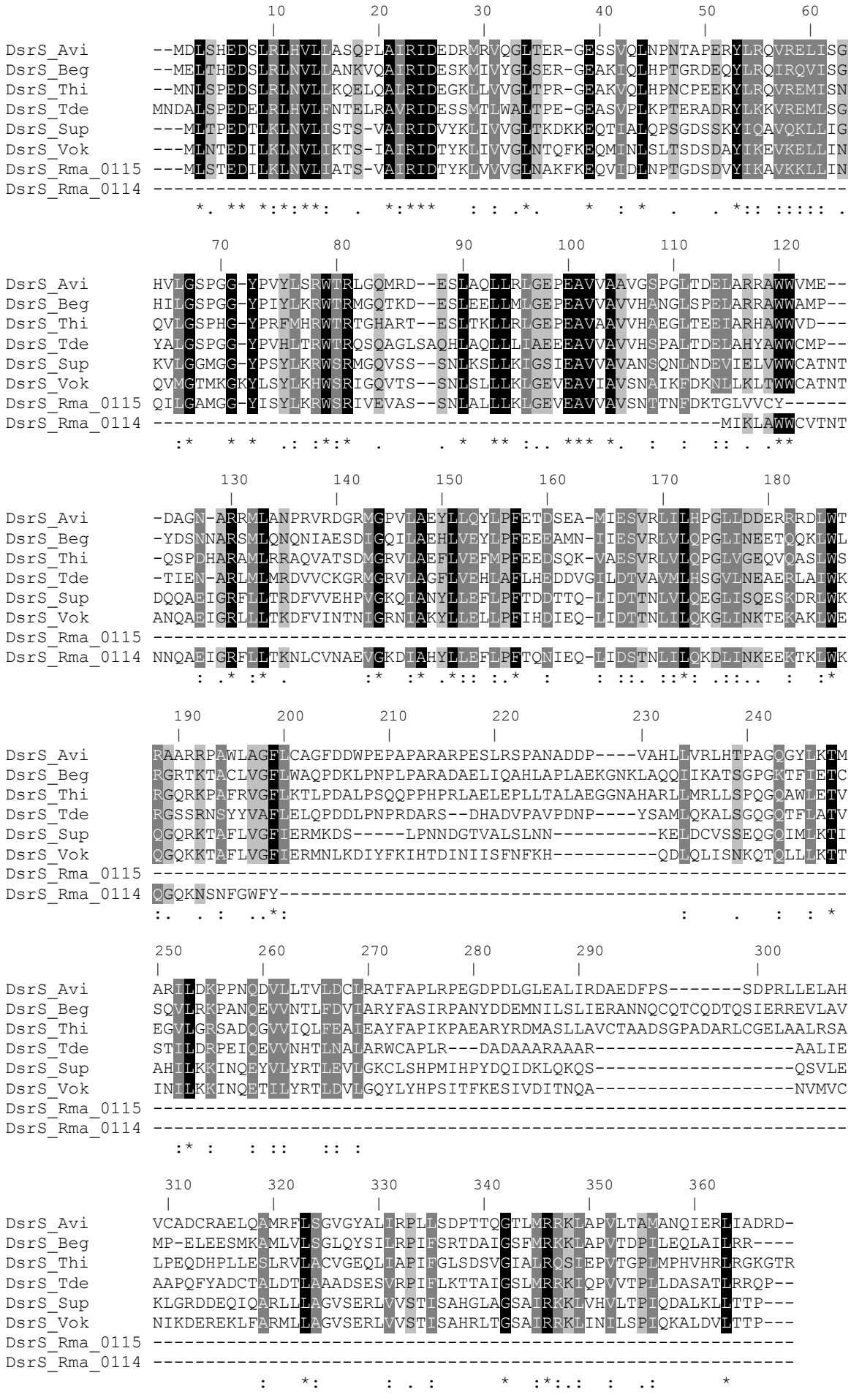
DsrS_Avi
DsrS_Beg
DsrS_Thi
DsrS_Tde
DsrS_Sup
DsrS_Vok
DsrS_Rma_0115
DsrS_Rma_0114

A. vinosum is so far the only organism in which *dsrS* is part of the *dsr* gene cluster. In other sulfur-oxidizing bacteria the gene is located elsewhere in the genome (Figure III.31), surrounded by quite a diverse gene neighborhood.

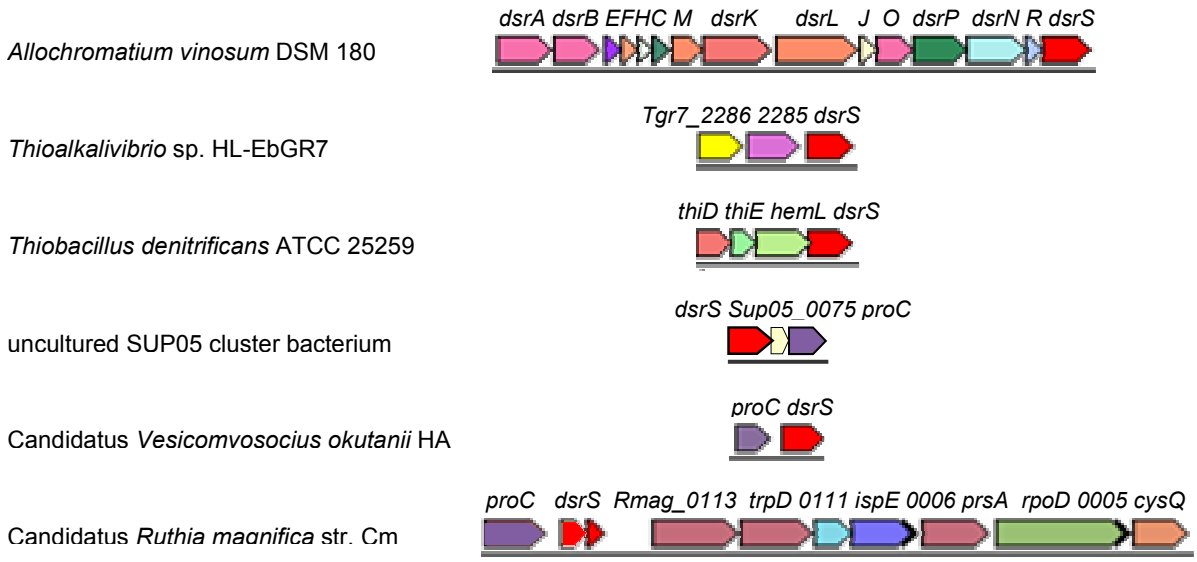

Figure III.31. The gene regions surrounding *dsrS* in *dsrS*-containing organisms. The schematic representations of the gene regions were created using the genome neighborhood tool of the IMG homepage. Walsh *et al*. (2009) identified a partial *dsr* operon in the metagenome of the uncultured bacterium SUP05 from an oceanic oxygen minimum zone (accession no. ACSG01000000). Predictions concerning the gene neighborhood in *Beggiatoa* sp. PS could not be made as only fragmented shotgun sequences were available. Genes homologous to *dsrS* are marked red.

In Thioalkalivibrio sp. HL-EbGR7, the *dsrS* homologous gene is preceded by two open reading frames (Tgr7_2286 and Tgr7_2285) that encode for hypothetical proteins. The first exhibits similarities to a metallo-peptidase and the second is indicated to have an ATPase activity, but the function of both proteins is not resolved.

In *Thiobacillus denitrificans* ATCC 25259, the *dsrS* homologue is preceded by three open reading frames (Tbd_2555, Tbd_2556, and Tbd_2557) that encode for a ThiD, a ThiE and an HemL homologue, respectively. ThiD is a phosphomethylpyrimidine kinase that is involved in the thiamin metabolism. It catalyzes the phosphorylation of hydroxymethylpyrimidine to hydroxymethylpyrimidine phosphate as well as the phosphorylation of hydroxymethyl-pyrimidine phosphate to hydroxymethylpyrimidine pyrophosphate in the thiamin biosynthesis pathway (Rodionov *et al.*, 2002). The subsequent coupling of hydroxymethylpyrimidine pyrophosphate and hydroxyethylthiazole phosphate to form thiamin monophosphate is mediated by the thiamin-phosphate synthase ThiE (Rodionov *et al.*, 2002). HemL is a glutamate 1-semialdehyde aminotransferase that catalyzes the transamination of glutamate-

1-semialdehyde to 5-aminolevulinate, the first committed precursor of the porphyrin biosynthesis (Ilag *et al.*, 1991). All three gene products are involved in co-factor synthesis.

In the uncultured bacterium SUP05 (Walsh *et al.*, 2009) the *dsrS* homologue is succeeded by two genes, Sup05_0075 and Sup05_0076. Sup05_0075 encodes a hypothetical protein of unknown function, whereas Sup05_0075 encodes ProC, a pyrroline-5-carboxylate reductase that catalyzes the reduction of pyrroline-5-carboxylate to proline as final step in the proline biosynthesis (Deutch *et al.*, 1982). A ProC homologue also precedes the *dsrS*-like genes in Candidatus *Vesicomyosocius okutanii* and Candidatus *Ruthia magnifica*, which is not surprising considering the close phylogenetic relationship of SUP05, *V. okutanii* and *R. magnifica* (Walsh *et al.*, 2009).

In the latter, the *dsrS*-encoding genes are succeeded by nine coding regions in the same reading direction (Rmag_0113, Rmag_0112, Rmag_0111, Rmag_0110, Rmag_0006, Rmag_0109, Rmag_0108, Rmag_0005, and Rmag_0107) of which two (Rmag_0006 and Rmag_0005) encode the tRNA for glutamate and methionine.

The open reading frames Rmag_0113, Rmag_0111 and Rmag_108 encode a Xaa-Pro aminopeptidase, a 3'-5' exoribonuclease and RpoD, the σ^{70} subunit of the RNA polymerase, respectively.

Rmag_0112 encodes a protein with similarities to TrpD, an anthranilate phosphoribosyl-transferase. TrpD is involved in the tryptophane synthesis and catalyzes the third of seven reactions leading to L-tryptophane, that is the conversion of anthranilate and 5-phospho-ribosyl-1-pyrophosphate to phosphoribosylanthranilate (Kim *et al.*, 2002).

An IspE homologue, a 4-diphosphocytidyl-2*C*-methyl-D-erythritol kinase, is encoded by Rmag_0110. IspE is an essential enzyme in the non-mevalonate pathway of isopentenyl diphosphate and dimethylallyl diphosphate biosynthesis. These isomers are the universal five-carbon precursors of isoprenoids. IspE catalyzes the ATP-dependent phosphorylation of the 2-hydroxyl group of 4-(diphosphocytidyl)-2*C*-methyl-D-erythritol, the fourth step of the non-mevalonate pathway, to yield 4-(diphosphocytidyl)-2*C*-methyl-D-erythritol 2-phosphate (Wada *et al.*, 2003; Miallau *et al.*, 2003).

Rmag_0109 encodes a PrsA homologue, a ribose-phosphate pyrophosphokinase that catalyzes the conversion of ribose-5-phosphate to phosphoribosylpyrophosphate (PRPP) at a key junction in intermediary metabolism. The enzyme diverts ribose 5-phosphate from energy generation by the pentose phosphate pathway to biosynthesis via the intermediate PRPP. PRPP is a precursor of the pyrimidine, purine, and pyridine nucleotide synthesis, as well as of the biosynthesis of the amino acids histidine and tryptophane (Hove-Jensen *et al.*, 1986).

A CysQ homologue, a 3'-phosphoadenosine-5'-phosphosulfate (PAPS) 3'-phosphatase, is encoded by Rmag_0107. CysQ controls the intracellular levels of PAPS, which is toxic at

high concentrations. PAPS is an intermediate in cysteine biosynthesis, a principal route of sulfur assimilation. PAPS is also utilized as a sulfate donor for sulfotransferase, yielding 3'-phosphoadenosine-5'-phosphate (PAP). CysQ further dephosphorylates PAP to AMP, preventing the intracellular trapping of adenine nucleotides and the inhibition of PAPS reductase, sulfotransferase, and oligoribonuclease by the metabolite (Neuwald *et al.*, 1992; Murguia *et al.*, 1995).

Except for the repeated occurrence of *proC* in close proximity to *dsrS* in three of the *dsrS*-containing sulfur-oxidizers, no similarities in the gene neighborhoods were found. Conclusions about a probable function of DsrS based on the gene neighborhood could therefore not be drawn.

3.2. Biochemical characterization of DsrS

According to sequence analyses, DsrS is a soluble protein of 41.1 kDa and does not contain any co-factors (Pott-Sperling, 2000; Dahl *et al.*, 2005). This has, however, so far not been experimentally investigated.

3.2.1. Production and purification of recombinant DsrS protein

A recombinant DsrS protein was produced in the *E. coli* strain BL21(DE3) under aerobic conditions. An N-terminal His-tag was added to the DsrS protein sequence by cloning the *A. vinosum dsrS* gene into the expression plasmid pET-15b, yielding the *dsrS* expression plasmid pDsrS-N.

As inclusion bodies were observed in the microscopic picture of the over-production culture, it was not surprising that most of the produced protein occurred in the insoluble fraction (resuspended pellet of the disrupted cells after centrifugation) (Figure III.32). The solubility was improved by lowering the growth temperature from 37°C to 25°C and by reducing the IPTG concentration to 2 µM. The alternative use of a C-terminal His-tag did not result in a higher yield of soluble protein but instead lead to a severely reduced recombinant protein yield.

DsrS was isolated from the soluble fraction using nickel-chelate affinity chromatography. The protein was eluted by step-wise increasing concentrations of imidazole. The observed size of the protein of ~45 kDa in the SDS polyacrylamide gel is in accordance with the sequence deduced molecular mass of 43.3 kDa for the recombinant protein (Figure III.32). The additional 2.2 kDa are due to the His-tag. The prominent band at approx. 25 kDa most likely represents a degradation or processing fragment of DsrS, consisting of the N-terminal part of the protein. This fragment was detected utilizing a His-tag-specific as well as a DsrS-specific antiserum (*cf.* III.3.2.2). The antiserum was raised against a potentially highly immunogenic synthetic peptide derived from the *A. vinosum dsrS* nucleotide sequence (Grimm, 2004). This peptide represents the aa 214-229 of the native 368 aa DsrS protein and thus an

unconserved region in the junction between the highly conserved N-terminal and the less conserved C-terminal part of DsrS (*cf.* Figure III.30). The minimal molecular mass of a fragment containing the N-terminal His-tag as well as the immunogenic region is 27.9 kDa.

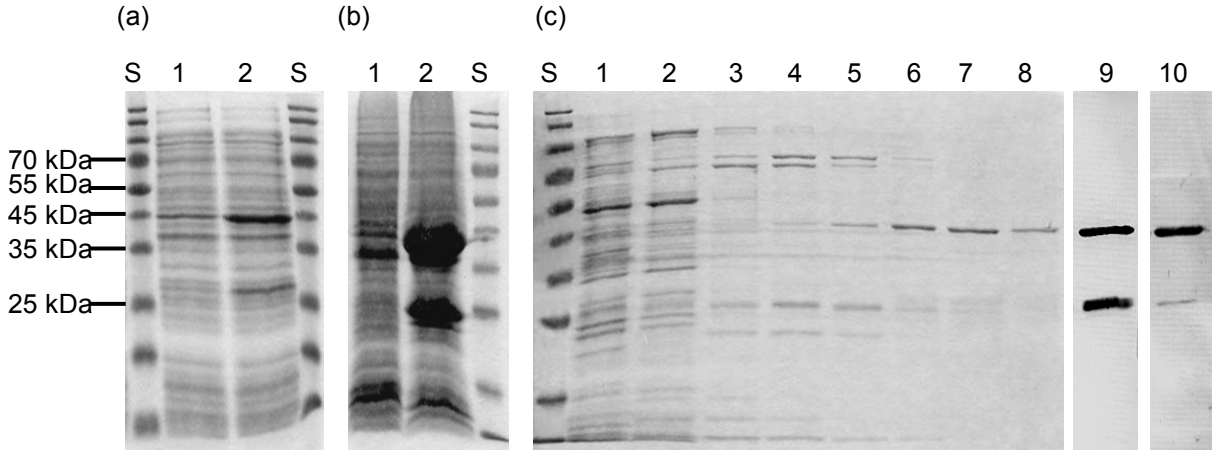

Figure III.32. Coomassie-stained SDS polyacrylamide gels documenting the production and purification of recombinant DsrS. (a) *E. coli* BL21(DE3) cells carrying pDsrS-N. 1: non-induced cells, 2: cells induced with IPTG. **(b)** Fractions after centrifugation of the disrupted cells. 1: soluble fraction, 2: resuspended insoluble fraction **(c)** Purification of recombinant DsrS by Ni-NTA chromatography. 1: wash (20 mM imidazole), 2-8: eluates (40, 60, 80, 100, 150, 200 and 250 mM imidazole), 9-10: Western blot analysis of 8 with specific antibodies against DsrS (9) and His-tag (10). S: PageRuler Prestained Protein Ladder.

3.2.2. Testing of DsrS-specific antiserum and detection of DsrS in *A. vinosum*

The formation of the DsrS protein within the *A. vinosum* cell was investigated utilizing a DsrS-specific antiserum. The antiserum was raised against a potentially highly immunogenic synthetic peptide derived from the *A. vinosum dsrS* nucleotide sequence (Grimm, 2004). The functionality of the antiserum was tested using the recombinant DsrS protein.

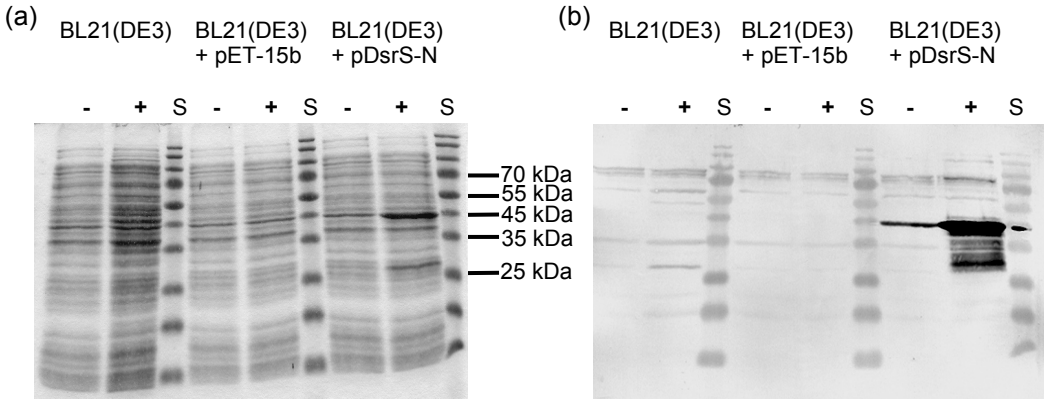

Figure III.33. Testing of DsrS-specific antiserum. (a) Coomassie-stained SDS polyacrylamide gel. **(b)** Western blot with antiserum against DsrS. The cell samples were take before (-) or after (+) induction with IPTG. S: PageRuler Prestained Protein Ladder.

The strongest signal was detected for a ~45 kDa fragment occuring in the pDsrS-N-carrying *E. coli* BL21(DE3) cells, demonstrating that the antiserum binds to DsrS. Besides the 45 kDa band, a second fragment at approximately 25 kDa was detected in the plasmid-carrying cells after induction with IPTG. This fragment most likely represents the N-terminal fragment of the protein, produced by degradation or post-translational processing (*cf*. III.3.2.1). Background signals are due to crossreactivity of the antiserum with *E. coli* BL21(DE3) specific proteins, as the same signals were detected in the BL21(DE3) samples.

The formation of DsrS in *A. vinosum* was investigated using photolithoautotrophically grown cells that were disrupted by sonication. The membrane fraction was separated from the soluble fraction by ultracentrifugation. The presence of DsrS in these fractions could not be confirmed. The DsrS protein content might have been to low to enable detection.

3.2.3. State of oligomerization of DsrS

The molecular mass and state of oligomerization of DsrS was determined by gel filtration chromatography. The protein was loaded onto a precalibrated Superdex-200 column and the elution of the protein was monitored by absorption at 280 nm (Figure III.34).

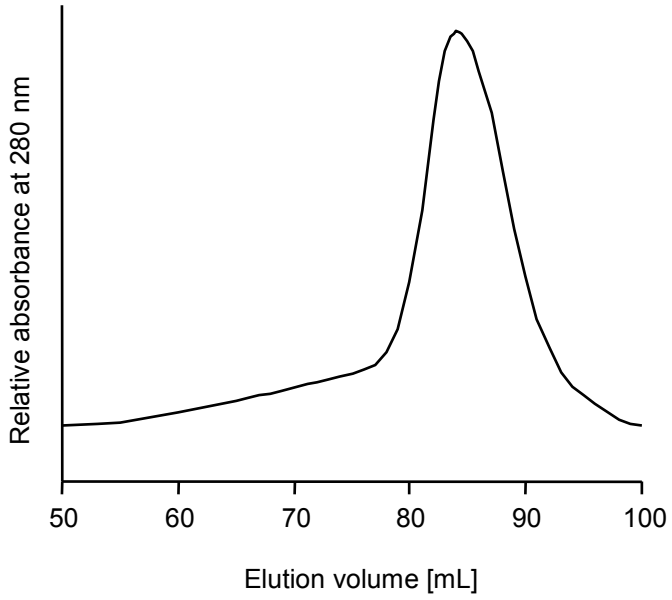

Figure III.34. Gel filtration chromatogram of recombinant DsrS. The protein was loaded onto a Superdex-200 column. The elution was monitored by absorption at 280 nm. The column had been calibrated with several proteins of known molecular mass.

DsrS eluted in one clear peak at an elution volume of 84 mL. This volume corresponds to a molecular mass of 43.3 kDa, which is in accordance with the sequence deduced mass for the recombinant protein. DsrS does not oligomerize and occurs as a monomer.

A peak corresponding to the ~25 kDa fragment seen in the Western blots of the recombinant protein was not observed. This might be due to the low protein concentration, as this fragment was hardly detectable in the Coomassie-stained gel of the purified recombinant

protein (*cf*. Figure III.32 (c)). A corresponding peak might have been below the detection limit.

UV-Vis spectra of the purified recombinant DsrS protein did not indicate the presence of any co-factors (Figure III.35), as was to be expected in light of the sequence analyses. Nevertheless, it cannot be discounted that this could also be due to the recombinant production of the protein.

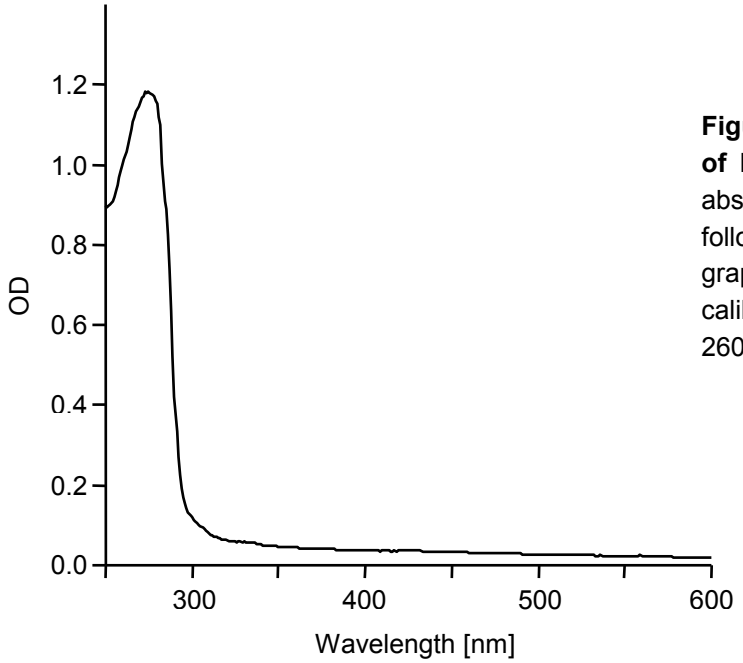

Figure III.35. UV-Vis spectrum of DsrS. Shown is the UV-visible absorption spectra of DsrS following gel filtration chromatography. The spectrum was calibrated to an absorbance at 260 nm of 1.0.

3.3. Physiological characterization of DsrS

The importance of DsrS for the oxidation of intracellularly stored sulfur in *A. vinosum* had previously been investigated by creating an in frame deletion mutant of *dsrS*. First experiments had shown the oxidation of intermediary stored sulfur to be clearly affected in the Δ*dsrS* strain (Grimm, 2004).

As *dsrS* is the last gene of the operon, down-stream effects caused by the deletion are quite unlikely. Nevertheless, in order to confirm that the observed phenotype was solely due to the deletion of *dsrS*, the complementation of the Δ*dsrS* mutant was attempted by reintroducing *dsrS in trans*. The oxidation rate of reduced sulfur compounds was quantified and compared between the *A. vinosum* mutant strains and the wild-type. Furthermore, the effect of the deletion of *dsrS* on the formation of several Dsr proteins was investigated.

3.3.1. Complementation of a *dsrS* deletion mutant

The complementation of the Δ*dsrS* mutant was carried out essentially as described for the deletion mutant Δ*dsrR* (*cf*. III.2.3.1). The *dsrS* gene was reintroduced *in trans* under control of the *dsrA* promoter. The *A. vinosum dsrS* gene and the subsequent *dsr* terminator region

were amplified using the primer pair DsrSNhef1 and TermDsrXbar1, that introduced a *Nhe*I and *Xba*I resitriction site at the 5'- and 3'-ends of the amplicon respectively. The digested PCR fragment was ligated to the *Nhe*I/XbaI fragment of pBBR*dsr*PT1, resulting in the complementation plasmid pBBR*dsr*PT-*dsrS* (Figure III.36). The plasmid was transferred into *A. vinosum* Δ*dsrS* via conjugation, thereby producing the complementation strain Δ*dsrS*+*dsrS*.

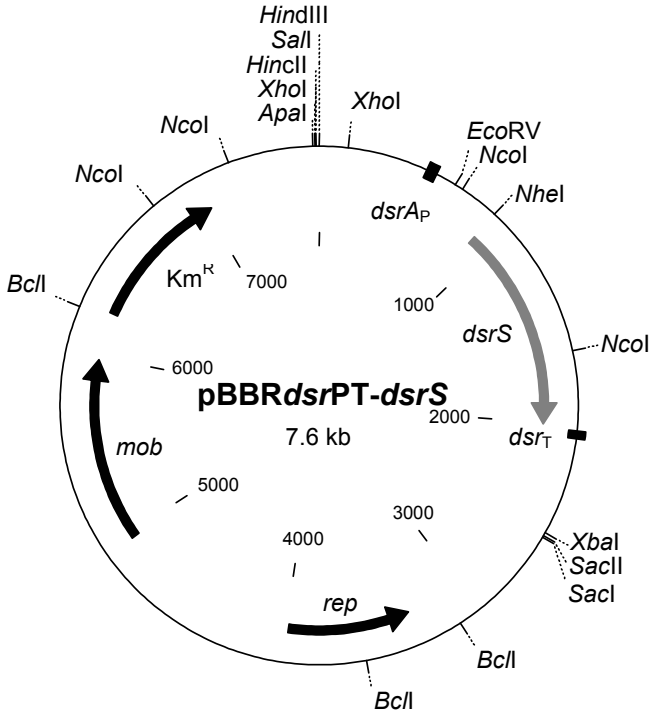

Figure III.36. Map of the complementation plasmid pBBR*dsr*PT-*dsrS*.

3.3.2. Phenotypical characterization of the complementation mutant

In order to examine the phenotype of *A. vinosum* Δ*dsrS*+*dsrS* and compare it to the wild-type and the deletion mutant, the strains were grown photolithoautotrophically in batch culture with 2 mM sulfide as electron source. As expected for a classical purple sulfur bacterium like *A. vinosum*, sulfide was immediately oxidized to zero-valent sulfur that was stored in periplasmic sulfur globules (Brune, 1995b). Following sulfide depletion, the stored sulfur was further metabolized to the end product sulfate. Sulfite was not detected during sulfur oxidation (Figure III.37).

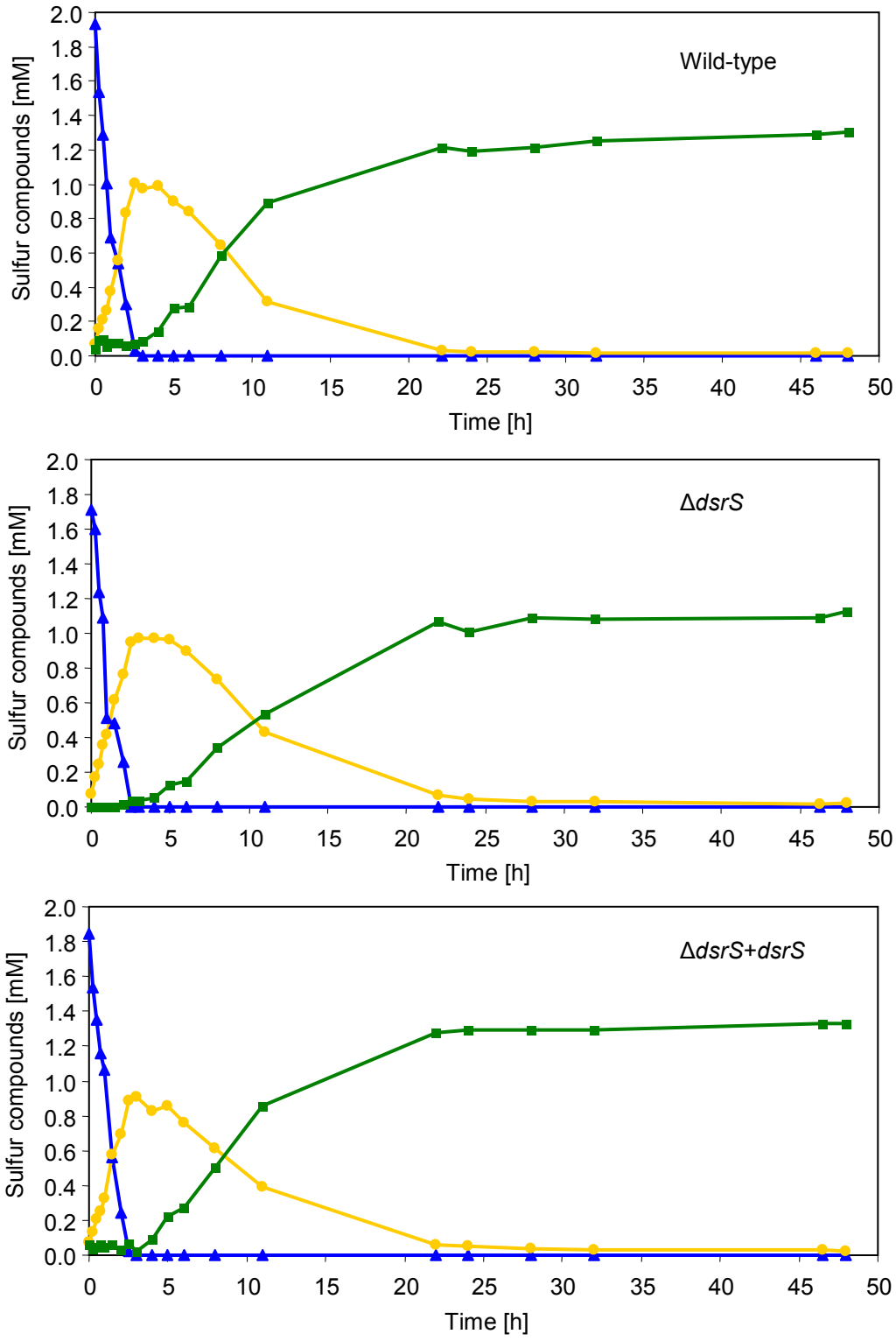

Figure III.37. Time-course of sulfide metabolization by *A. vinosum* Δ*dsrS* and *A. vinosum* Δ*dsrS*+*dsrS* compared to the wild-type. The oxidation of sulfide (▲), formation and degradation of sulfur (●) and production of sulfate (■) were examined in a thermostatted fermenter with modified Pfennig's medium containing 2 mM sulfide. Sulfide could not be completely recovered as sulfate due to loss of gaseous H_2S during sampling. The protein contents of the cultures were 49.7 µg mL^{-1} (wild-type), 90.3 µg mL^{-1} (Δ*dsrS*), and 74.1 µg mL^{-1} (Δ*dsrS*+*dsrS*) at the start of the experiment. Representatives of three independent growth experiments for each strain are shown.

Neither the sulfide oxidation rate, the rate of sulfur globule formation nor the growth yield were affected by the deletion of *dsrS* or by the complementation (Table III.10). Also, the formation of intermediary polysulfides during the oxidation of sulfide to sulfur (Gehrke, 2000; Prange *et al.*, 2004) was neither affected in the Δ*dsrS* mutant nor in the complementation mutant (data not shown). The oxidation of intermediary stored sulfur was evidently not blocked by the deletion of *dsrS* and Δ*dsrS* was still able to form sulfate as end product. However, compared to the wild-type, the deletion mutant exhibited a specific sulfur oxidation rate that was reduced by ~30% (Table III.10). Complementation of the *A. vinosum ΔdsrS* strain did not restore the wild-type oxidation rate, but further reduced the sulfur oxidation rate to 45% of the wild-type rate (Table III.10).

Apparently, contrary to the Δ*dsrR*+*dsrR* strain, a gene expression comparable to the wild-type was not achieved by the complementation *in trans* using the *dsrA* promoter. The expression of *dsrS* obviously requires a different regulation than provided solely by the *dsrA* promoter region.

Nevertheless, the deletion mutant clearly demonstrated that, although DsrS is not absolutely essential for the oxidation of intermediary stored sulfur, it still plays an important role in ensuring an undisturbed process.

Table III.10. Characteristics of the *A. vinosum* Δ*dsrS* deletion mutant compared to the wild-type and the complementation mutant *A. vinosum* Δ*dsrS*+*dsrS*. The results represent the means and standard deviations of three independent growth experiments. Initial sulfide concentration was 2 mM. Oxidation and formation rates are given as nmol min^{-1} (mg protein)$^{-1}$. The growth yield is given as g protein (mol sulfide)$^{-1}$.

	A. vinosum strain		
	Wild-type	Δ*dsrS*	Δ*dsrS*+*dsrS*
Sulfide oxidation rate	199.0 ± 18.2	210.4 ± 2.6	196.9 ± 9.9
Sulfur globule formation rate	90.7 ± 0.6	91.6 ± 3.3	88.9 ± 9.1
Sulfur oxidation rate	24.1 ± 0.3	17.5 ± 0.2	10.8 ± 0.9
Growth yield	8.8 ± 0.9	8.9 ± 0.5	8.9 ± 0.5

3.3.3. Formation of Dsr proteins in the deletion and complementation mutant

Comparative immunoblot analysis of *A. vinosum* wild-type and *ΔdsrS* soluble cell fractions (Figure III.38) did not reveal any apparent influence of the lack of DsrS on the formation of the proteins DsrE, DsrC, DsrK, DsrL and DsrR. Interestingly, the formation of DsrE and DsrL appeared to be disturbed in the *ΔdsrS*+*dsrS* complementation strain, though the formation of DsrR appeared not to be influenced. DsrE and DsrL are known to be essential for sulfur oxidation (Lübbe *et al.*, 2006; Dahl *et al.*, 2008b). Both of these proteins could only be weakly

detected in cells harvested while they were still oxidizing internal sulfur globules (Figure III.38). In a later phase of sulfur oxidation, however, when sulfur globules had essentially vanished from the cells, both proteins were apparently no longer adversely affected. At that point, the same or even higher amounts of both proteins were detected in the *ΔdsrS*+*dsrS* strain as compared to the wild-type or the *ΔdsrS* mutant.

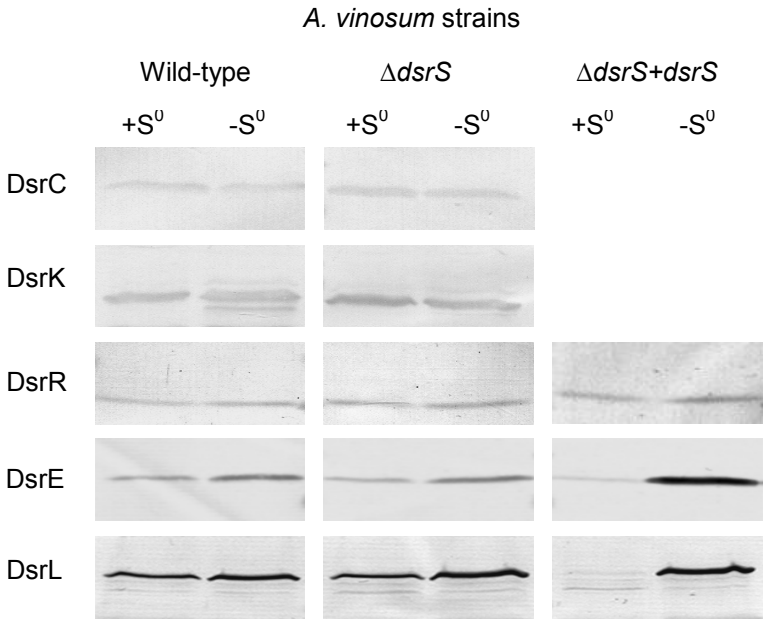

Figure III.38. Formation of several Dsr proteins in *A. vinosum* Δ*dsrS* and *A. vinosum* Δ*dsrS*+*dsrS* compared to the wild-type. Western blot analyses with antisera against DsrC (12.6 kDa), DsrK (58.5 kDa), DsrR (11.4 kDa), DsrE (14.6 kDa), and DsrL (71.4 kDa) were performed with soluble fractions of *A. vinosum* (96 µg protein), *A. vinosum* Δ*dsrS* (96 µg protein), and *A. vinosum* Δ*dsrS*+*dsrS* (96 µg) grown in batch culture on 2 mM sulfide and harvested either at the maximum content of intracellularly stored sulfur (+S^0) or after the sulfur had been completely metabolized (-S^0).

3.4. Influence of the *dsrS* deletion on the expression of other *dsr* genes

The experiments done earlier on the expression of the *dsr* operon showed *dsrS* to be transcribed with similar pattern and levels as the *dsrC* gene and to be probably controlled by a secondary promoter in the *dsrNR* gene region (*cf*. III.1.2). To elucidate if DsrS has an influence on the expression of other *dsr* genes, the expression levels of six *dsr* genes were determined in the *dsrS* deletion mutant via RT-PCR under sulfur-oxidizing conditions and in the absence of sulfur compounds. Furthermore, the *dsrA* expression on a translational level was examined in the *ΔdsrS* mutant by introducing a translational *dsrA*'-*lacZ* gene fusion plasmid and comparing the results to a transcriptional $dsrA_P$-*lacZ* fusion.

3.4.1. Expression studies by real-time RT-PCR

The transcript pattern and levels of the *dsr* genes are largely unchanged in the *dsrS* deletion mutant compared to the wild-type, with the expected exception of the absence of a *dsrS* transcript (Figure III.39). The deletion of *dsrS* does not appear to have a major effect on the transcription of the *dsr* genes.

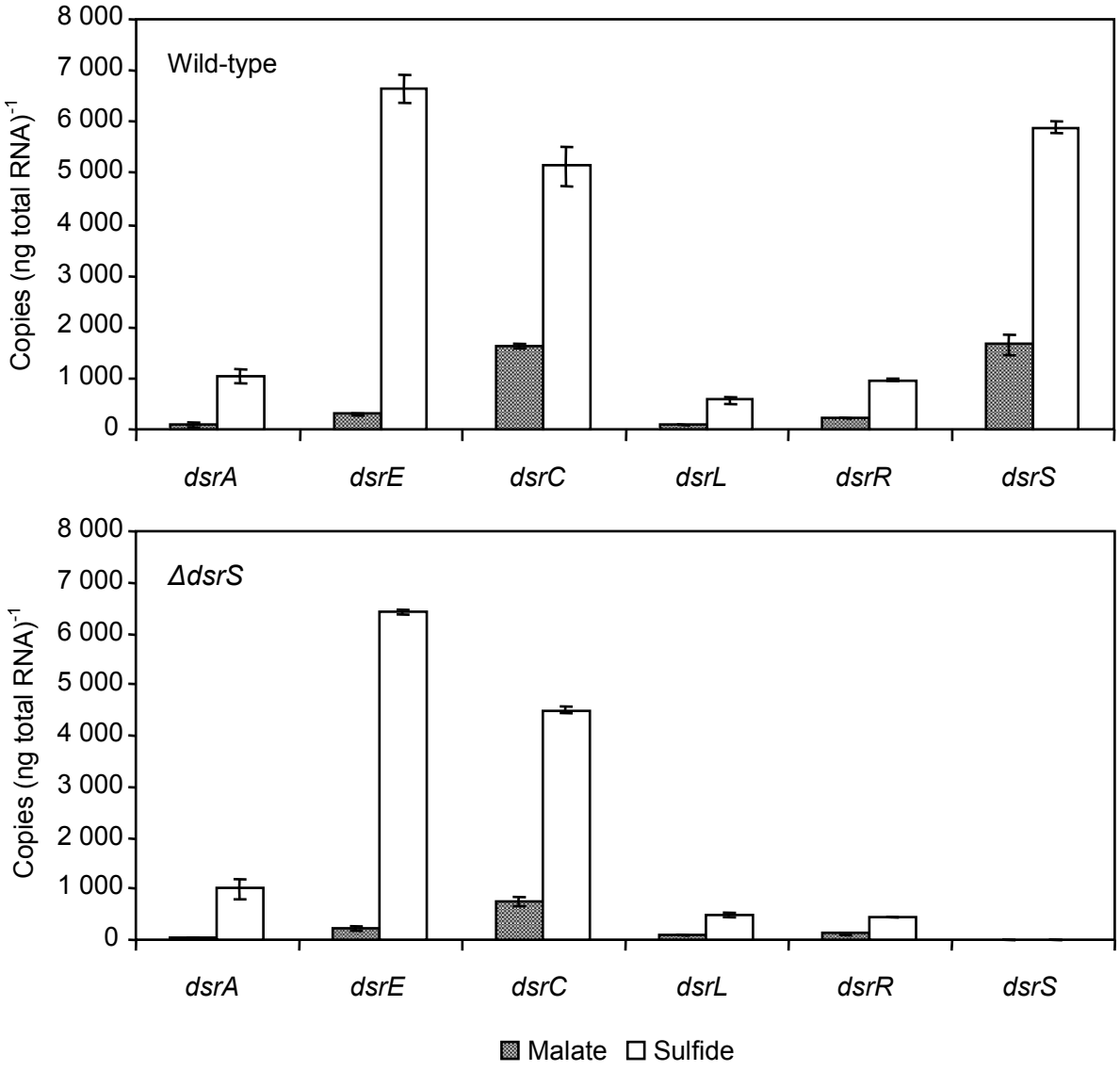

Figure III.39. Expression levels of six *dsr* genes in the *A. vinosum ΔdsrS* mutant compared to the wild-type under photoorganoheterotrophic (malate) and photolithoautotropic (sulfide) conditions determined by real-time RT-PCR. 250 ng of total RNA were used as template. Quantified external RNA fragments containing the target sequence served as standards.

3.4.2. Expression studies by reporter gene fusions

A gene fusion of the main *dsr* promoter $dsrA_P$ and a truncated *dsrA* to a truncated *lacZ* gene was introduced to the *dsrS* deletion mutant in order to assess if DsrS has any effect on the expression of *dsrA* on the translational level. The expression was examined under photo-organoheterotrophic and photolithoautotrophic growth conditions. The resulting β-galacto-sidase activities were compared to those achieved with a transcriptional gene fusion that consists of the $dsrA_P$ fused to *lacZ*.

The specific β-galactosidase activities were at a low level in malate-grown cells and increased approximately three-fold under sulfur-oxidizing conditions (Table III.11, Figure III.40). In accordance with the RT-PCR results, the *ΔdsrS* mutant carrying the transcriptional fusion exhibited the same activities as the wild-type. DsrS has no apparent effect on the transcription of *dsrA*. On the other hand, the *ΔdsrS* mutant carrying the translational fusion showed a ~35 % reduction of β-galactosidase activities compared to the wild-type. The effect was independent of the tested growth conditions.

Table III.11. Specific β-galactosidase activities in *A. vinosum ΔdsrS* and the wild-type carrying transcriptional or translational gene fusions. Photoorganoheterotrophically grown cultures containing transcriptional ($dsrA_P$-*lacZ*) or translational (*dsrA'-lacZ*) gene fusion plasmids were used to inoculate modified Pfennig's medium containing 2 mM of the indicated electron source. The specific β-galactosidase activity is given in nmol *o*-nitrophenol min^{-1} (mg protein)$^{-1}$. The average protein content amounted to 500 µg mL^{-1}. The results represent the means and standard deviations of three independent measurements.

	Specific β-galactosidase activity	
A. vinosum strain	Malate	Sulfide
Wild-type		
$dsrA_P$-*lacZ*	2.9 ± 0.7	9.1 ± 0.9
dsrA'-lacZ	42.6 ± 1.7	96.2 ± 27.1
ΔdsrS		
$dsrA_P$-*lacZ*	2.8 ± 0.3	8.8 ± 1.9
dsrA'-lacZ	26.1 ± 4.2	65.0 ± 2.1

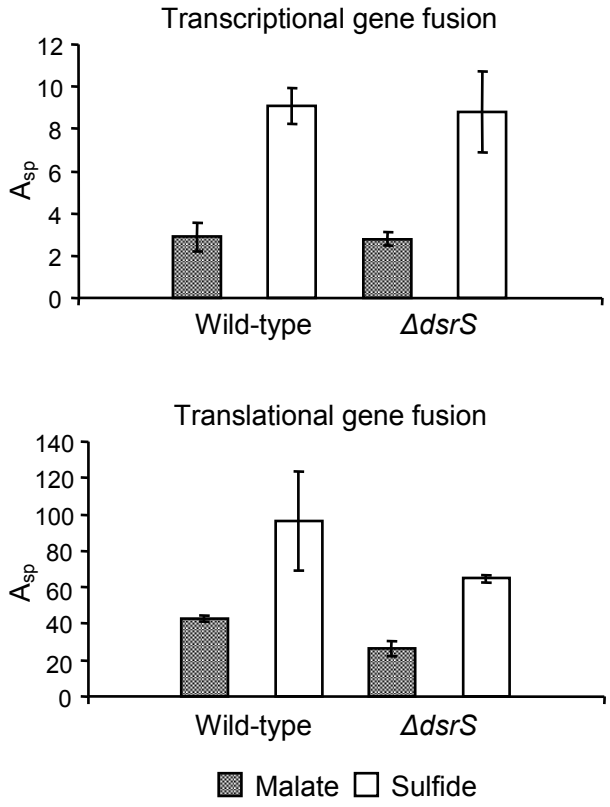

Figure III.40. Specific β-galactosidase activities in the *dsrS* deletion mutant and the wild-type carrying transcriptional or translational gene fusions. Photoorganoheterotrophically grown cultures containing transcriptional or translational gene fusion plasmids were used to inoculate modified Pfennig's medium containing 2 mM of the indicated electron source. The specific β-galactosidase activity A_{sp} is given in nmol *o*-nitrophenol min^{-1} (mg protein)$^{-1}$ (*cf.* Table III.11).

Indeed, the same percentage of reduction was observed with sulfide of different concentrations or thiosulfate as electron source (Table III.12, Figure III.41, Table III.13, *cf.* III.1.1.4). This implicates DsrS as a factor in post-transcriptional control as apparently less DsrA'-LacZ is formed when DsrS is lacking, compared to when it is present..

Table III.12. Influence of the concentration of sulfide on the expression level of DsrA'-LacZ in the *dsrS* deletion mutant. Photoorganoheterotrophically grown cultures containing translational (*dsrA'-lacZ*) gene fusion plasmid were used to inoculate modified Pfennig's medium with the indicated sulfide concentrations. The specific β-galactosidase activity is given in nmol *o*-nitrophenol min^{-1} (mg protein)$^{-1}$. The average protein content amounted to 500 µg mL^{-1}. The results represent the means and standard deviations of three independent measurements.

	Specific β-galactosidase activity	
Sulfide	Wild-type	*ΔdsrS*
0.0 mM	36.7 ± 3.8	25.5 ± 0.6
0.2 mM	44.0 ± 0.2	28.2 ± 5.9
0.5 mM	57.0 ± 8.6	35.8 ± 4.5
2.0 mM	85.1 ± 10.5	52.2 ± 11.5
6.0 mM	110.7 ± 8.0	70.7 ± 8.2

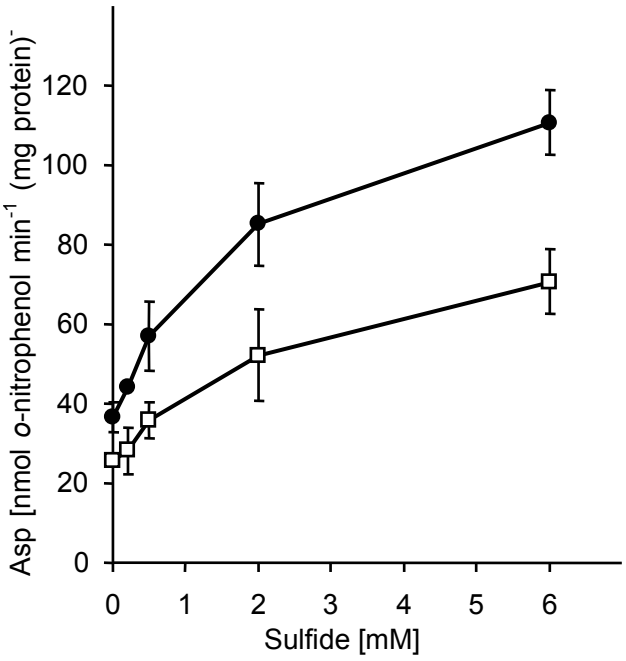

Figure III.41. Influence of the initial concentration of sulfide on the expression level of DsrA'-LacZ in the *dsrS* deletion mutant (squares) compared to the wild-type (circles). Photoorganoheterotrophically grown cultures containing the translational gene fusion plasmid were incubated for 24 h in modified Pfennig's medium with different concentrations of sulfide before the β-galactosidase activities were determined (*cf*. Table III.12).

The addition of malate or sulfite to media already containing sulfide did not reduce the specific β-galactosidase activity any further in the *dsrS* deletion mutant (Table III.13). This demonstrates again that these substances have no influence on the expression of *dsrA* under the tested conditions.

Table III.13. Influence of thiosulfate, malate or sulfite on the expression of DsrA'-LacZ in the *dsrS* deletion mutant. Photoorganoheterotrophically grown culture containing translational gene fusion plasmid was used to inoculate modified Pfennig's medium containing 2 mM of the indicated electron source. The specific β-galactosidase activity is given in nmol *o*-nitrophenol min^{-1} (mg protein)$^{-1}$. The average protein content amounted to 500 µg mL^{-1}. The results represent the means and standard deviations of three independent measurements.

	Specific β-galactosidase activity	
Electron source	Wild-type	*ΔdsrS*
Thiosulfate	89.5 ± 9.4	51.8 ± 6.5
Sulfide	96.2 ± 27.1	65.0 ± 2.1
Malate	42.6 ± 1.7	26.1 ± 4.2
Malate + sulfide	96.4 ± 10.5	67.8 ± 13.4
Sulfite	39.0 ± 7.4	29.7 ± 6.3
Sulfite + sulfide	94.3 ± 30.9	57.4 ± 9.8

IV. Discussion

Insights into the regulation of the *dsr* operon

The investigation of the expression of several *dsr* genes via real-time RT-PCR showed the transcript levels to be low under heterotrophic conditions in the absence of reduced sulfur compounds and to be increased under sulfur-oxidizing conditions. This observation agrees with earlier Northern blot analyses that showed an increased *dsrAB* mRNA level under sulfur-oxidizing conditions (Pott and Dahl, 1998). These findings are further corroborated by the results gained by Dahl *et al.* (2005) who used Western blot analyses to demonstrate the increased formation of the Dsr proteins DsrE, DsrH, DsrC, DsrK, and DsrL under sulfur-oxidizing conditions. On the other hand, the low expression level of sulfite reductase under heterotrophic conditions is not in agreement with observations by Schedel *et al.* (1979). The authors were not able to detect sulfite reductase in malate-grown cells probably because the enzyme level was below the detection limit.

The upregulation of *dsr* gene expression by reduced sulfur compounds has so far only been described for *A. vinosum*. In the chemotrophic sulfur oxidizer *Thiobacillus denitrificans* the *dsr* genes are highly and most likely constitutively expressed (Beller *et al.*, 2006a; Beller *et al.*, 2006b). As the green sulfur bacterium *Chlorobaculum tepidum* is dependent on sulfide, thiosulfate or sulfur for growth (Chan *et al.*, 2008), it can be assumed that *dsr* genes are constitutively expressed in this organism as well. Indeed, recent proteomic analysis of *C. tepidum* showed the abundance of the DsrAB protein to be not exceptionally different between early and late growth phase where the cells had consumed almost all reduced sulfur compounds. Interestingly, the cellular level of DsrEFH was less abundant in the late growth phase which could be due to the change in available sulfur substrates (Falkenby *et al.*, 2011).

Time-course experiments showed that the expression of *dsrA* was not enhanced before the vast majority of sulfide had been metabolized and sulfur globules had been formed. Therefore, sulfide is most likely not the direct inducing factor of *dsr* gene expression. Nevertheless, experiments with varying sulfide concentrations showed the expression level to be dependent on the strength of the inducing signal. Apparently, the expression can be modified according to demand.

Sulfate concentration in the time-course experiments increased concurrently to the β-galactosidase activities, implicating the oxidation of stored sulfur to sulfite as the rate-limiting step in the oxidation of sulfur to sulfate. This corresponds to the fact that sulfite is hardly detected during sulfur oxidation in *A. vinosum* (Steudel *et al.*, 1990; Dahl, 1996; Dahl *et al.*, 2008b). Considering the high reactivity and toxicity of free sulfite in the cytoplasm, it is not surprising that the organism protects itself by a fast turn-over. The mechanism of sulfite

oxidation in phototrophic sulfur-oxidizing bacteria is still under debate, though several candidates were identified (Frigaard and Dahl, 2009). For a number of chemo- and photo-lithotrophic sulfur oxidizers (*e.g. T. denitrificans, A. vinosum, C. tepidum*) the simultaneous occurrence of at least two sulfite-oxidizing pathways has been observed (Dahl, 1996; Kappler and Dahl, 2001; Frigaard and Dahl, 2009). The possession of an additional periplasmically located pathway might serve the organism in the oxidation of externally added sulfite (Kappler and Dahl, 2001). This could explain why externally added sulfite had no influence on the expression of the *dsr* genes.

The alternative electron donor malate had no effect on the expression of *dsrA*. In the past, it had been observed that in *A. vinosum* the reduced sulfur compound thiosulfate is metabolized in the presence of an organic carbon and electron donor, like pyruvate or acetate (Hurlbert and Lascelles, 1963; Hurlbert, 1968). Moreover, thiosulfate exerts a repressive effect on the utilization of pyruvate. The synthesis of ribulose-1,5-bisphosphate carboxylase, which catalyzes the main CO_2 fixation reaction in *Chromatiaceae* (Sahl and Trüper, 1977), is inhibited by the presence of an organic compound (Fuller *et al.*, 1961). But the repression is not complete and a residual activity can be detected, depending on the presence of reduced sulfur compounds (Hurlbert and Lascelles, 1963). Therefore, pure photoheterotrophy apparently only occurs when reduced sulfur compounds are limited. These observations suggest a preferential utilization of reduced sulfur compounds over organic compounds as electron donors.

Based on the RT-PCR results, additional secondary promoters involved in the expression of *dsrC* and *dsrS* were postulated. This conclusion is corroborated by the differential regulation of the genes in other organisms. In several sulfate-reducing prokaryotes, like *Desulfovibrio vulgaris* Hildenborough, the *dsrC* gene is located separately from *dsrAB* and the expression of these genes is not co-ordinately regulated (Karkhoff-Schweizer *et al.*, 1993). *dsrS* homologues are found in several sulfur-oxidizing bacteria, like *T. denitrificans* and Candidatus *Vesicomyosocius okutanii*, but only in *A. vinosum dsrS* is part of the *dsr* operon (Dahl *et al.*, 2005; Sander *et al.*, 2006). Northern blot experiments showed a 0.9 kb mRNA detectable by *dsrC* probe that was present in the 21D mutant (Pott and Dahl, 1998), leading the authors to suggest a secondary promoter for *dsrC*. *In silico* analyses revealed potential promoter sequences in the respective upstream regions of *dsrC* and *dsrS*.

The *dsrC* and *dsrS* mRNA levels under sulfur-oxidizing conditions were increased in the wild-type and reduced in the 21D and 34D mutants, indicating the regulatory signals of $dsrC_P$ and $dsrS_P$ to be different from those of $dsrA_P$ as the expression of *dsrA* in the mutants was unchanged from wild-type expression. The *dsrA* promoter appears to be solely responsible for the upregulation of the expression of *dsr* genes in the presence of reduced sulfur compounds.

The increased mRNA level of *dsrS* under sulfur-oxidizing conditions clearly implies that DsrS plays a role in the oxidation of sulfur in *A. vinosum*. Indeed, an in frame deletion mutant of *dsrS* in *A. vinosum* displayed a ~30% reduction of the specific sulfur oxidation rate compared to the wild-type. On the other hand, the presence of *dsrS* is not essential for sulfur oxidation, as many sulfur-oxidizing bacteria like *C. tepidum* and *H. halophila* do not contain a copy of the gene (Sander *et al.*, 2006; Frigaard and Dahl, 2009). DsrS exhibits no significant homologies to proteins of known function and contains no identifiable domain or co-factor binding sites. The later discussed involvement of DsrS in the post-transcriptional regulation of the *dsr* gene expression might explain the need for a differential regulation of *dsrS*.

dsrC is part of the core set of *dsr* genes present in all sulfur-oxidizing bacteria and sulfate-reducing prokaryotes (Sander *et al.*, 2006; Frigaard and Dahl, 2009). A high transcript level of *dsrC* has also been noted in *T. denitrificans* (Beller *et al.*, 2006a; Beller *et al.*, 2006b), *D. vulgaris* (Haveman *et al.*, 2003), and the endosymbiont of the coastal bivalve *Solemya velum* (Stewart *et al.*, 2011). DsrC is highly similar to TusE, a protein involved in the sulfur relay mechanism leading to biosynthesis of thiouridine at the wobble position of tRNA (Numata *et al.*, 2006; Cort *et al.*, 2008). DsrC from the sulfate-reducing organisms *Desulfovibrio vulgaris*, *Desulfovibrio gigas*, and *Desulfomicrobium norvegicum* interacts closely with DsrAB: The highly conserved C-terminal arm of DsrC has been shown to be able to reach the active site of the reductase (Oliveira *et al.*, 2008; Hsieh *et al.*, 2010; Oliveira *et al.*, 2011). Based on these findings it has been proposed that DsrC from *A. vinosum* is part of a substrate delivery system for the reverse sulfite reductase (Cort *et al.*, 2008; Dahl *et al.*, 2008b). Interestingly, DsrEFH, the protein complex encoded immediately upstream of *dsrC*, shows high similarities to TusBCD, the sulfur donor of TusE (Dahl *et al.*, 2008b). In fact, recent experiments showed *A. vinosum* DsrEFH to be capable of transferring sulfur to DsrC *in vitro* (Yvonne Stockdreher, personal communication). The reason for the differential regulation of *dsrC* might therefore be found in the function of DsrC as co-substrate for sulfite reductase. The continuous presence of DsrC even at non sulfur-oxidizing conditions might be advantageous as it guarantees a fast turn-over rate. The surprisingly high transcript level of *dsrE* under sulfur-oxidizing conditions might be due to the need of the organism to quickly build up enough DsrEFH to ensure a fast sulfur transfer to DsrC.

The proposed DNA-binding ability of DsrC (Cort *et al.*, 2008) was confirmed by DNA mobility shift assays. DsrC binds specifically to a 538 bp DNA fragment, bordered by *Xho*I and *Eco*RV restriction sites, that is located 236 nt upstream of the *dsrA* starting codon. Analysis of the sequence with Neural Network Promoter Prediction and BPROM online tools revealed a potential promoter region within the fragment that is in accordance with the *dsrA* promoter region previously proposed by A. Pott-Sperling (2000). A nearly perfect 20 bp palindrome (aaactgtaat-attagagttt) was identified that is situated immediately upstream of the potential

promoter region. Motifs with pronounced dyad symmetry are typically bound by symmetric transcription factor homodimers where each subunit binds to one half of the motif via a helix-turn-helix motif. In this respect it is interesting to note that DsrC has been reported to form homodimers (Cort *et al.*, 2008). The length of the potential transcription factor recognition site and its immediate vicinity to the proposed -35 region of the promoter is reminiscent of the situation found for a number of well-characterized transcription factors of the LuxR family, *e.g.* TraR which regulates genes of the tumor-inducing plasmid of *Agrobacterium tumefaciens* (White and Winans, 2007).

These results suggest a second function for DsrC as a regulatory protein. The utilization of the same protein for two distinct functions has already been described for several polypeptides. One well documented example is PutA from *E. coli*. This protein catalyzes the two-step oxidation of proline to glutamate and serves as a transcriptional repressor of the proline utilization (*put*) genes (Lee *et al.*, 2003).

Several copies of putative *dsrC* homologues are present in the genomes of *T. denitrificans* (Beller *et al.*, 2006a) and *A. vinosum*. In *T. denitrificans* only the *dsrC* gene which is part of the *dsr* operon contains the two C-terminal conserved cysteine residues. The other DsrC candidates contain only one or none of these cysteine residues, making a participation in sulfur oxidation unlikely. The *dsrC* copies show a wide variability in their expression pattern (Beller *et al.*, 2006b). *A. vinosum* possesses five *dsrC* homologues, two of which contain both cysteine residues, the *dsrC* copy in the *dsr* operon (YP_003443227.1) and Alvin_0345 (YP_003442339.1). The latter is not encoded in the vicinity of sulfur oxidation related genes. The function of the DsrC homologue with one conserved cysteine residues corresponding to Cys100 (YP_003442712.1) as well as the function of the cysteine-lacking DsrC homologues (YP_003443473.1, YP_003442032.1) is unclear. TusE-like proteins contain a conserved cysteine residue corresponding to Cys111 of *A. vinosum* DsrC but lack a conserved Cys100 residue (Ikeuchi *et al.*, 2006).

While the C-terminus with its conserved cysteine residues is important for the function as substrate carrier, the overall DsrC fold might serve another, possibly regulatory, function that is preserved in these other DsrC-like proteins. DsrC exhibiting a second function would also explain why *dsrC* cannot be stably deleted from the *A. vinosum* genome (Cort *et al.*, 2008). The deletion mutant could not be maintained in liquid culture, neither on media containing malate nor in the presence of reduced sulfur compounds (Cort *et al.*, 2008). Comparable phenotypes were not observed for other *dsr* deletion mutants, including a *dsrE* deficient mutant. The severity of this phenotype is therefore not in accordance with the previous assumption that DsrC has only a single function as part of a substrate delivery system.

The additional function of DsrC as a regulatory protein suggests another reason for the differential regulation of *dsrC*. The protein could function as a transcriptional activator and

might be constitutively expressed to provide a low protein level, so that transcription can quickly be induced in changing environmental conditions. Such a mechanism has already been reported for *Salmonella typhimurium* EutR, the transcriptional activator of the *eut* operon. The latter encodes ethanolamine utilization genes. EutR is expressed from a weak constitutive promoter within the operon as well as from the main promoter. The expression of *eutR* increases when the expression of the operon is induced, creating a positive feedback loop that is necessary for maximal operon expression (Roof and Roth, 1992).

Characterization of the DsrR protein

Based on the sequence similarity to IscA, a protein involved in iron-sulfur cluster maturation (Krebs *et al.*, 2001; Tokumoto and Takahashi, 2001; Ding *et al.*, 2005), it is tempting to assume that DsrR could exhibit a similar function. Considering that several iron-sulfur cluster containing proteins are encoded within the *dsr* operon (DsrAB, DsrK, DsrO and DsrL), it even appears appropriate to provide these with a protein specific iron-sulfur cluster scaffold, similar to ^{Nif}IscA and the IscA homologue ErpA. In *Azotobacter vinelandii,* ^{Nif}IscA supposedly serves as alternative scaffold to NifU in nitrogen fixation specific iron-sulfur cluster assembly (Krebs *et al.*, 2001). In *Escherichia coli* ErpA, just as DsrR in *A. vinosum*, is not encoded near any other Fe-S cluster biogenesis genes. Nevertheless, ErpA is essential for isopentenyl diphosphate (IPP) biosynthesis, as it is probably involved in the maturation of the iron-sulfur cluster containing key enzymes IspG and IspH (Loiseau *et al.*, 2007).

Despite the high sequential and structural similarity that has been shown by the NMR structure, the DsrR protein family lacks all of the three invariant cysteine residues that are involved in the coordination of iron or iron-sulfur clusters (Jensen and Culotta, 2000; Bilder *et al.*, 2004; Cupp-Vickery *et al.*, 2004; Ding *et al.*, 2004). Conserved acidic amino acid residues present in DsrR-like proteins (Asp35, Asp45, Asp50, and Asp95 of *A. vinosum* DsrR) could indicate a reduced iron-binding capability of DsrR. However, the UV-Vis spectra of DsrR after purification and after reconstitution with iron or with iron and sulfide showed no indication of bound iron or bound iron-sulfur clusters. Moreover, gel filtration analysis showed DsrR to be a monomer, contrary to IscA which occurs as a mixture of oligomeric forms with dimer and tetramer predominating (Ollagnier-de-Choudens *et al.*, 2001; Wu *et al.*, 2002). The NMR spectra of DsrR corroborated these results, as neither bound iron nor an indication for a multimeric species of DsrR could be found. IscA monomers associate to form a dimer of dimers with a central channel within which the conserved cysteine residues are presumed to form a “cysteine pocket” and where mononuclear iron or iron-sulfur cluster can be coordinated in a subunit bridging manner (Krebs *et al.*, 2001; Bilder *et al.*, 2004; Cupp-Vickery *et al.*, 2004). The loss of the cysteine residues as well as the lack of a higher oligomerization state and the inability to bind iron ions or iron-sulfur clusters strongly

disabuse the notion that DsrR serves as a Dsr protein specific iron-sulfur cluster scaffold or as iron chaperone delivering iron ions to nascent iron-sulfur clusters.

The DsrR protein family is clearly a subgroup belonging to the IscA protein superfamily. DsrR-like proteins apparently only occur in sulfur-oxidizing bacteria that use the reverse acting sulfite reductase DsrAB to oxidize intracellularly stored sulfur. The subgroup, as stated above, is characterized by the striking absence of the three invariant cysteine residues present in hundreds of IscA superfamily sequences. DsrR must have acquired a specialized role in sulfur oxidation following gene duplication of an ancestral *iscA* gene. This role does not require binding of iron ions or Fe-S clusters directly and the loss of the cysteine residues actually may have been driven by negative selection for Fe-S- or iron binding activity. *A. vinosum* and other organisms with *dsrR* still contain *iscA* or *erpA* genes.

The structural similarity between DsrR and IscA-like proteins and conservation of several surface residues suggest that DsrR retains functional characteristics other than coordination of Fe-S clusters or iron-binding in common with its IscA-like paralogues. One possibility is that DsrR assists in recruitment of iron or Fe-S cluster donors and facilitation of metal transfer to a Fe-S cluster-containing Dsr protein such as DsrAB, DsrK, DsrO or DsrL without actually interacting with the metal itself. In this sense, DsrR would not be unlike other IscA paralogues such as ^{Nif}IscA and ErpA that are specialized in the maturation of specific Fe-S cluster containing proteins, except that DsrR would not interact directly with iron or the Fe-S cluster. There is some evidence suggesting cysteine-less scaffold proteins as mediators of protein-protein interaction. The iron-sulfur cluster scaffold protein NfuA of *E. coli* consists of two domains. NfuA is essential for *E. coli* to grow under oxidative stress and iron-starvation (Angelini *et al.*, 2008). The C-terminus resembles the Nfu domain of NifU and the N-terminal domain shows similarity to A-type scaffold proteins (IscA, SufA, ErpA), but, like DsrR, has lost the three invariant cysteine residues of this protein family. The NfuA N-terminal domain is not particularly similar to DsrR however, so this appears to be a second instance of loss of cysteine residues from an ancestral IscA-like protein, rather than the occurrence of a DsrR-like protein in an organism that does not have other *dsr* genes and does not oxidize intracellularly stored sulfur. Complementation studies showed that both domains are essential for the function of NfuA *in vivo* (Angelini *et al.*, 2008). Interestingly, several transcriptomic analyses reported that *nfuA* (also known as *yhgI* and *gntY*) is upregulated in response to translational stress, either due to misfolded protein (Lesley *et al.*, 2002), kanamycin (Shaw *et al.*, 2003), or heat-shock (Nonaka *et al.*, 2006) and, of course, under iron limitation (McHugh *et al.*, 2003). These facts led Angelini *et al.* (2008) to the conclusion, that NfuA possesses a function as a chaperone and in repairing damaged iron-sulfur proteins.

A similar case involving loss of cysteine residues from one domain of a protein with duplicate domains involved in Fe-S cluster assembly is found in OsCnfU-1A of *Oryza sativa* (Saio *et al.*, 2007). The two domains of OsCnfU-1A resemble the Nfu domain of NifU, the IscU-like iron-sulfur cluster scaffold for maturation of the nitrogenase iron-sulfur cluster in *Azotobacter vinelandii* (Dos Santos *et al.*, 2004; Smith *et al.*, 2005). The second domain does not have the invariant cysteine residues typical for Nfu domains. It is responsible for the mediation of the interaction to the apo-protein ferredoxin through an extensive basic surface which makes it ideal for the interaction with the predominantly negatively charged ferredoxin (Saio *et al.*, 2007). DsrR could in principle be another example of a cysteine-less scaffold protein mediating protein-protein interaction.

In this context, it is interesting to note that highly conserved residues typical for DsrR-like proteins (the fully conserved motif Met42-Gly43-Phe44-Asp45 and the highly conserved hydrophobic motif Ile89-Phe90-Leu91) are located on the surface of the cleft of the protein structure (Figure III.21). In IscA-like proteins residues located in the cleft have been implicated to be important for the stabilization of dimer/tetramer interaction (Bilder *et al.*, 2004; Morimoto *et al.*, 2006).

A first look at potential interaction partners of DsrR using a coprecipitation method showed DsrR to interact with the essential Dsr proteins DsrEFH, DsrC, and DsrL. DsrEFH and DsrC, as mentioned above, are thought to be part of the substrate delivery system for the reverse sulfite reductase DsrAB (Cort *et al.*, 2008; Dahl *et al.*, 2008b). DsrL is a cytoplasmic iron-sulfur flavoprotein with NADH:acceptor oxidoreductase activity and a C-terminal thioredoxin motif (Lübbe *et al.*, 2006; Dahl, 2008). A potential disulfide reductase activity has been proposed but the corresponding activity could so far not be confirmed (Lübbe, 2005; Kammler, 2009). The function of DsrL in the oxidation of sulfur is uncertain but it has been put forward that it could be involved in the reductive release of sulfide from a perthiolic organic carrier molecule that transportes sulfur from the periplasmic sulfur globules to the cytoplasm (Dahl, 2008; Frigaard and Dahl, 2009; Sander and Dahl, 2009). DsrL has also been proposed to be responsible for the reduction of an intramolecular disulfide bond in DsrC that could form upon release of sulfide as substrate for DsrAB or upon the relase of the product sulfite following the oxidation of DsrC-bound sulfide by the reverse-acting sulfite reductase (Cort *et al.*, 2008; Kammler, 2009). DsrR might function as a chaperon mediating the interactions between these proteins and thus enhance the sulfur relay system.

In the genome of *Candidatus* Ruthia magnifica (Newton *et al.*, 2007), the sulfur-oxidizing symbiont of the giant hydrothermal vent clam *Calyptogena magnifica*, *dsrR* is fused to *dsrN* which is located immediately upstream (Figure III.12). A separate ribosome binding site is not apparent for the *dsrR* gene, indicating co-translation of the two genes in *R. magnifica*. The authors Harada *et al.* (2009) proposed that the intergenic region between *dsrR* and *dsrN*

was deleted during the reductive genome evolution (the reduction of a symbiont genome to those genes that are essential for intracellular symbiotic life). This observation provoked the idea that DsrN and DsrR may act together or even be subunits of a heterooligomeric protein (Sander and Dahl, 2009; Frigaard and Dahl, 2009). DsrN is a siroheme amidase and responsible for the amidation of siroheme to siroamide, the prosthetic group of the reverse-acting sulfite reductase in *A. vinosum* (Lübbe *et al.*, 2006). A *dsrN* deletion mutant showed a similar phenotype to the *dsrR* deletion mutant, *i.e.* a severe reduction but not cessation of sulfur oxidation (Lübbe *et al.*, 2006). In light of these observations the assumption that the two proteins are connected appeared plausible. However, *dsrR* and *dsrN* do not always occur together, as *dsrR* is neither present in the genome sequences of green sulfur bacteria, *e.g. C. tepidum*, nor in that of the purple sulfur bacterium *H. halophila*. Contrary to *dsrR*, *dsrN* is part of the core set of *dsr* genes present in all prokaryotes utilizing Dsr proteins in dissimilatory sulfur metabolism (Sander *et al.*, 2006). Therefore, the proposal that DsrN and DsrR might be subunits of a heterooligomeric protein may have been premature. Furthermore, co-expression and co-purification of His-tagged DsrN with DsrR gave no indication on a closer interaction of these two proteins in *A. vinosum*. A weaker intermediary interaction of these two proteins cannot be excluded, but it appears unlikely that DsrR is a subunit in a DsrNR protein complex.

During the course of this work, another potential function for DsrR was identified, *i.e.* the participation of DsrR in post-transcriptional regulation. The comparison of the effects of a deletion of *dsrR* on transcriptional versus translational reporter gene fusions showed that transcription was not affected but that translation was diminished by ~83 %. The LacZ activities measured where comparable to those obtained with the transcriptional gene fusion. The lack of DsrR apparently has a similar effect on the expression as the lack of the *dsrA* specific 5'-untranslated region. Reporter gene activities in the Δ*dsrR* strain for the translational gene fusion decreased to approximately the same extent as the sulfur oxidation rate (~88 %). The decreased sulfur oxidation rate and the diminished presence of DsrE and DsrL, both of which are absolutely essential for sulfur oxidation (Lübbe *et al.*, 2006; Dahl *et al.*, 2008b), could be explained by a reduced rate of post-transcriptional processes in the *ΔdsrR* mutant. The unchanged presence of DsrC might be due to the differential regulation of the *dsrC* gene. The cause of the unaffected presence of the membrane-associated cytoplasmic protein DsrK is uncertain and requires further reasearch. A possible explanation might be that, as DsrR is implicated to interact with the proteins DsrEFH, DsrC, DsrL, and even maybe DsrAB in order to facilitate the sulfur relay system, it could be that DsrR is only involved in the regulation of the post-transcriptional processes of these proteins. As DsrC performs a second function as a transcriptional regulator and is itself additionally regulated

by a secondary promoter it may be exempt from the regulation facilitated by the DsrR protein.

These findings suggest DsrR as a player in post-transcriptional regulation. The protein could either be involved in stabilizing ribosome-mRNA interaction, thus enhancing translation, or play a role during translational attenuation, *i.e.* inducing a conformational change in the mRNA and thereby permitting translation initiation. Interestingly, the entire Shine-Dalgarno sequence of *dsrA* is part of a predicted stem-loop formation possibly preventing ribosomal access (Figure IV.1).

```
880 cacaaaccatatccgttcctggttatatcgataggagagaccgcgcaatggctatcgacaagcacgcgacc 950
                                rbs          >---dsrA'--------------'
```

Figure IV.1. The location of the potential stem-loop formation that encompasses the entire Shine-Delgarno sequence of *dsrA* as predicted by DINAMelt. The stem-part of the stem-loop formation is marked in blue bold face, the loop-part is in green bold face. The predicted free energy of forming is -38 kJ mol^{-1}. The sequence can be found under the GenBank acc. no. U84760.4.

It is also interesting to note in this respect that Balasubramanian *et al.* (2006) suggested a regulatory role for IscA, in addition to its function as an Fe-S cluster assembly scaffold. The authors described IscA as part of the sense and/or response cascade set into action upon iron limitation in cyanobacteria.

As the NMR structure of DsrR did not reveal any RNA-binding motifs, it seems unlikely that DsrR itself binds directly to mRNA. More detailed experiments need to be performed in the future to elucidate the most likely indirect contribution of DsrR to post-transcriptional regulation as part of a signal-transducing reporter chain cascade.

Characterization of the DsrS protein

Compared to previous analyses (Dahl *et al.*, 2005), the updated sequence analyses of the *dsrS* gene did not reveal further insights into the function of the protein encoded by the last gene of the *dsr* operon. Neither conserved domains nor motifs were identified in the sequence and significant similarities to proteins of known function were not apparent. Furthermore, the gene neighborhood of *dsrS* gene homologues of other sulfur-oxidizing organisms, *dsrS* is only part of the *dsr* gene cluster in *A. vinsoum*, gave no indications to a potential function of the DsrS protein. The function and indeed the involvement of the DsrS protein in the sulfur-oxidation in *A. vinosum* had been uncertain (Dahl *et al.*, 2005; Dahl, 2008; Frigaard and Dahl, 2009; Sander and Dahl, 2009).

In this work, the previous sequence-deduced postulations concerning DsrS were confirmed; the gene *dsrS* encodes a monomeric protein of the deduced 41.1 kDa molecular mass and appears not to contain cofactors. The DsrS protein might be post-translationally processed by cleaving the less conserved C-terminal part of the protein. This is suggested by sequence

comparison of DsrS homologues and an N-terminal ~25 kDa fragment of DsrS observed in cells producing the recombinant protein.

The *dsrS* gene is transcribed at a high level under photoorganoheterotrophic conditions in the absence of reduced sulfur compounds and the mRNA level increased under sulfur-oxidizing conditions, indicating direct or indirect involvement of the encoded protein in the sulfur-oxidizing process. The transcript levels were similar to those observed for the constitutively and highly expressed gene *dsrC* for which a secondary promoter has been postulated. They were significantly higher than those for *dsrA* under photoorganoheterotrophic conditions in the absence of reduced sulfur compounds, even though *dsrA* encodes a subunit of the key enzyme for intracellular sulfur oxidation, dissimilatory sulfite reductase.

Characterization of a Δ*dsrS* mutant showed DsrS to be important though not essential for the oxidation of intracellularly stored sulfur (Grimm, 2004). Quantification of the specific sulfur oxidation rate showed a 30 % reduction in the *dsrS* deletion mutant compared to the wild-type. Complementation *in trans* of the Δ*dsrS* strain with *dsrS* under control of the main *dsr* promoter $dsrA_P$ did not restore the sulfur oxidation rate to wild-type levels; indeed, the oxidation rate was further reduced to 45 % of the wild-type oxidation rate. Comparable plasmids carrying *dsr* genes cloned immediately downstream of $dsrA_P$ had already been successfully used for complementation of *A. vinosum* mutants carrying deletions of the respective *dsr* genes (Lübbe *et al.*, 2006; Sander *et al.*, 2006; Dahl *et al.*, 2008b). In all cases described so far, wild-type oxidation rates were restored or at least significantly improved compared to the deletion mutant. The *ΔdsrS*+*dsrS* strain clearly behaved differently, indicating that the *dsrA* promoter may not be able to provide the cell with the necessary level of DsrS and pointing at the presence of further regulatory element(s) for *dsrS*.

As mentioned before, a differential regulation of the *dsrS* gene expression, potentially mediated by a secondary promoter, is not surprising, considering that *dsrS* is not part of the *dsr* operon in other sulfur-oxidizing bacteria. Furthermore, the presence of a secondary promoter for *dsrS* is in agreement with the results of the comparative analysis of the *dsr* gene transcription in *A. vinosum* wild-type and the mutants 21D and 34D that contain transcriptional and translational blocks in the *dsrB* and *dsrH* gene region, respectively. Even though the transcription of genes located downstream should thus be prevented, high transcription levels were nevertheless found for *dsrS*. *In silico* analysis of the upstream region of *dsrS* revealed potential promoter sequences in the *dsrNR* intergenic region.

A comparison of the transcription patterns of several *dsr* genes in the wild-type to those in the Δ*dsrS* deletion mutant revealed no major differences. The *dsrS*-encoded protein is apparently not involved in the regulation of the *dsr* gene transcription. This observation fits well with the results of the immunoblot analysis, as a perceptible reduction in the formation of DsrC, DsrK, DsrR, DsrE, and DsrL could not be observed in the deletion mutant.

Nevertheless, translational gene fusion experiments suggest a participation of DsrS in the post-transcriptional control of the *dsr* operon. The formation of the translational fusion of DsrA'-LacZ was diminished by 35 % in the deletion mutant compared to the wild-type. It is possible that the method of choice, immunoblot analysis, was not sensitive enough to detect an approx. 30 % reduction in the protein levels. A more sensitive approach combined with quantification techniques might allow for a more differentiated statement. It is also possible that DsrS is only involved in the post-transcriptional regulation of DsrA and thus the formation of downstream encoded Dsr proteins is not affected by the lack of DsrS in the *ΔdsrS* mutant.
On the other hand, the formation of DsrE and DsrL appears to be negatively affected in the *ΔdsrS*+*dsrS* complementation strain. Compared to the wild-type and the deletion mutant, the proteins could only be faintly detected in cells harvested while they were still oxidizing internal sulfur globules. In a later phase of sulfur oxidation, when sulfur globules had essentially vanished from the cells, both proteins were apparently no longer adversely affected. At that point, the same or even higher amounts of both proteins were detected in the *ΔdsrS*+*dsrS* strain compared to the wild-type or the *ΔdsrS* mutant. This suggests that the DsrS protein level has an effect on the formation of these proteins as well.
The reduction of the specific sulfur oxidation rate observed in the *dsrS* deletion mutant could thus be due to a reduced presence of essential Dsr proteins like DsrA, DsrE, and DsrL. The further reduction of the specific sulfur oxidation rate in the Δ*dsrS* complementation strain may be due to the time-delayed formation of the essential Dsr proteins DsrE and DsrL. Whether the formation of DsrA is similarly affected in the complementation mutant remains to be investigated.
The exact mechanism of the post-transcriptional regulation by DsrS is still unclear. Similar to the proposed function of DsrR, DsrS could influence the post-transcriptional regulation either indirectly as part of a signal transducing reporter chain cascade or directly by stabilizing the ribosome-mRNA interaction and thus enhancing translation. Another possibility is that DsrS is involved in translational attenuation, *i.e.* induces a conformational change in the mRNA thereby permitting translational initiation. The reader may be reminded that the entire Shine-Dalgarno sequence of *dsrA* is part of a potential stem-loop formation that could prevent ribosomal access. As the gene fusion experiments showed, the region encompassing the *dsrA* ribosome binding site is required for the downregulation of the accumulation of DsrA protein in the absence of DsrS.
Further studies are, however, clearly necessary to elucidate the exact mechanism of the post-transcriptional regulation of DsrA, and possibly of further Dsr proteins, by DsrS. Apparently the regulation of the *dsr* operon and the function of DsrS may be more intricate than previously expected.

V. Summary

This work represents the first in depth investigation of the *dsr* gene expression in a phototrophic sulfur-oxidizing organism. Although over the last decade some observations were made concerning regulation a more detailed survey had been missing until now.

An increase in expression of *dsr* genes under sulfur-oxidizing conditions was shown on the transcriptional as well as translational level and probable secondary promoters involved in the expression of *dsrC* and *dsrS* were identified. Sulfide was disproven to be a direct inducing factor of the *dsr* gene expression, although the strength of the expression was dependent on the sulfide concentration. The oxidation of intermediary stored sulfur to sulfite was identified as the rate-limiting step in the oxidation of sulfur to sulfate. The proposed product of the reverse sulfite reductase sulfite as well as the alternative electron donor malate had no effect on the expression of *dsrA*. The proposed DNA-binding capability of DsrC could be confirmed, thus identifying DsrC as a potential regulatory protein of *dsr* gene expression.

Furthermore, the importance of the previously barely investigated proteins DsrR and DsrS for the oxidation of intermediary stored sulfur in *A. vinosum* was examined more closely. The similarities and differences of DsrR to the A-type scaffold IscA, a protein involved in the maturation of iron-sulfur clusters, were shown on the structural as well as on the functional level and a potential direct involvement of DsrR in the maturation of Dsr protein specific iron-sulfur clusters could be negated. Interaction of DsrR with DsrEFH, DsrC, and DsrL opened up the possibility that DsrR might mediate the protein interaction of these Dsr proteins that could be involved in the substrate delivery system for the sulfite reductase. The effects of the deletion of *dsrR* and *dsrS* on the expression of other *dsr* genes were examined and, based on the results, a potential function for the proteins DsrR and DsrS as post-transcriptional regulators was proposed.

VI. References

Altschul, S.F., Madden, T.L., Schäffer, A.A., Zhang, J., Zhang, Z., Miller, W., and Lipman, D.J. (1997) Gapped BLAST and PSI-BLAST: A new generation of protein database search programs. *Nucleic Acids Res* **25:** 3389-3402.

Angelini, S., Gerez, C., Ollagnier-de-Choudens, S., Sanakis, Y., Fontecave, M., Barras, F., and Py, B. (2008) NfuA, a new factor required for maturing Fe/S proteins in *Escherichia coli* under oxidative stress and iron starvation conditions. *J Biol Chem* **283:** 14084-14091.

Ausubel, F.A., Brent, R., Kingston, R.E., Moore, D.D., Seidman, J.G., Smith, J.A., and Struhl, K. (1997) *Current Protocols in Molecular Biology.* New York: John Wiley & Sons.

Ayala-Castro, C., Saini, A., and Outten, F.W. (2008) Fe-S cluster assembly pathways in bacteria. *Microbiol Mol Biol Rev* **72:** 110-125.

Balasubramanian, R., Shen, G., Bryant, D.A., and Golbeck, J.H. (2006) Regulatory roles for IscA and SufA in iron homeostasis and redox stress responses in the cyanobacterium *Synechococcus* sp. strain PCC 7002. *J Bacteriol* **188:** 3182-3191.

Bartlett, P.D., and Skoog, D.A. (1954) Colorimetric determination of elemental sulfur in hydrocarbons. *Anal Chem* **26:** 1008-1011.

Bazaral, M., and Helinski, D.R. (1968) Circular DNA forms of colicinogenic factors E1, E2 and E3 from *Escherichia coli*. *J Mol Biol* **36:** 185-194.

Beller, H.R., Chain, P.S.G., Letain, T.E., Chakicherla, A., Larimer, F.W., Richardson, P.M., Coleman, M.A., Wood, A.P., and Kelly, D.P. (2006a) The genome sequence of the obligately chemolithoautotrophic, facultatively anaerobic bacterium *Thiobacillus denitrificans*. *J Bacteriol* **188:** 1473-1488.

Beller, H.R., Letain, T.E., Chakicherla, A., Kane, S.R., Legler, T.C., and Coleman, M.A. (2006b) Whole-genome transcriptional analysis of chemolithoautotrophic thiosulfate oxidation by *Thiobacillus denitrificans* under aerobic versus denitrifying conditions. *J Bacteriol* **188:** 7005-7015.

Bertani, G. (2004) Lysogeny at mid-twentieth century: P1, P2, and other experimental systems. *J Bacteriol* **186:** 595-600.

Bilder, P.W., Ding, H., and Newcomer, M.E. (2004) Crystal structure of the ancient, Fe-S scaffold IscA reveals a novel protein fold. *Biochemistry* **43:** 133-139.

Bradford, M. (1976) A rapid and sensitive method for the quantitation of microgram quantities of protein utilizing the principle of protein-dye binding. *Anal Biochem* **72:** 248-254.

Brown, K.A. (1982) Sulfur in the environment: a review. *Environ Pollut* **3B:** 47-80.

Brune, D.C. (1989) Sulfur oxidation by phototrophic bacteria. *Biochim Biophys Acta* **975:** 189-221.

Brune, D.C. (1995a) Isolation and characterization of sulfur globule proteins from *Chromatium vinosum* and *Thiocapsa roseopersicina*. *Arch Microbiol* **163:** 391-399.

Brune, D.C. (1995b) Sulfur compounds as photosynthetic electron donors. In *Anoxygenic Photosynthetic Bacteria*. Blankenship, R.E., Madigan, M.T., and Bauer, C.E. (eds). Dordrecht: Kluwer Academic Publishers, pp. 847-870.

Brüser, T., Lens, P., and Trüper, H.G. (2000) The biological sulfur cycle. In *Environmental Technologies to Treat Sulfur Pollution*. Lens, P., and Pol, L.H. (eds). London: IWA Publishing, pp. 47-86.

Bryantseva, I.A., Gorlenko, V.M., Tourova, T.P., Kuznetsov, B.B., Lysenko, A.M., Bykova, S.A., Galchenko, V.F., Mityushina, L.L., and Osipov, G.A. (2000) *Heliobacterium sulfidophilum* sp. nov. and *Heliobacterium undosum* sp. nov.: Sulfide-oxidizing heliobacteria from thermal sulfidic springs. *Microbiology* **69:** 325-334.

Cavanaugh, C.M., McKiness, Z.P., Newton, I.L.G., and Stewart, F.J. (2006) Marine chemosynthetic symbioses. In *The Prokaryotes*. Dworkin, M., Falkow, S., Rosenberg, E., Schleifer, K.-H., and Stackebrandt, E. (eds). New York: Springer, pp. 475-507.

Chan, L.-K., Margan-Kiss, R., and Hanson, T.E. (2008) Sulfur oxidation in *Chlorobium tepidum* (syn. *Chlorobaculum tepidum*): genetic and proteomic analyses. In *Microbial Sulfur Metabolism*. Dahl, C., and Friedrich, C.G. (eds). Heidelberg Berlin: Springer, pp. 117-126.

Chenna, R., Sugawara, H., Koike, T., Lopez, R., Gibson, T.J., Higgins, D.G., and Thompson, J.D. (2003) Multiple sequence alignment with the Clustal series of programs. *Nucleic Acids Res* **31:** 3497-3500.

Coligen, J.E., Dum, B.M., Ploegh, H.L., Speicher, D.W., and Wingfield, W.T. (1997) *Current Protocols in Protein Science.* New York: John Wiley & Sons.

Cort, J.R., Mariappan, S.V.S., Kim, C.-Y., Park, M.S., Peat, T.S., Waldo, G.S., Terwilliger, T.C., and Kennedy, M.A. (2001) Solution structure of *Pyrobaculum aerophilum* DsrC, an archaeal homologue of the gamma subunit of dissimilatory sulfite reductase. *Eur J Biochem* **268:** 5842-5850.

Cort, J.R., Selan, U., Schulte, A., Grimm, F., Kennedy, M.A., and Dahl, C. (2008) *Allochromatium vinosum* DsrC: Solution-state NMR structure, redox properties, and interaction with DsrEFH, a protein essential for purple sulfur bacterial sulfur oxidation. *J Mol Biol* **382:** 692-707.

Cupp-Vickery, J.R., Silberg, J.J., Ta, D.T., and Vickery, L.E. (2004) Crystal structure of IscA, an iron-sulfur cluster assembly protein from *Escherichia coli*. *J Mol Biol* **338:** 127-137.

Dagert, M., and Ehrlich, S.D. (1974) Prolonged incubation in calcium chloride improves competence of *Escherichia coli* cells. *Gene* **6:** 23-28.

Dahl, C. (1996) Insertional gene inactivation in a phototrophic sulphur bacterium: APS-reductase-deficient mutants of *Chromatium vinosum*. *Microbiology* **142:** 3363-3372.

Dahl, C. (2008) Inorganic sulfur compounds as electron donors in purple sulfur bacteria. In *Sulfur Metabolism in Phototrophic Organisms*. Hell, R., Dahl, C., Knaff, D.B., and Leustek, T. (eds). Dordrecht: Springer, pp. 289-317.

Dahl, C., and Prange, A. (2006) Bacterial sulfur globules: Occurrence, structure and metabolism. In *Inclusions in Prokaryotes*. Shively, J.M. (ed). Heidelberg: Springer-Verlag, pp. 21-51.

Dahl, C., and Trüper, H.G. (1994) Enzymes of dissimilatory sulfide oxidation in phototrophic bacteria. *Meth Enzymol* **243:** 400-421.

Dahl, C., Prange, A., and Steudel, R. (2002) Natural polymeric sulfur compounds. In *Miscellaneous Bioploymers and Biodegradation of Synthetic Polymers*. Steinbüchel, A. (ed). Weinheim: Wiley-VCH, pp. 35-62.

Dahl, C., Engels, S., Pott-Sperling, A.S., Schulte, A., Sander, J., Lübbe, Y., Deuster, O., and Brune, D.C. (2005) Novel genes of the *dsr* gene cluster and evidence for close interaction of Dsr proteins during sulfur oxidation in the phototrophic sulfur bacterium *Allochromatium vinosum*. *J Bacteriol* **187:** 1392-1404.

Dahl, C., Schulte, A., and Shin, D.H. (2007) Cloning, expression, purification, crystallization and preliminary X-ray diffraction analysis of DsrEFH from *Allochromatium vinosum*. *Acta Crystallogr Sect F Struct Biol Cryst Commun* **63:** 890-892.

Dahl, C., Hell, R., Leustek, T., and Knaff, D.B. (2008a) Introduction to sulfur metabolism on phototrophic organisms. In *Sulfur Metabolism in Phototrophic Organisms*. Hell, R., Dahl, C., Knaff, D.B., and Leustek, T. (eds). Dordrecht: Springer, pp. 1-14.

Dahl, C., Schulte, A., Stockdreher, Y., Hong, C., Grimm, F., Sander, J., Kim, R., Kim, S.-H., and Shin, D.H. (2008b) Structural and molecular genetic insight into a widespread sulfur oxidation pathway. *J Mol Biol* **384:** 1287-1300.

Denkmann, K. (2011) Biochemische und enzymkinetische Analyse des ungewöhnlichen *c*-Typ Cytochroms Thiosulfatdehydrogenase aus *Allochromatium vinosum*. Diploma thesis, University of Bonn.

Deutch, A.H., Smith, C.J., Rushlow, K.E., and Kretschmer, P.J. (1982) *Escherichia coli* Δ^1-pyrroline-5-carboxylate reductase: Gene sequence, protein overproduction and purification. *Nucleic Acids Res* **10:** 7701-7714.

Ding, H., and Clark, R.J. (2004) Characterization of iron binding in IscA, an ancient iron-sulphur cluster assembly protein. *Biochem J* **379:** 433-440.

Ding, H., Clark, R.J., and Ding, B. (2004) IscA mediates iron delivery for assembly of iron-sulfur clusters in IscU under the limited accessible free iron conditions. *J Biol Chem* **279:** 37499-37504.

Ding, H., Harrison, K., and Lu, J. (2005) Thioredoxin reductase system mediates iron binding in IscA and iron delivery for the iron-sulfur cluster assembly in IscU. *J Biol Chem* **280:** 30432-30437.

Dos Santos, P.C., Smith, A.D., Frazzon, J., Cash, V.L., Johnson, M.K., and Dean, D.R. (2004) Iron-sulfur cluster assembly. NifU-directed activation of the nitrogenase Fe protein. *J Biol Chem* **279:** 19705-19711.

Eisen, J.A., Nelson, K.E., Paulsen, I.T., Heidelberg, J.F., Wu, M., Dodson, R.J., Deboy, R., Gwinn, M.L., Nelson, W.C., Haft, D.H., Hickey, E.K., Peterson, J.D., Durkin, A.S., Kolonay, J.L., Yang, F., Holt, I., Umayam, L.A., Mason, T., Brenner, M., Shea, T.P., Parksey, D., Nierman, W.C., Feldblyum, T.V., Hansen, C.L., Craven, M.B., Radune, D., Vamathevan, J., Khouri, H., White, O., Gruber, T.M., Ketchum, K.A., Venter, J.C., Tettelin, H., Bryant, D.A., and Fraser, C.M. (2002) The complete genome sequence of *Chlorobium tepidum* TLS, a photosynthetic, anaerobic, green-sulfur bacterium. *Proc Natl Acad Sci U S A* **99:** 9509-9514.

Embury, S.H., Scharf, S., Saiki, R.K., Gholson, M.A., Golbus, M., Arnheim, N., and Erlich, H.A. (1987) Rapid prenatal diagnosis of sickle cell anemia by a new method of DNA analysis. *N Engl J Med* **316:** 656-661.

Falkenby, L.G., Szymanska, M., Holkenbrink, C., Habicht, K.S., Andersen, J.S., Miller, M., and Frigaard, N.-U. (2011) Quantitative proteomics of *Chlorobaculum tepidum*: insights into the sulfur metabolism of a phototrophic green sulfur bacterium. *FEMS Microbiol Lett* **323:** 142-150.

Fey, A., Eichler, S., Flavier, S., Christen, R., Höfle, M.G., and Guzmán, C.A. (2004) Establishment of a real-time PCR-based approach for accurate quantification of bacterial RNA targets in water, using *Salmonella* as a model organism. *Appl Environ Microbiol* **70:** 3618-3623.

Franz, B. (2010) Untersuchungen zum Sox-Multienzymkomplex in *Allochromatium vinosum* und zur Verwertung von Elementarschwefel in phototrophen Schwefeloxidierern. Doctoral thesis, University of Bonn.

Friedrich, C.G., Rother, D., Bardischewsky, F., Quentmeier, A., and Fischer, J. (2001) Oxidation of reduced inorganic sulfur compounds by bacteria: Emergence of a common mechanism? *Appl Environ Microbiol* **67:** 2873-2882.

Friedrich, C.G., Bardischewsky, F., Rother, D., Quentmeier, A., and Fischer, J. (2005) Prokaryotic sulfur oxidation. *Curr Opin Microbiol* **8:** 253-259.

Frigaard, N.-U., and Dahl, C. (2009) Sulfur metabolism in phototrophic sulfur bacteria. *Adv Microb Physiol* **54:** 103-200.

Fuller, R.C., Smillie, R.M., Sisler, E.C., and Kronberg, H.L. (1961) Carbon metabolism in *Chromatium*. *J Biol Chem* **236:** 2140-2149.

Gehrke, T. (2000) Identifizierung und Charakterisierung niedermolekularer Thiole in dem phototrophen Schwefelbakterium *Allochromatium vinosum*. Diploma thesis, University of Bonn.

Ghosh, W., and Dam, B. (2009) Biochemistry and molecular biology of lithotrophic sulfur oxidation by taxonomically and ecologically diverse bacteria and archaea. *FEMS Microbiol Rev* **33:** 999-1043.

Glaser, F., Pupko, T., Paz, I., Bell, R.E., Bechor-Shental, D., Martz, E., and Ben-Tal, N. (2003) ConSurf: Identification of functional regions in proteins by surface-mapping of phylogenetic information. *Bioinformatics* **19:** 163-164.

Gourse, R.L., Gaal, T., Bartlett, M.S., Appleman, J.A., and Ross, W. (1996) rRNA transcription and growth rate-dependent regulation of ribosome synthesis in *Escherichia coli*. *Annu Rev Microbiol* **50:** 645-677.

Grein, F., Pereira, I.A.C., and Dahl, C. (2010a) Biochemical characterization of individual components of the *Allochromatium vinosum* DsrMKJOP transmembrane complex aids understanding of complex function *in vivo*. *J Bacteriol* **192:** 6369-6377.

Grein, F., Venceslau, S.S., Schneider, L., Hildebrandt, P., Todorovic, S., Pereira, I.A., and Dahl, C. (2010b) DsrJ, an essential part of the DsrMKJOP transmembrane complex in the purple sulfur bacterium *Allochromatium vinosum*, is an unusual triheme cytochrome *c*. *Biochemistry* **49:** 8290-8299.

Griesbeck, C., Schütz, M., Schödl, T., Bathe, S., Nausch, L., Mederer, N., Vielreicher, M., and Hauska, G. (2002) Mechanism of sulfide-quinone oxidoreductase investigated using site-directed mutagenesis and sulfur analysis. *Biochemistry* **41:** 11552-11565.

Grimm, F. (2004) In-frame-Mutagenese der Gene *dsrAB*, *dsrEFH*, *dsrC*, *dsrR* und *dsrS* in *Allochromatium vinosum*. Diploma thesis, University of Bonn.

Grimm, F., Franz, B., and Dahl, C. (2008) Thiosulfate and sulfur oxidation in purple sulfur bacteria. In *Microbial Sulfur Metabolism*. Dahl, C., and Friedrich, C.G. (eds). Berlin Heidelberg: Springer-Verlag, pp. 101-116.

Hanahan, D. (1983) Studies on transformation of *Escherichia coli* with plasmids. *J Mol Biol* **166:** 557-580.

Harada, M., Yoshida, T., Kuwahara, H., Shimamura, S., Takaki, Y., Kato, C., Miwa, T., Miyake, H., and Maruyama, T. (2009) Expression of genes for sulfur oxidation in the intracellular chemoautotrophic symbiont of the deep-sea bivalve *Calyptogena okutanii*. *Extremophiles* **13:** 895-903.

Haveman, S.A., Brunelle, V., Voordouw, J.K., Voordouw, G., Heidelberg, J.F., and Rabus, R. (2003) Gene expression analysis of energy metabolism mutants of *Desulfovibrio vulgaris* Hildenborough indicates an important role for alcohol dehydrogenase. *J Bacteriol* **185:** 4345-4353.

Haveman, S.A., Greene, E.A., Stilwell, C.P., Voordouw, J.K., and Voordouw, G. (2004) Physiological and gene expression analysis of inhibition of *Desulfovibrio vulgaris* Hildenborough by nitrite. *J Bacteriol* **186:** 7944-7950.

He, Q., Huang, K.H., He, Z., Alm, E.J., Fields, M.W., Hazen, T.C., Arkin, A.P., Wall, J.D., and Zhou, J. (2006) Energetic consequences of nitrite stress in *Desulfovibrio vulgaris* Hildenborough, inferred from global transcriptional analysis. *Appl Environ Microbiol* **72:** 4370-4381.

Hensen, D. (2006) Biochemical and genetic analysis of the Sox multienzyme complex in the purple sulfur bacterium *Allochromatium vinosum*. Doctoral thesis, University of Bonn.

Hensen, D., Sperling, D., Trüper, H.G., Brune, D.C., and Dahl, C. (2006) Thiosulfate oxidation in the phototrophic sulfur bacterium *Allochromatium vinosum*. *Mol Microbiol* **62:** 794-810.

Hildebrandt, T.M., and Grieshaber, M.K. (2008) Three enzymatic activities catalyze the oxidation of sulfide to thiosulfate in mammalian and invertebrate mitochondria. *FEBS J* **275:** 3352-3361.

Hipp, W.M., Pott, A.S., Thum-Schmitz, N., Faath, I., Dahl, C., and Trüper, H.G. (1997) Towards the phylogeny of APS reductases and sirohaem sulfite reductases in sulfate-reducing and sulfur-oxidizing prokaryotes. *Microbiology* **143:** 2891-2902.

Horton, R.M. (1995) PCR-mediated recombination and mutagenesis: SOEing together tailor-made genes. *Mol Biotechnol* **3:** 93-99.

Hove-Jensen, B., Harlow, K.W., King, C.J., and Switzer, R.L. (1986) Phosphoribosyl-pyrophosphate synthetase of *Escherichia coli.* Properties of the purified enzyme and primary structure of the *prs* gene. *The journal of biological chemistry* **261:** 6765-6771.

Hsieh, Y.C., Liu, M.Y., Wang, V.C., Chiang, Y.L., Liu, E.H., Wu, W.G., Chan, S.I., and Chen, C.J. (2010) Structural insights into the enzyme catalysis from comparison of three forms of dissimilatory sulphite reductase from *Desulfovibrio gigas*. *Mol Microbiol* **78:** 1101-1116.

Hübner, P., Willison, J.C., Vignais, P., and Bickle, T.A. (1991) Expression of regulatory *nif* genes in *Rhodobacter capsulatus*. *J Bacteriol* **173:** 2993-2999.

Hurlbert, R.E. (1968) Effect of thiol-binding reagents on the metabolism of *Chromatium* D. *J Bacteriol* **95:** 1706-1712.

Hurlbert, R.E., and Lascelles, J. (1963) Ribulose diphosphate carboxylase in Thiorhodaceae. *J Gen Microbiol* **33:** 445-458.

Ikeuchi, Y., Shigi, N., Kato, J.-I., Nishimura, A., and Suzuki, T. (2006) Mechanistic insights into sulfur relay by multiple sulfur mediators involved in thiouridine biosynthesis at tRNA wobble positions. *Mol Cell* **21:** 97-108.

Ilag, L.L., Jahn, D., Eggertsson, G., and Söll, D. (1991) The *Escherichia coli hemL* gene encodes glutamate 1-semialdehyde aminotransferase. *J Bacteriol* **173:** 3408-3413.

Imhoff, J.F. (2003) Phylogenetic taxonomy of the family *Chlorobiaceae* on the basis of 16S rRNA and *fmo* (Fenna-Matthews-Olson protein) gene sequences. *Int J Syst Evol Microbiol* **53:** 941-951.

Imhoff, J.F., Süling, J., and Petri, R. (1998) Phylogenetic relationships among the *Chromatiaceae*, their taxonomic reclassification and description of the new genera *Allochromatium*, *Halochromatium*, *Isochromatium*, *Marichromatium*, *Thiococcus*, *Thiohalocapsa*, and *Thermochromatium*. *Int J Syst Bacteriol* **48:** 1129-1143.

Jensen, L.T., and Culotta, C. (2000) Role of *Saccharomyces cerevisiae ISA1* and *ISA2* in iron homeostasis. *Mol Cell Biol* **20:** 3918-3927.

Johnson, D.C., Dean, D.R., Smith, A.D., and Johnson, M.K. (2005) Structure, function, and formation of biological iron-sulfur clusters. *Annu Rev Biochem* **74:** 247-281.

Kammler, L. (2009) Heterologe Produktion und Charakterisierung des purpurbakteriellen Eisen-Schwefel-Flavoproteins DsrL aus *Allochromatium vinosum*. Diploma thesis, University of Bonn.

Kämpf, C., and Pfennig, N. (1980) Capacity of Chromatiaceae for chemotrophic growth. Specific respiration rates of *Thiocystis violacea* and *Chromatium vinosum*. *Arch Microbiol* **127:** 125-135.

Kappler, U. (1999) Molekularbiologie und Enzymologie der direkten Oxidation von Suflit durch die Sulfit:Akzeptor Oxidoreduktase in photo- und chemotrophen Schwefelbakterien. Doctoral thesis, University of Bonn.

Kappler, U., and Dahl, C. (2001) Enzymology and molecular biology of prokaryotic sulfite oxidation. *FEMS Microbiol Lett* **203:** 1-9.

Karkhoff-Schweizer, R.R., Bruschi, M., and Voordouw, G. (1993) Expression of the γ-subunit gene of desulfoviridin-type dissimilatory sulfite reductase and of the α- and β-subunit genes is not coordinately regulated. *Eur J Biochem* **211:** 501-507.

Keller, K.L., and Wall, J.D. (2011) Genetics and molecular biology of the electron flow for sulfate respiration in *Desulfovibrio*. *Front Microbio* **2:**135: 1-17.

Kim, C., Xuong, N.-H., Edwards, S., Madhusudan, Yee, M.-C., Spraggon, G., and Mills, S.E. (2002) The crystal structure of anthranilate phosphoribosyltransferase from the enterobacterium *Pectobacterium carotovorum*. *FEBS Lett* **523:** 239-246.

Kovach, M.E., Elzer, P.H., Hill, D.S., Robertson, G.T., Farris, M.A., Roop, R.M.II., and Peterson, K.M. (1995) Four new derivatives of the broad-host-range cloning vector pBBR1MCS, carrying different antibiotic-resistance cassettes. *Gene* **166:** 175-176.

Krebs, C., Agar, J.N., Smith, A.D., Frazzon, J., Dean, D.R., Huynh, B.H., and Johnson, M.K. (2001) IscA, an alternate scaffold for Fe-S cluster biosynthesis. *Biochemistry* **40:** 14069-14080.

Kuwahara, H., Yoshida, T., Takaki, Y., Shimamura, S., Nishi, S., Harada, M., Matsuyama, K., Takishita, K., Kawato, M., Uematsu, K., Fujiwara, Y., Sato, T., Kato, C., Kitagawa, M., Kato, I., and Maruyama, T. (2007) Reduced genome of the thioautotrophic intracellular symbiont in a deep-sea clam, *Calyptogena okutanii*. *Curr Biol* **17:** 881-886.

Laemmli, U.K. (1970) Cleavage of structural proteins during the assembly of the head of bacteriophage T4. *Nature* **227:** 680-685.

Lane, D., Prentki, P., and Chandler, M. (1992) Use of gel retardation to analyze protein-nucleic acid interactions. *Microbiol Rev* **56:** 509-528.

Lee, Y.-H., Nadaraia, S., Gu, D., Becker, D.F., and Tanner, J.J. (2003) Structure of the proline dehydrogenase domain of the multifunctional PutA flavoprotein. *Nat Struct Biol* **10:** 109-114.

Lehmann, M. (2010) Überproduktion und biochemische Charakterisierung des komplexen purpurbakteriellen *c*-Typ Cytochroms SoxXAK aus *Allochromatium vinosum*. Bachelor thesis, University of Bonn.

Lens, P.N.L., and Kuenen, J.G. (2001) The biological sulfur cycle: novel opportunities for environmental biotechnology. *Water Sci Technol* **44:** 57-66.

Lesley, S.A., Graziano, J., Cho, C.Y., Knuth, M.W., and Klock, H.E. (2002) Gene expression response to misfolded protein as a screen for soluble recombinant protein. *Protein Eng* **15:** 153-160.

Loiseau, L., Gerez, C., Bekker, M., Ollagnier-de-Choudens, S., Py, B., Sanakis, Y., Teixeira de Mattos, J., Fontecave, M., and Barras, F. (2007) ErpA, an iron-sulfur (Fe-S) protein of the A-type essential for respiratory metabolism in *Escherichia coli*. *Proc Natl Acad Sci U S A* **104:** 13626-13631.

Lübbe, Y. (2005) Biochemische und molekularbiologische Untersuchungen zur Funktion von DsrN und DsrL im dissimilatorischen Schwefelstoffwechsel von *Allochromatium vinosum*. Doctoral thesis, University of Bonn.

Lübbe, Y., Youn, H.-S., Timkovich, R., and Dahl, C. (2006) Siro(haem)amide in *Allochromatium vinosum* and relevance of DsrL and DsrN, a homolog of cobyrinic acid *a,c*-diamide synthase, for sulphur oxidation. *FEMS Microbiol Lett* **261:** 194-202.

Matias, P.M., Pereira, I.A.C., Soares, C.M., and Carrondo, M.A. (2005) Sulphate respiration from hydrogen in *Desulfovibrio* bacteria: A structural biology overview. *Prog Biophys Mol Biol* **89:** 292-329.

Matthews, J.C., Timkovich, R., Liu, M.-Y., and Le Gall, J. (1995) Siroamide: A prosthetic group isolated from sulfite reductases in the genus *Desulfovibrio*. *Biochemistry* **34:** 5248-5251.

McHugh, J.P., Rodríguez-Quinones, F., Abdul-Tehrani, H., Svistunenko, D.A., Poole, R.K., Cooper, C.E., and Andrews, S.C. (2003) Global iron-dependent gene regulation in *Escherichia coli*. A new mechanism for iron homeostasis. *J Biol Chem* **278:** 29478-29486.

Miallau, L., Alphey, M.S., Kemp, L.E., Leonard, G.A., McSweeney, S.M., Hecht, S., Bacher, A., Eisenreich, W., Rohdich, F., and Hunter, W.N. (2003) Biosynthesis of isoprenoids: Crystal structure of 4-diphosphocytidyl-2*C*-methyl-D-erythritol kinase. *Proc Natl Acad Sci U S A* **100:** 9173-9178.

Middelburg, J. (2000) The geochemical sulfur cycle. In *Environmental Technologies to Treat Sulfur Pollution*. Lens, P., and Hulshoff Pol, L. (eds). London: IWA Publishing, pp. 33-46.

Miller, J.H. (1972) Assay of β-galactosidase. In *Experiments in Molecular Genetics*. Miller, J.H. (ed). Cold Spring Harbor, N.Y.: Cold Spring Harbor Laboratory, pp. 352-355.

Mittenhuber, G., Sonomoto, K., Egert, M., and Friedrich, C.G. (1991) Identification of the DNA region responsible for sulfur-oxidizing ability of *Thiosphaera pantotropha*. *J Bacteriol* **173:** 7340-7344.

Morimoto, K., Yamashita, E., Kondou, Y., Lee, S.J., Arisaka, F., Tsukihara, T., and Nakai, M. (2006) The asymmetric IscA homodimer with an exposed [2Fe-2S] cluster suggests the structural basis of the Fe-S cluster biosynthetic scaffold. *J Mol Biol* **360:** 117-132.

Mullis, K.B., Faloona, F., Scharf, S., Saiki, R.K., Horn, G.T., and Erlich, H.A. (1986) Specific enzymatic amplification of DNA in vitro: The polymerase chain reaction. *Cold Spring Harb Symp Quant Biol* **51:** 263-273.

Murguia, J.R., Belles, J.M., and Serrano, R. (1995) A salt-sensitive 3'(2'),5'-bisphosphate nucleotidase involved in sulfate activation. *Science* **267:** 232-234.

Murzin, A.G., Brenner, S.E., Hubbard, T., and Chothia, C. (1995) SCOP: A structural classification of proteins database for the investigation of sequences and structures. *J Mol Biol* **247:** 536-540.

Neretin, L.N., Schippers, A., Pernthaler, A., Hamann, K., Amann, R., and Jørgensen, B.B. (2003) Quantification of dissimilatory (bi)sulphite reductase gene expression in *Desulfobacterium autotrophicum* using real-time RT-PCR. *Environ Microbiol* **5:** 660-671.

Neuwald, A.F., Krishnan, B.R., Brikun, I., Kulakauskas, S., Sužiedelis, K., Tomcsanyi, T., Leyh, T.S., and Berg, D.E. (1992) *cysQ*, a gene needed for cysteine synthesis in *Escherichia coli* K-12 only during aerobic growth. *J Bacteriol* **174:** 415-425.

Newton, I.L.G., Woyke, T., Auchtung, T.A., Dilly, G.F., Dutton, R.J., Fisher, M.C., Fontanez, K.M., Lau, E., Stewart, F.J., Richardson, P.M., Barry, K.W., Saunders, E., Detter, J.C., Wu, D., Eisen, J.A., and Cavanaugh, C.M. (2007) The *Calyptogena magnifica* chemoautotrophic symbiont genome. *Science* **315:** 998-1000.

Nonaka, G., Blankschien, M., Herman, C., and Gross, C.A. (2006) Regulon and promoter analysis of the *E. coli* heat-shock factor, σ^{32}, reveals a multifaceted cellular response to heat stress. *Genes Dev* **20:** 1776-1789.

Numata, T., Fukai, S., Ikeuchi, Y., Suzuki, T., and Nureki, O. (2006) Structural basis for sulfur relay to RNA mediated by heterohexameric TusBCD complex. *Structure* **14:** 357-366.

Ogawa, T., Furusawa, T., Nomura, R., Seo, D., Hosoya-Matsuda, N., Sakurai, H., and Inoue, K. (2008) SoxAX binding protein, a novel component of the thiosulfate-oxidizing multienzyme system in the green sulfur bacterium *Chlorobium tepidum*. *J Bacteriol* **190:** 6097-6110.

Oliveira, T.F., Vonrhein, C., Matias, P.M., Venceslau, S.S., Pereira, I.A.C., and Archer, M. (2008) The crystal structure of *Desulfovibrio vulgaris* dissimilatory sulfite reductase bound to DsrC provides novel insights into the mechanism of sulfate respiration. *J Biol Chem* **283:** 34141-34149.

Oliveira, T.F., Franklin, E., Alfonso, J.P., Kahn, A.R., Oldham, N.J., Pereira, I.A.C., and Archer, M. (2011) Structural insights into dissimilatory sulfite reductases: Structure of desulforubidin from *Desulfomicrobium norvegicum*. *Front Microbio* **2:**71: 1-12.

Ollagnier-de-Choudens, S., Mattioli, T., Takahashi, Y., and Fontecave, M. (2001) Iron-sulfur cluster assembly. Characterization of IscA and evidence for a specific and functional complex with ferredoxin. *J Biol Chem* **276:** 22604-22607.

Overmann, J., Fischer, U., and Pfennig, N. (1992) A new purple sulfur bacterium from saline littoral sediments, *Thiorhodovibrio winogradskyi* gen. nov. and sp. nov. *Arch Microbiol* **157:** 329-335.

Pattaragulwanit, K. (1994) Antibiotika-Sensitivität und konjugativer Transfer von Resistenzplasmiden bei *Chromatium vinosum*. Diploma thesis, University of Bonn.

Pattaragulwanit, K., and Dahl, C. (1995) Development of a genetic system for a purple sulfur bacterium: Conjugative plasmid transfer in *Chromatium vinosum*. *Arch Microbiol* **164:** 217-222.

Pattaragulwanit, K., Brune, D.C., Trüper, H.G., and Dahl, C. (1998) Molecular genetic evidence for extracytoplasmic localization of sulfur globules in *Chromatium vinosum*. *Arch Microbiol* **169:** 434-444.

Pereira, P.M., He, Q., Valente, F.M.A., Xavier, A.V., Zhou, J., Pereira, I.A.C., and Louro, R.O. (2008a) Energy metabolism in *Desulfovibrio vulgaris* Hildenborough: Insights from transcriptome analysis. *Antonie van Leeuwenhoek* **93:** 347-362.

Pereira, P.M., He, Q., Xavier, A.V., Zhou, J., Pereira, I.A.C., and Louro, R.O. (2008b) Transcriptional response of *Desulfovibrio vulgaris* Hildenborough to oxidative stress mimicking environmental conditions. *Arch Microbiol* **189:** 451-461.

Pereira, I.A.C., Ramos, A.R., Grein, F., Marques, M.C., Marques da Silva, S., and Venceslau, S.S. (2011) A comparative genomic analysis of energy metabolism in sulfate reducing bacteria and archaea. *Front Microbio* **2:**69: 1-22.

Pfennig, N., and Trüper, H.G. (1989) Anoxygenic phototrophic bacteria. In *Bergey's Manual of Systematic Bacteriology, Vol. 3*. Staley, J.T., Bryant, M.P., Pfennig, N., and Holt, J.G. (eds). Baltimore: Williams & Wilkins, pp. 1635-1653.

Pires, R.H., Venceslau, S.S., Morais, F., Teixeira, M., Xavier, A.V., and Pereira, I.A.C. (2006) Characterization of the *Desulfovibrio desulfuricans* ATCC 27774 DsrMKJOP complex - A membrane-bound redox complex involved in the sulfate respiratory pathway. *Biochemistry* **45:** 249-262.

Pott, A.S., and Dahl, C. (1998) Sirohaem sulfite reductase and other proteins encoded in the *dsr* locus of *Chromatium vinosum* are involved in the oxidation of intracellular sulfur. *Microbiology* **144:** 1881-1894.

Pott-Sperling, A.S. (2000) Das *dsr*-Operon von *Allochromatium vinosum*: molekular-biologische Charakterisierung der Gene für die Schwefeloxidation. Doctoral thesis, University of Bonn.

Prange, A., Arzberger, I., Engemann, C., Modrow, H., Schumann, O., Trüper, H.G., Steudel, R., Dahl, C., and Hormes, J. (1999) *In situ* analysis of sulfur in the sulfur globules of phototrophic sulfur bacteria by X-ray absorption near edge spectroscopy. *Biochim Biophys Acta* **1428:** 446-454.

Prange, A., Chauvistre, R., Modrow, H., Hormes, J., Trüper, H.G., and Dahl, C. (2002) Quantitative speciation of sulfur in bacterial sulfur globules: X-ray absorption spectroscopy reveals at least three different speciations of sulfur. *Microbiology* **148:** 267-276.

Prange, A., Engelhardt, H., Trüper, H.G., and Dahl, C. (2004) The role of the sulfur globule proteins of *Allochromatium vinosum*: Mutagenesis of the sulfur globule protein genes and expression studies by real-time RT PCR. *Arch Microbiol* **182:** 165-174.

Reinartz, M., Tschäpe, J., Brüser, T., Trüper, H.G., and Dahl, C. (1998) Sulfide oxidation in the phototrophic sulfur bacterium *Chromatium vinosum*. *Arch Microbiol* **170:** 59-68.

Rethmeier, J., Rabenstein, A., Langer, M., and Fischer, U. (1997) Detection of traces of oxidized and reduced sulfur compounds in small samples by combination of different high-performance liquid chromatography methods. *J Chromatogr A* **760:** 295-302.

Rodionov, D.A., Vitreschak, A.G., Mironov, A.A., and Gelfand, M.S. (2002) Comparative genomics of thiamin biosynthesis in procaryotes. *J Biol Chem* **277:** 48949-48959.

Roof, D.M., and Roth, J.R. (1992) Autogenous regulation of ethanolamine utilization by a transcriptional activator of the *eut* operon in *Salmonella typhimurium*. *J Bacteriol* **174:** 6634-6643.

Sabehi, G., Loy, A., Jung, K.-H., Partha, R., Spudich, J.L., Isaacson, T., Hirschberg, J., Wagner, M., and Béjà, O. (2005) New insights into metabolic properties of marine bacteria encoding proteorhodopsins. *PLoS Biol* **3:** e273.

Sahl, H.G., and Trüper, H.G. (1977) Enzymes of CO_2 fixation in *Chromatiaceae*. *FEMS Microbiol Lett* **2:** 129-132.

Saiki, R.K., Scharf, S., Faloona, F., Mullis, K.B., Horn, G.T., Erlich, H.A., and Arnheim, N. (1985) Enzymatic amplification of β-globin genomic sequences and restriction site analysis for diagnosis of sickle cell anemia. *Science* **230:** 1350-1354.

Saiki, R.K., Bugawan, T.L., Horn, G.T., Mullis, K.B., and Erlich, H.A. (1986) Analysis of enzymatically amplified β-globin and HLA-DQα DNA with allele-specific oligonucleotide probes. *Nature* **324:** 163-166.

Saio, T., Kumeta, H., Ogura, K., Yokochi, M., Asayama, M., Katoh, E., Teshima, K., and Inagaki, F. (2007) The cooperative role of OsCnfU-1A domain I and domain II in the iron-sulphur cluster transfer process as revealed by NMR. *J Biochem* **142:** 113-121.

Sambrook, J., Fritsch, E.F., and Maniatis, T. (1989) *Molecular Cloning: a Laboratory Manual.* Cold Spring Harbor, N.Y.: Cold Spring Harbor Laboratory.

Sanchez, O., Ferrera, I., Dahl, C., and Mas, J. (2001) *In vivo* role of APS reductase in the purple sulfur bacterium *Allochromatium vinosum*. *Arch Microbiol* **176:** 301-305.

Sander, J., and Dahl, C. (2009) Metabolism of inorganic sulfur compounds in purple bacteria. In *The Purple Phototrophic Bacteria*. Hunter, C.N., Daldal, F., Thurnauer, M.C., and Beatty, J.T. (eds). Dordrecht: Springer, pp. 595-622.

Sander, J., Engels-Schwarzlose, S., and Dahl, C. (2006) Importance of the DsrMKJOP complex for sulfur oxidation in *Allochromatium vinosum* and phylogenetic analysis of related complexes in other prokaryotes. *Arch Microbiol* **186:** 357-366.

Schäfer, A., Tauch, A., Jager, W., Kalinowski, J., Thierbach, G., and Pühler, A. (1994) Small mobilizable multi-purpose cloning vectors derived from the *Escherichia coli* plasmids pK18 and pK19: selection of defined deletions in the chromosome of *Corynebacterium glutamicum*. *Gene* **145:** 69-73.

Schedel, M., and Trüper, H.G. (1980) Anaerobic oxidation of thiosulfate and elemental sulfur in *Thiobacillus denitrificans*. *Arch Microbiol* **124:** 205-210.

Schedel, M., Vanselow, M., and Trüper, H.G. (1979) Siroheme sulfite reductase isolated from *Chromatium vinosum*. Purification and investigation of some of its molecular and catalytic properties. *Arch Microbiol* **121:** 29-36.

Schmidt, G.L., Nicolson, G.L., and Kamen, M.D. (1971) Composition of the sulfur particle of *Chromatium vinosum*. *J Bacteriol* **105:** 1137-1141.

Shahak, Y., and Hauska, G. (2008) Sulfide oxidation from cyanobacteria to humans: Sulfide-quinone oxidoreductase (SQR). In *Sulfur Metabolism in Phototrophic Organisms*. Hell, R., Dahl, C., Knaff, D.B., and Leustek, T. (eds). Dordrecht: Springer, pp. 319-335.

Shaw, K.J., Miller, N., Liu, X., Lerner, D., Wan, J., Bittner, A., and Morrow, B.J. (2003) Comparison of the changes in global gene expression of *Escherichia coli* induced by four bactericidal agents. *J Mol Microbiol Biotechnol* **5:** 105-122.

Simon, R., Priefer, U., and Pühler, A. (1983) A broad host range mobilization system for *in vivo* genetic engineering: Transposon mutagenesis in gram negative bacteria. *Bio/Technology* **1:** 784-791.

Smith, A.D., Jameson, G.N.L., Dos Santos, P.C., Agar, J.N., Naik, S., Krebs, C., Frazzon, J., Dean, D.R., Huynh, B.H., and Johnson, M.K. (2005) NifS-mediated assembly of [4Fe-4S] clusters in the N- and C-terminal domains of the NifU scaffold protein. *Biochemistry* **44:** 12955-12969.

Smith, A.J., and Lascelles, J. (1966) Thiosulphate metabolism and rhodanese in *Chromatium* sp. strain D. *J Gen Microbiol* **42:** 357-370.

Southern, E.M. (1975) Detection of specific sequences among DNA fragments separated by gel electrophoresis. *J Mol Biol* **98:** 503-517.

Southern, E.M. (1979) Gel electrophoresis of restriction fragments. *Meth Enzymol* **68:** 152-176.

Steudel, R. (2000) The chemical sulfur cycle. In *Environmental Technologies to Treat Sulfur Pollution - Principles and Engineering*. Lens, P.N.L., and Hulshoff Pol, L. (eds). London: IWA Publishing, pp. 1-31.

Steudel, R., Holdt, G., Visscher, P.T., and van Gemerden, H. (1990) Search for polythionates in cultures of *Chromatium vinosum* after sulfide incubation. *Arch Microbiol* **155:** 432-437.

Stewart, F.J., Dmytrenko, O., DeLong, E.F., and Cavanaugh, C.M. (2011) Metatranscriptomic analysis of sulfur oxidation genes in the endosymbiont of *Solemya velum*. *Front Microbio* **2:**134: 1-10.

Stroupe, M.E., Leech, H.K., Daniels, D.S., Warren, M.J., and Getzoff, E.D. (2003) CysG structure reveals tetrapyrrole-binding features and novel regulation of siroheme biosynthesis. *Nat Struct Biol* **10:** 1064-1073.

Theissen, U., and Martin, W. (2008) Biochemical and evolutionary aspects of eukaryotes that inhabit sulfidic environments. In *Microbial Sulfur Metabolism*. Dahl, C., and Friedrich, C.G. (eds). Berlin Heidelberg: Springer, pp. 36-45.

Tokumoto, U., and Takahashi, Y. (2001) Genetic analysis of the *isc* operon in *Escherichia coli* involved in the biogenesis of cellular iron-sulfur proteins. *J Biochem* **130:** 63-71.

Towbin, H., Staehelin, T.L., and Gordon, J. (1979) Electrophoretic transfer of proteins from polyacrylamide gels to nitrocellulose sheets. Procedure and some applications. *Proc Natl Acad Sci U S A* **76:** 4350-4356.

Trüper, H.G. (1984) Phototrophic bacteria and their sulfur metabolism. In *Sulfur, Its Significance for Chemistry, for the Geo-, Bio-, and Cosmosphere and Technology*. Müller, A., and Krebs, B. (eds). Amsterdam: Elsevier Science Publishers B.V., pp. 367-382.

Trüper, H.G., and Fischer, U. (1982) Anaerobic oxidation of sulphur compounds as electron donors for bacterial photosynthesis. *Phil Trans R Soc Lond B* **298:** 529-542.

Trüper, H.G., and Pfennig, N. (1992) The family Chlorobiaceae. In *The Prokaryotes. A Handbook on the Biology of Bacteria: Ecophysiology, Isolation, Identification, Applications*. Balows, A., Trüper, H.G., Dworkin, M., Harder, W., and Schleifer, K.-H. (eds). New York: Springer Verlag, pp. 3583-3592.

Vandecasteele, S.J., Peetermans, W.E., Merckx, R., and van Eldere, J. (2001) Quantification of expression of *Staphylococcus epidermidis* housekeeping genes with Taqman quantitative PCR during in vitro growth and under different conditions. *J Bacteriol* **183:** 7094-7101.

Wada, K., Hasegawa, Y., Gong, Z., Minami, Y., Fukuyama, K., and Takahashi, Y. (2005) Crystal structure of *Escherichia coli* SufA involved in biosynthesis of iron-sulfur clusters: implications for a functional dimer. *FEBS Lett* **579:** 6543-6548.

Wada, T., Kuzuyama, T., Satoh, S., Kuramitsu, S., Yokoyama, S., Unzai, S., Tame, J.R.H., and Park, S.-Y. (2003) Crystal structure of 4-(cytidine 5-diphospho)-2-*C*-methyl-derythritol kinase, an enzyme in the non-mevalonate pathway of isoprenoid synthesis. *J Biol Chem* **278:** 30022-30027.

Walsh, D.A., Zaikova, E., Howea, C.G., Song, Y.C., Wright, J.J., Tringe, S.G., Tortell, P.D., and Hallam, S.J. (2009) Metagenome of a versatile chemolithoautotroph from expanding oceanic dead zones. *Science* **326:** 578-582.

Weaver, P.F., Wall, J.D., and Gest, H. (1975) Characterization of *Rhodopseudomonas capsulata*. *Arch Microbiol* **105:** 207-216.

Weissgerber, T., Zigann, R., Bruce, D., Chang, Y., Detter, J. C., Han, C., Hauser, L., Jeffries, C. D., Land, M., Munk, A. C., Tapia, R., and Dahl, C. (2011) Complete genome sequence of *Allochromatium vinosum* DSM 180^{T}. *In preparation*.

Wek, R.C., and Hatfield, G.W. (1986) Examination of the internal promoter, P_E, in the *ilvGMEDA* operon of *E. coli* K-12. *Nucleic Acids Res* **14:** 2763-2777.

Welte, C., Hafner, S., Krätzer, C., Quentmeier, A., Friedrich, C.G., and Dahl, C. (2009) Interaction between Sox proteins of two physiologically distinct bacteria and a new protein involved in thiosulfate oxidation. *FEBS Lett* **583:** 1281-1286.

White, C.E., and Winans, S.C. (2007) The quorum-sensing transcription factor TraR decodes its DNA binding site by direct contacts with DNA bases and by detection of DNA flexibility. *Mol Microbiol* **64:** 245-256.

Wollenberg, M., Berndt, C., Bill, E., Schwenn, J.D., and Seidler, A. (2003) A dimer of the FeS cluster biosynthesis protein IscA from cyanobacteria binds a [2Fe2S] cluster between two protomers and transfers it to [2Fe2S] and [4Fe4S] apo porteins. *Eur J Biochem* **270:** 1662-1671.

Wu, G., Mansy, S.S., Hemann, C., Hille, R., Surerus, K.K., and Cowan, J.A. (2002) Iron-sulfur cluster biosynthesis: characterization of *Schizosaccharomyces pombe* Isa1. *J Biol Inorg Chem* **7:** 526-532.

Xu, D., Liu, G., Xiao, R., Acton, T., Goldsmith-Fischman, S., Honig, B., Montelione, G.T., and Szyperski, T. (2004) NMR structure of the hypothetical protein AQ-1857 encoded by the Y157 gene from *Aquifex aeolicus* reveals a novel protein fold. *Proteins* **54:** 794-796.

Yang, J., Bitoun, J.P., and Ding, H. (2006) Interplay of IscA and IscU in biogenesis of iron-sulfur clusters. *J Biol Chem* **281:** 27956-27963.

VII. Publications

Parts of this thesis have already been published:

Grimm, F., Cort, J.R., and Dahl, C. (2010a) DsrR, a novel IscA-like protein lacking iron- and Fe-S-binding functions, involved in the regulation of sulfur oxidation in *Allochromatium vinosum*. *J Bacteriol* **192:** 1652-1661.

Grimm, F., Dobler, N., and Dahl, C. (2010b) Regulation of *dsr* genes encoding proteins responsible for the oxidation of stored sulfur in *Allochromatium vinosum*. *Microbiology* **156:** 764-773.

Grimm, F., Franz, B., and Dahl, C. (2011) Regulation of dissimilatory sulfur oxidation in the purple sulfur bacterium *Allochromatium vinosum*. *Front Microbio* **2:**51: 1-11.

Further publications

Cort, J.R., Selan, U., Schulte, A., Grimm, F., Kennedy, M.A., and Dahl, C. (2008) *Allochromatium vinosum* DsrC: solution-state NMR structure, redox properties, and interaction with DsrEFH, a protein essential for purple sulfur bacterial sulfur oxidation. *J Mol Biol* **382:** 692-707.

Dahl, C., Schulte, A., Stockdreher, Y., Hong, C., Grimm, F., Sander, J., Kim, R., Kim, S.-H., and Shin, D.H. (2008) Structural and molecular genetic insight into a widespread sulfur oxidation pathway. *J Mol Biol* **384:** 1287-1300.

Grimm, F., Franz, B., and Dahl, C. (2008) Thiosulfate and sulfur oxidation in purple sulfur bacteria. In *Microbial Sulfur Metabolism*. Dahl, C., and Friedrich, C.G. (eds). Berlin Heidelberg: Springer-Verlag, pp. 101-116.

Conference contributions

Grimm, F. and Dahl, C. (2005). DsrR and DsrS from *Allochromatium vinosum*: Proteins involved in the regulation of the dsr operon? Abstract, Jahrestagung der VAAM 2005, Göttingen. Biospektrum Tagungsband zum 2. Gemeinsamen Kongress der DGHM und VAAM, p. 124.

Grimm, F. and Dahl, C. (2006). DsrR and DsrS from *Allochromatium vinosum*. Abstract, 12th International Symposium on Phototrophic Prokaryotes, Pau, France. Conference volume, p. 148.

Grimm, F. and Dahl, C. (2006). The significance of DsrR ans DsrS in the dissimilatory sulfur-oxidizing pathway of *Allochromatium vinosum*. Abstract, International Symposium on Microbial Sulfur Metabolism, Münster, Germany. Conference volume p.112.

Grimm, F. and Dahl, C. (2006). DsrR and DsrS from *Allochromatium vinosum*. Abstract, Meeting on Microbial Respiratory Chains, Tomar, Portugal. Conference volume, P11.

Cort, J., Grimm, F., and Dahl C. (2009) NMR Structure of *Allochromatium vinosum* DsrR. Abstract, EMBO-FEMS Workshop on Microbial Sulfur Metabolism, Tomar, Portugal. Conference volume, p.130.

Grimm, F. and Dahl C. (2009) Insights into the Regulation of the *dsr* Operon of *Allochromatium vinosum*. Abstract, EMBO-FEMS Workshop on Microbial Sulfur Metabolism, Tomar, Portugal. Conference volume, p.146.

Stockdreher, Y., Dobler, N., Grimm, F., and Dahl, C. (2009) DsrEFH, DsrC and TusA: Potential Sulfur Transferases in the Phototrophic Sulfur Oxidizer *Allochromatium vinosum*. Abstract, EMBO-FEMS Workshop on Microbial Sulfur Metabolism, Tomar, Portugal. Conference volume, p.218.

VIII. Acknowledgments

I would like to sincerely thank the following persons for their support and help in the realization of this thesis:

apl. Prof. Dr. Christiane Dahl for the interesting subject, helpful discussions, and continuous support and encouragement.

Prof. Dr. Uwe Deppenmeier for his spontaneous agreement to give an opinion on this thesis.

Dr. John R. Cort for performing the solution state NMR analysis of DsrR and insightful discussions.

Dr. Jacob Bitoun for the guidelines to iron-binding assays and Dr. Bernd Masepohl for his helpful tips concerning gene fusion.

Dr. Bettina Franz and Dr. Daniela Hensen for insightful discussion and proof-reading of this thesis.

All members of the sulfur lab, especially Dr. Fabian Grein (for the introduction into and upkeep of the anaerobic chamber), Yvonne Stockdreher (for the provision of IscS and quick supply with publications), Brigit Hüttig, and Renate Zigann for their help whenever needed.

All other members of the IfMB for a good working atmosphere.

Dr. Beatrix Tappeser and the colleages of the Federal Agency for Nature Conservation for their encouragement and understanding.

My family for their ceaseless support, encouragement, and curiosity in the subject.